

# Voltage support strategies in a rural low voltage network with high photovoltaic penetration

K. Pantziris

Master of Science Thesis



# **Voltage support strategies in a rural low voltage network with high photovoltaic penetration**

Master of Science Thesis

For the degree of Master of Science in Sustainable Energy Technology  
at Delft University of Technology

**Kyriakos Pantziris**

**Delft University of Technology – Electrical Sustainable Energy Department  
DNV GL – Energy**

May 2014



**DELFT UNIVERSITY OF TECHNOLOGY**

**FACULTY OF**

**ELECTRICAL ENGINEERING, MATHEMATICS AND COMPUTER SCIENCE (EEMCS)**

**ELECTRICAL SUSTAINABLE ENERGY (ESE)**

The undersigned hereby certify that they have read and recommend to the Faculty of Applied Sciences (AS) for acceptance a thesis entitled

**VOLTAGE SUPPORT STRATEGIES IN A RURAL LV NETWORK**

**WITH HIGH PV PENETRATION**

by

**KYRIAKOS PANTZIRIS**

in partial fulfilment of the requirements for the degree of

**MASTER OF SCIENCE IN SUSTAINABLE ENERGY TECHNOLOGY**

May 27, 2014

Thesis committee members

Supervisors:	P. Bauer	.....
	P. Vaessen	.....
Readers:	J. A. Ferreira	.....
	L. M. Ramirez Elizondo	.....



# Abstract

The rapidly increasing penetration of rooftop PV systems in rural LV distribution networks calls for the attention of DNOs in order to secure end-user voltage range. In times of high photovoltaic generation and low load consumption, voltage at PCCs may exceed the specified upper limit and make PV inverters trip. This phenomenon hinders further PV integration in the network although MV/LV transformer and conductors are by far not used up to their full capacity yet.

In this thesis, voltage rise problem is analysed through load flows and simulations on a suitably designed rural test network model implemented in PowerFactory software. The suggested local voltage support strategies by the German directive VDE-AR-N 4105 and the recent European standard EN 50438, namely PF(P) and Q(V), which require reactive power control capability of photovoltaic inverters, are implemented, tested and analysed in order to check their effectiveness and compare their behaviour. As active power curtailment capability is also already required by some DNOs, a dynamic active power curtailment control algorithm is designed and tested as well, taking into account the local load demand and the network's feed-in limitations. Afterwards, local battery storage is also incorporated in every PV system model and all the three aforementioned strategies are tested and analysed again.

All studied strategies manage to mitigate the voltage rise problem up to a PV-integration level of 10 kW/household. However, their effectiveness is compared in terms of a set of evaluation criteria for a range of PV-integration levels. Subsequently, the best candidate strategy, among the ones studied, emerges through the help of experts' opinion and a suitably designed overall evaluation score number, for both the perspectives of a DNO and a PV system owner. It is revealed that the overall preference of a DNO is for a solution which involves active power curtailment and local storage, in contrast to the overall preference of a PV system owner for a reactive power based strategy without storage.

**Keywords:** distribution network, low voltage, distributed generation, photovoltaic systems, reverse power flow, voltage rise, inverters, voltage support, reactive power control, active power curtailment, storage, photovoltaic integration, hosting capacity, PowerFactory





# Contents

<b>Abstract .....</b>	<b>i</b>
<b>Contents.....</b>	<b>iii</b>
<b>List of Figures .....</b>	<b>vii</b>
<b>List of Tables.....</b>	<b>xi</b>
<b>List of Abbreviations .....</b>	<b>xiii</b>
<b>Acknowledgments .....</b>	<b>xv</b>
<b>1 Introduction.....</b>	<b>1</b>
1.1 Electric power systems and distributed generation history.....	1
1.2 Photovoltaic systems.....	3
1.3 PV grid integration.....	4
1.4 Problem statement.....	5
1.5 Project objective and research questions .....	7
1.6 Research approach .....	7
1.7 Watt connects.....	8
1.8 Thesis outline.....	8
<b>2 Regulations.....</b>	<b>11</b>
2.1 General .....	11
2.2 Voltage requirements.....	12
2.2.1 Supply voltage variations .....	12
2.2.2 Flicker .....	12
2.2.3 Voltage dips/swells.....	13
2.2.4 Voltage unbalance.....	13
2.3 Power factor - Reactive power capability.....	14
2.4 Active power curtailment .....	15
<b>3 Voltage rise and mitigation solutions.....</b>	<b>17</b>
3.1 Voltage rise in a LV feeder.....	17
3.2 Solutions to voltage rise problem.....	18
3.2.1 Grid reinforcement.....	18
3.2.2 MV/LV transformers with OLTC .....	19
3.2.3 Reactive power control strategies .....	20
3.2.3.1 Fixed PF .....	21

3.2.3.2	PF in terms of injected active power PF(P) .....	21
3.2.3.3	Voltage-dependent reactive power Q(V) .....	23
3.2.4	Active power curtailment (APC) .....	25
3.2.5	Storage.....	27
3.3	Categorisation of strategies based on their communication requirements .....	28
3.3.1	Local strategies .....	28
3.3.2	Decentralised strategies .....	28
3.3.3	Central strategies.....	29
<b>4</b>	<b>Simulation setup.....</b>	<b>31</b>
4.1	Rural test network model .....	31
4.1.1	External grid.....	33
4.1.2	MV/LV transformer .....	33
4.1.3	Feeders and conductor types .....	34
4.1.4	Loads, PV generators and batteries.....	35
4.2	Load model .....	35
4.2.1	“Load profile” block .....	36
4.2.2	“Load data process” block .....	37
4.2.3	“Load” block .....	38
4.3	PV-Battery system model .....	38
4.3.1	“Irradiance” block.....	39
4.3.2	“PV generation profile” block.....	40
4.3.3	“Load Profile” blocks .....	41
4.3.4	“Voltage” block.....	41
4.3.5	“Active Power Control” block.....	41
4.3.6	“Reactive Power Control” block .....	42
4.3.7	“Battery Control” block .....	45
4.3.8	“PV Generator” and “Battery” blocks.....	47
4.4	General simulation assumptions .....	47
<b>5</b>	<b>Implementation and test results .....</b>	<b>49</b>
5.1	High PV integration without voltage support.....	49
5.2	Voltage sensitivity analysis of test network .....	51
5.3	Reactive power control strategies .....	53
5.3.1	PF(P) control mode.....	56
5.3.1.1	PF(P) without storage.....	57

---

5.3.1.2	PF(P) with battery storage .....	58
5.3.2	Q(V) control mode.....	60
5.3.2.1	Q(V) without storage.....	62
5.3.2.2	Q(V) with battery storage .....	63
5.3.3	Comparison of reactive power based voltage support strategies .....	64
5.4	Dynamic active power curtailment strategies.....	68
5.4.1	DAPC without storage .....	68
5.4.2	DAPC with battery storage.....	69
5.4.3	Comparison of the DAPC voltage support strategies.....	70
5.5	Overall comparison.....	72
5.5.1	Formulation of an overall evaluation criterion .....	72
5.5.2	Relative weighting of the evaluation criteria .....	74
5.5.3	Choosing the best strategy.....	75
<b>6</b>	<b>Conclusions and future work .....</b>	<b>77</b>
6.1	Conclusions.....	77
6.1.1	Main conclusions.....	77
6.1.2	Specific findings.....	77
6.2	Recommendations for future work.....	79
	<b>Appendix A - OHL modelling.....</b>	<b>81</b>
	<b>Appendix B - DSL models' code .....</b>	<b>83</b>
	<b>Appendix C - DPL commands .....</b>	<b>85</b>
	<b>Bibliography .....</b>	<b>89</b>



# List of Figures

Figure 1.1: Conventional electric power system [2] .....	1
Figure 1.2: Connection of distributed generators [2] .....	2
Figure 1.3: Evolution of global cumulative installed capacity 2000-2013 [13] .....	4
Figure 1.4: Evolution of European PV cumulative installed capacity 2000-2012 [12] .....	5
Figure 1.5: PV contribution to the energy demand in the EU 27 in 2012 based on cumulative installed capacity in 2012 [12] .....	5
Figure 1.6: Voltage profile on an exemplary feeder with distributed generation [11].....	6
Figure 1.7: Watt connects interactive table.....	8
Figure 2.1: Evolution of the German grid codes and regulations compared with PV deployment (GW) [11].....	11
Figure 2.2: Reactive power capability in load reference frame [20].....	14
Figure 2.3: Reactive power control characteristic [20].....	14
Figure 2.4: PF(P) characteristic according to VDE-AR-N 4105 [22] .....	15
Figure 3.1: Simplified schematic of a PV generator and a load connected to a LV feeder .....	17
Figure 3.2: Phasor diagram of voltage rise calculation .....	18
Figure 3.3: Fixed PF characteristic.....	21
Figure 3.4: PF(P) characteristic.....	22
Figure 3.5: Q(V) characteristic.....	23
Figure 3.6: P(V) characteristic .....	25
Figure 3.7: Dynamic active power curtailment strategy for a feeder with 5 kW/household maximum net generation.....	26
Figure 3.8: Categorisation of voltage support strategies based on their communication requirements [15] .....	28
Figure 4.1: Single-phase diagram of the test rural network structure .....	32
Figure 4.2: External Grid element connected to the MV busbar of the transformer .....	33
Figure 4.3: Histograms and associated Weibull distribution of the average house distance for rural, village and suburban networks [47] .....	34
Figure 4.4: Household load, farm load, PV generator and battery system connected to the last terminal of the first feeder.....	35
Figure 4.5: Load frame .....	36
Figure 4.6: Example of daily household load profile.....	36

Figure 4.7: Example of farm load profile.....	37
Figure 4.8: 3-phase load model in PowerFactory.....	38
Figure 4.9: PV-Battery system frame .....	39
Figure 4.10: Weekly irradiance profile used in the simulations.....	40
Figure 4.11: Fixed PF characteristic.....	43
Figure 4.12: PF(P) characteristic.....	44
Figure 4.13: Q(V) characteristic.....	44
Figure 5.1: Voltage profile of feeder 1 under low load and high PV generation conditions (10 kW/household and 27 kW/farm) for both conductor types.....	50
Figure 5.2: Voltage profile of feeder 2 under low load and high PV generation conditions (10 kW/household and 27 kW/farm) for both conductor types.....	50
Figure 5.3: Voltage measurements for the weakest point of the network under normal load conditions and high PV integration (10 kW/household and 27 kW/farm) throughout the weekly simulation.....	51
Figure 5.4: Voltage sensitivities to P and Q variation for the terminals of feeder 1.....	52
Figure 5.5: Voltage sensitivities to P and Q variation for the terminals of feeder 2.....	53
Figure 5.6: Flowchart of the script executed to calculate the PV hosting capacity of the network for different power factors of the PV generators .....	54
Figure 5.7: Plot of the PV hosting capacity with respect to the power factor of a household PV system .....	56
Figure 5.8: Selection of the appropriate PF(P) characteristic .....	57
Figure 5.9: Comparison of the selected PF(P) characteristic with the hosting capacity limits in case of maximum PV hosting capacity .....	57
Figure 5.10: Voltage at the weakest terminal in case of PF(P) strategy without storage.....	58
Figure 5.11: Active and reactive power injection of a household PV system for a PV-integration level of 10 kW/household .....	58
Figure 5.12: Voltage at the weakest terminal in case of PF(P) strategy with battery storage.....	59
Figure 5.13: State of charge of one of the household battery systems throughout the weekly simulation.....	59
Figure 5.14: Sensitivity of Q(V) characteristic in the selection of its parameters: a) for the $V_{sp}$ parameter, b) for the $V_{max}$ parameter.....	60
Figure 5.15: Flowchart of the script executed to calculate the highest value of $V_{max}$ which allows for each PV-integration level the use of Q(V) strategy .....	61
Figure 5.16: Voltage at the weakest terminal in case of Q(V) strategy without storage.....	63
Figure 5.17: Comparison of the behaviour of Q(V) strategy at different terminals: a) daily voltage measurements, b) active and reactive power injection.....	63

---

Figure 5.18: Voltage at the weakest terminal in case of Q(V) strategy with battery storage .....	64
Figure 5.19: Weekly grid losses comparison for the reactive power control strategies .....	65
Figure 5.20: Weekly losses of all the battery systems .....	65
Figure 5.21: Maximum reactive power demand from the external grid .....	66
Figure 5.22: Difference in reactive power requirement between PF(P) and Q(V) strategies.....	67
Figure 5.23: Quality index comparison among the reactive power control strategies .....	68
Figure 5.24: Voltage at the weakest terminal in case of DAPC strategy without storage .....	69
Figure 5.25: Operation of DAPC strategy without storage for one of the PV systems connected in the network.....	69
Figure 5.26: Voltage at the weakest terminal in case of DAPC strategy with battery storage.....	70
Figure 5.27: Operation of DAPC strategy with battery storage for one of the PV systems connected in the network.....	70
Figure 5.28: Weekly grid losses comparison for the DAPC strategies .....	71
Figure 5.29: Yield losses comparison .....	71
Figure 5.30: Overview of the performance of all strategies in the evaluation criteria: a) grid losses, b) battery losses, c) maximum reactive power demand from the external grid, d) reactive power performance index and e) yield loss.....	73
Figure 5.31: Ranking of the studied voltage support strategies .....	75
Figure 5.32: OEC comparison with respect to the PV-integration level according to the DNO's perspective.....	76
Figure 5.33: OEC comparison with respect to the PV-integration level according to the PV system owner's perspective .....	76
Figure A.1: Geometry of overhead lines for a typical European LV network [48].....	81





# List of Tables

Table 2.1: Interface protection settings in case of under-voltage .....	13
Table 2.2: Interface protection settings in case of over-voltage .....	13
Table 3.1: Operational intervals of PF(P) characteristic.....	22
Table 3.2: Parameters of PF(P) characteristic .....	22
Table 3.3: Operational intervals of Q(V) characteristic.....	24
Table 3.4: Parameters of Q(V) characteristic .....	24
Table 4.1: MV equivalent network parameters .....	33
Table 4.2: Transformer characteristics .....	33
Table 4.3: Characteristics of the conductors available in the model .....	34
Table 4.4: Line segments of the feeders and their corresponding lengths .....	35
Table 4.5: Inputs of "Load data process" block.....	37
Table 4.6: Parameters of "Load data process" block .....	38
Table 4.7: Solar irradiance data parameters [55] .....	39
Table 4.8: Inputs of "Active Power Control" block.....	41
Table 4.9: Parameters of "Active Power Control" block .....	41
Table 4.10: Outputs of "Active Power Control" block.....	42
Table 4.11: Inputs of "Reactive Power Control" block.....	42
Table 4.12: Reactive power based control strategy selection .....	43
Table 4.13: Parameters of "Reactive Power Control" block .....	43
Table 4.14: Inputs of "Battery Control" block.....	45
Table 4.15: Parameters of "Battery Control" block .....	45
Table 5.1: Transformer and conductor loading for the worst case conditions (low load – high PV generation).....	50
Table 5.2: PV hosting capacity of the network for the range of permitted power factors of the PV generators .....	55
Table 5.3: PV hosting capacity with respect to $V_{max}$ parameter.....	62
Table 5.4: Selection of $V_{max}$ parameter for different PV-integration levels .....	62
Table 5.5: Differences of evaluation criteria.....	72
Table 5.6: Relative weights of the evaluation criteria .....	74
Table A.1: Characteristics of the OHLs used in the model [48, 60].....	81

Table A.2: Phase impedance matrix after Kron reduction ( $\Omega/\text{km}$ ) [48] .....	81
--	----

# List of Abbreviations

<b>Abbreviation</b>	<b>Meaning</b>
APC	active power curtailment
CHP	combined heat and power
DAPC	dynamic active power curtailment
DG	distributed generation (or distributed generator)
DNO	distribution network operator
DPL	DlgSILENT programming language
DSL	DlgSILENT simulation language
DSM	demand side management
DSO	distribution system operator
EN	European norm
FiT	feed-in tariff
GMR	geometric mean radius
HV	high voltage
HVDC	high voltage direct current
IEC	international electrotechnical commission
LV	low voltage
MV	medium voltage
OEC	overall evaluation criterion
OHL	overhead line
OLTC	on-load tap changer
PCC	point of common coupling
PF	power factor
PV	photovoltaic
QC	quality concept
RES	renewable energy sources
RMS	root mean square
STC	standard test conditions
TSO	transmission system operator
VDE	verband der elektrotechnik
VDEW	verband der elektrizitätswirtschaft



# Acknowledgments

First of all, I would like to express my gratitude to Peter Vaessen, and by extension DNV GL, for the continuous guidance and monitoring throughout the completion of this thesis as well as for the opportunity I was given to work on Watt connects project. Furthermore, I would like to express my appreciation to my TU Delft supervisor, Pavol Bauer, for his trust and support.

Special thanks should be given also to my family for its endless support throughout these years. Last but not least, I would like to thank Aspa for her patience and support.



# Chapter 1

## Introduction

### 1.1 Electric power systems and distributed generation history

Originally, public electricity supply was developed in the form of local generation feeding local loads. The first complete electric power system was built by Thomas Edison; the historic Pearl Street Station in New York city that served a number of factories, residences and street lighting [1]. Thereafter, more individual small power systems were being built and operated by independent companies providing electricity to a limited geographic region [2]. The systems were isolated, without connections among them [3]. During the early years, up to around 1930, this proved quite sufficient. However, it was then recognised that an integrated system was needed to ensure an electricity supply that was both reasonably secure and economic. Improved security resulted from the mutual emergency assistance that electric companies (often called utilities) could provide. Improved economy resulted from the need for less generating reserve capacity on each system [4].

It did not take very long for electric companies to realize that economies of scale caused a dramatic lowering of costs [5]. An economy of scale simply means that it tends to be less expensive to build and operate one large generator than several smaller ones [1]. This led to large centrally located generators, built in areas close to large water reservoirs or near available fuel supply routes.

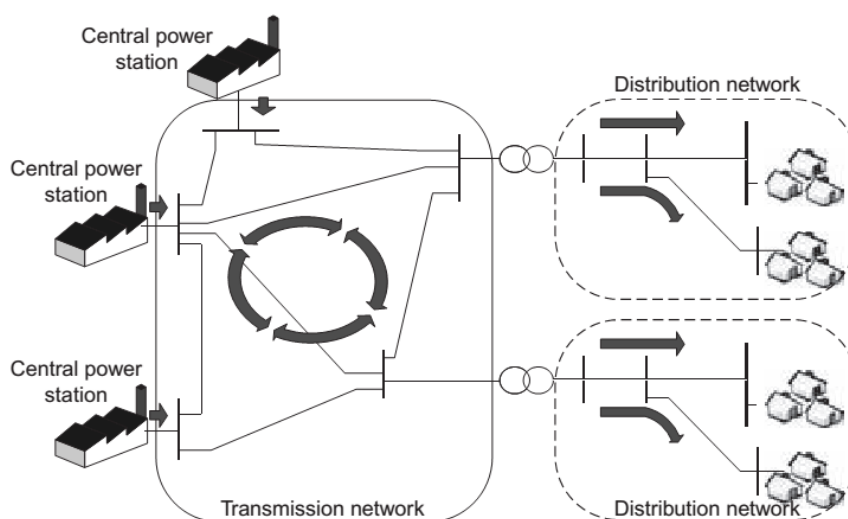


Figure 1.1: Conventional electric power system [2]

As the electricity demand was increasing so did the need for transmitting larger amounts of power over longer distances creating an incentive to use progressively higher voltage levels in order to reduce current flow and therefore resistive losses in the lines [4]. Soon the familiar

power system structure was formed, generally split up into three parts: generation, transmission and distribution (Figure 1.1). The transmission system interconnects all major generating stations and main load centres in the system. It forms the backbone of the integrated power system and operates at the highest voltage levels. Large industrial customers are often supplied directly from the transmission system. The distribution system is the final stage in the transfer of power to the individual customers and it is usually operated at medium and low voltage levels [4].

However, from around 1990, there has been a revival of interest in smaller generating units mainly based on renewable energy technologies and this has come to be known as distributed generation (DG). The term describes electric power generation that is geographically distributed or spread out across the grid, generally smaller in scale than traditional power plants and located closer to the load, often on customers' property [1].

There are various reasons for introducing these new types of production into the power system. First, the open electricity market, which has been introduced in many countries since the early '90s, has made it easier for new players to enter the market. Second, in order to cope with the environmental impact of conventional power plants and reduce the greenhouse gas emissions the interest in renewable energy sources, such as sun and wind, is growing. Third, the margin between the highest consumption and the likely available production is getting rather small for some regions or countries. Building large conventional power stations is not always politically acceptable for, among others, environmental reasons. It also requires large investments and can take 10 years or longer to complete. Small-scale generation based on renewable sources of energy does not suffer from these limitations. The total costs may be higher, but as the investments can be spread over many owners, the financing may actually be easier [6].

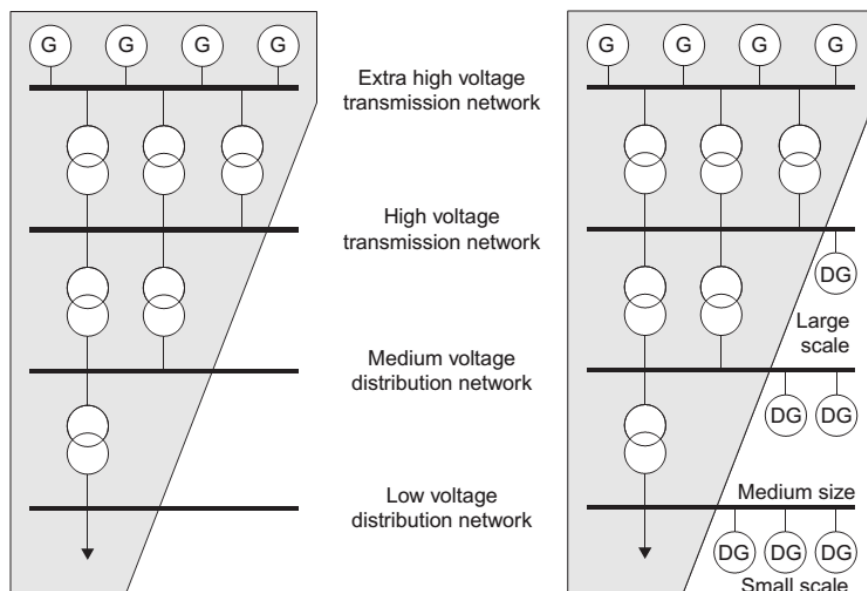


Figure 1.2: Connection of distributed generators [2]

Distributed generation may be connected at a number of voltage levels from 120/230 V to 150 kV. Only very small generators may be connected to the lowest voltage networks, but large



installations of some hundreds of megawatts are connected to the busbars of high voltage transmission systems (Figure 1.2) [2].

A wide variety of generating plant types is being connected to the medium and low voltage distribution networks. Examples include the well-established technologies of small-scale hydro generation, combined heat and power (CHP), wind turbines and PV systems, with the latter being the centre of interest in this thesis.

## 1.2 Photovoltaic systems

Solar energy conversion into electricity takes place in a specially treated semiconductor device that is called a solar cell. A solar cell is a unit that delivers only a certain amount of electrical power. In order to use solar electricity for practical devices, which require a particular voltage or current for their operation, a number of solar cells has to be connected together to form a solar panel (also called PV module or PV panel). For higher generation PV panels are connected together to form PV arrays [7].

Solar panels are only a part of a complete PV system. Their produced energy is transferred to the load or to the electric grid by means of a subsystem that is generally referred to as the “balance of system” (BOS). It encompasses all components of a PV system other than the PV panels and may include the following [8, 9]:

- supporting structures for mounting PV modules
- power conditioning units, that adjust and convert the produced DC power to AC power (inverters)
- cables and protection devices, that allow a safe passage for current
- storage devices that store PV generated electricity to be used when generation is not sufficient

For many years, the major application of PV systems was off-grid for high-value, small electric loads that were a long way from the nearest distribution network (e.g. vaccine refrigerators and remote communication systems). PV systems have also been used as a power source for satellites and space vehicles [3]. More recently, stimulated by financial support incentives, such as Feed-in-Tariffs (FiT), their use as grid-connected distributed generators has increased dramatically.

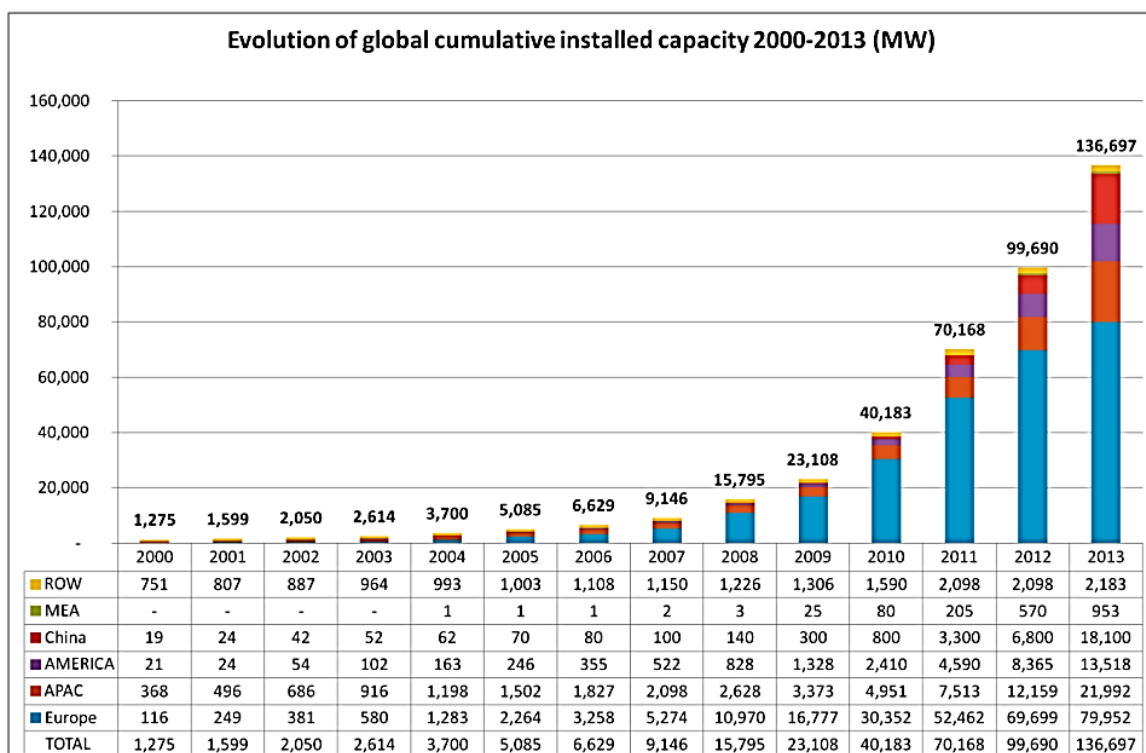
Most solar PV systems are installed on homes and businesses in developed areas. By connecting to the local electricity network, owners can sell their excess or total energy production, feeding it back into the grid. When solar energy is not available, electricity can be drawn from the grid. Under a FiT regime, the owner of the PV system is paid by the local electricity provider for the electric energy generated [10]. The photovoltaic modules may be roof mounted or incorporated into the fabric of buildings in order to reduce overall cost and space requirements. Thus, these PV installations (typically from 1 to 100 kW) are connected directly at customers' premises and so to the LV distribution network [2].

Large PV systems, with a capacity of hundreds of kilowatts (kW) to several megawatts (MW), are usually connected in the MV distribution network. The solar panels of these systems are usually

mounted on frames on the ground. However, they can also be installed on large industrial buildings such as warehouses, airport terminals or railway stations.

### 1.3 PV grid integration

Until recently, the PV market has been assisted in its development by financial support schemes, such as Feed-in-Tariffs which have proven to be the most effective [11]. As a result, installations of PV systems have grown over the past decade at a remarkable rate, even under difficult economic circumstances (Figure 1.3). The majority of these PV systems are connected to the grid, with off-grid ones accounting for less than 1 % of the installed PV capacity in Europe [12]. Europe remains the world's leading region in terms of cumulative installed capacity, with almost 80 GW as of 2013. This represents about 60 % of the world's cumulative PV capacity [13].



Source: EPIA

ROW: Rest of the World. MEA: Middle East and Africa. APAC: Asia Pacific.

Figure 1.3: Evolution of global cumulative installed capacity 2000-2013 [13]

Europe's market development is the result of a few countries that have taken the lead year after year, with Germany showing a constant commitment from policymakers to support the development of PV. Together with Italy the two countries have the largest portion of the European installed PV capacity (Figure 1.4). Based on the capacity installed and connected to the grid at the end of 2012, PV can currently provide a significant share of Europe's electricity mix, covering 2.6 % of the demand (Figure 1.5) and roughly 5.2 % of the peak demand [12]. The increasing shares of PV electricity in the European energy mix is one of many factors that will require modifications in the electricity system at national and European levels [11].

Evolution of European PV cumulative installed capacity 2000-2012 (MW)

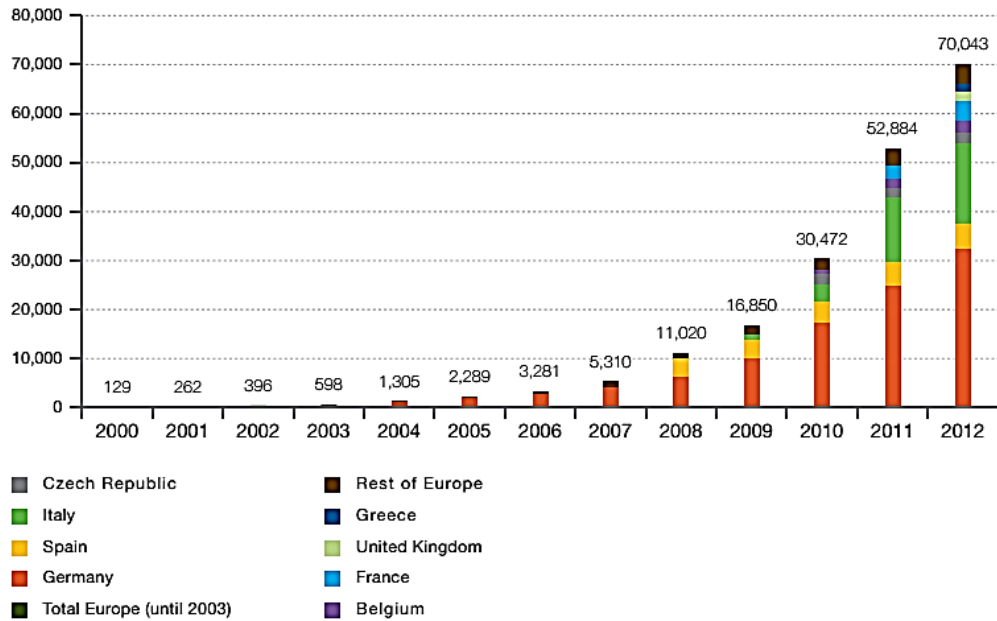


Figure 1.4: Evolution of European PV cumulative installed capacity 2000-2012 [12]

PV contribution to the electricity demand in the EU 27 in 2012\* (%)

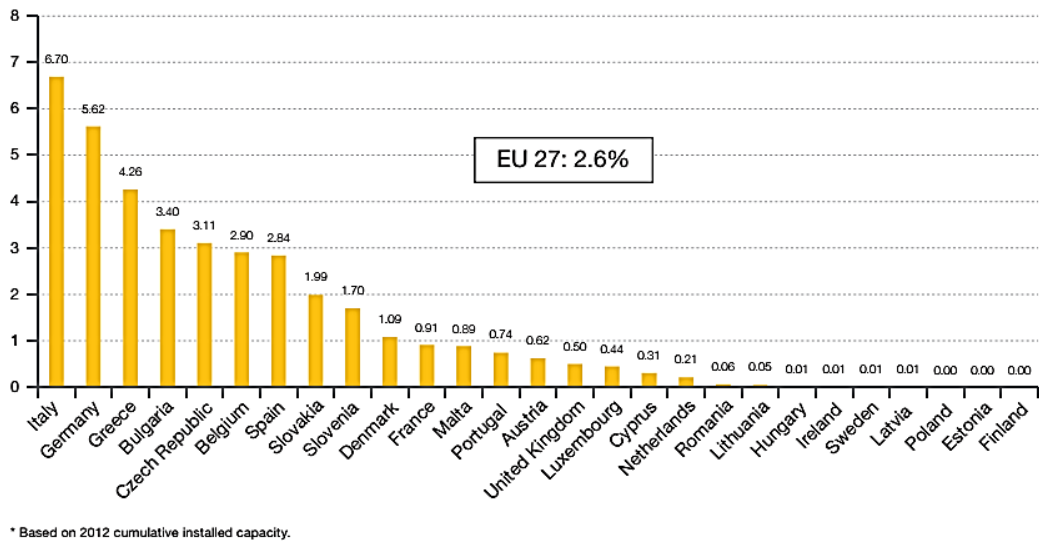


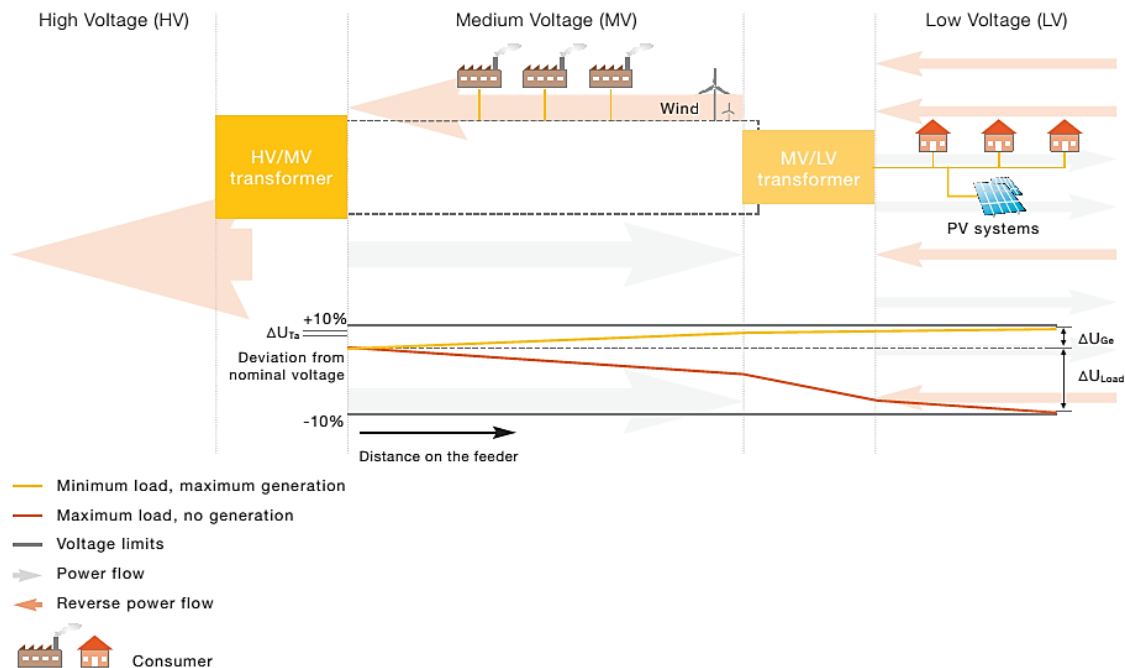
Figure 1.5: PV contribution to the energy demand in the EU 27 in 2012 based on cumulative installed capacity in 2012 [12]

### 1.4 Problem statement

The continuously increasing installation of distributed photovoltaics in residential areas around the world calls for detailed assessment of distribution grid impacts. Both photovoltaic generation and domestic electricity demand exhibit characteristic variations on short and long time scales

and are to a large extent negatively correlated, especially at high latitudes (where electric cooling devices are rarely used during midday hours in contrast with regions of lower latitudes). With a more extensive integration of PV systems in residential areas, it is important to assure that power quality and end-user voltages are not negatively affected [14].

On a distribution feeder, when the power consumed is lower than the power produced, a reverse flow occurs. The electricity flows from the distributed generation to other consumers or to higher voltage levels (Figure 1.6). As the distribution grid has not been built to host distributed generation, reverse power flows introduce some issues that must be tackled. The reverse flows may create grid bottlenecks that lead to voltage problems (voltage rise and possible excess of the upper voltage limit) or equipment (lines or transformers) overload [11]:



source: EPIA, based on AIT and E.ON Bavaria analysis, 2011

Figure 1.6: Voltage profile on an exemplary feeder with distributed generation [11]

Voltage rise represents one of the main impacts of distributed generation [11]. In the case of weak and/or long networks, voltage rise is common in times of low consumption and high power feed-in by DG (Figure 1.6). Therefore, the possibility of upper voltage limit violation may limit the PV-integration in a distribution network.

It is common to classify distribution grids in two different categories: urban and rural. Urban grids supply many households in a small area; the transformer capacity and the number of consumers powered are high and the length of the line is short. Rural grids are characterised by much longer lines with lower transformer capacity and a lower number of powered households. Overvoltage problems due to PV are virtually non-existent in urban networks as they are characterised by a greater load and less space for PV. In rural grids, however, overvoltages are more probable due to the longer line lengths and larger available space for PV installations [11].

As mentioned before, most PV systems are connected to the LV distribution network. In Germany, for example, about 70 % of the installed PV capacity is connected to the LV grid. South German distribution grids, with a high concentration of PV systems, already experience grid-integration challenges related to PV. In some LV grids, the installed PV capacity can even exceed the peak load by a factor of ten [15].

Taking into account the facts presented so far, the problem, which constitutes the motivation of this project, is defined as follows:

*“Voltage rise in a rural LV network with high PV penetration”*

The problem has to be solved so as to simplify the integration of more RES in the power systems and achieve a sustainable future energy supply.

### **1.5 Project objective and research questions**

Aiming to achieve higher levels of PV integration by mitigating the voltage rise problem, new studies, directives and standards demand from PV systems connected to the LV network to be able to support the local voltage either by the provision of reactive power or by active power curtailment.

The objective of this project is to test a selection of the suggested local voltage support strategies and check their attributes, for a range of PV-integration levels, in a typical rural LV network model. A series of research questions need to be answered:

- i. What are the characteristics of a typical rural LV network?
- ii. What are the PV-integration limits of such a network and how much can they be increased with the studied voltage support strategies?
- iii. What are the impacts of the studied voltage support strategies on grid operation and how these depend on the PV-integration level?
- iv. How these impacts are influenced by the inclusion of battery storage in the PV systems?
- v. Which strategy is the best candidate from the viewpoint of a DNO and a PV system owner?

### **1.6 Research approach**

The research approach is based on the following steps:

- i. study of current regulations regarding the connection of DG in a LV network
- ii. study of the suggested voltage support strategies in literature
- iii. design of the appropriate network, load and PV-Battery system models
- iv. execution of a series of load flow calculations and simulations
- v. analysis of the results
- vi. comparison of the studied strategies based on a set of technical evaluation criteria
- vii. weighted rating of the evaluation criteria by experts
- viii. estimation of the best voltage support strategy

## 1.7 Watt connects

Watt connects is a demonstration project on smart grids, initiated by three main partners, DNV GL (formerly DNV KEMA), Alliander and TenneT. It consists of an interactive demonstration table and simulation tools that create insight and enable new models, smart grid technologies and research results to be tested, validated and presented to stakeholders. The most important reason for using this procedure is to reduce the risk that a component, system or even an entirely new technology fails, before it is used in the real world [16].

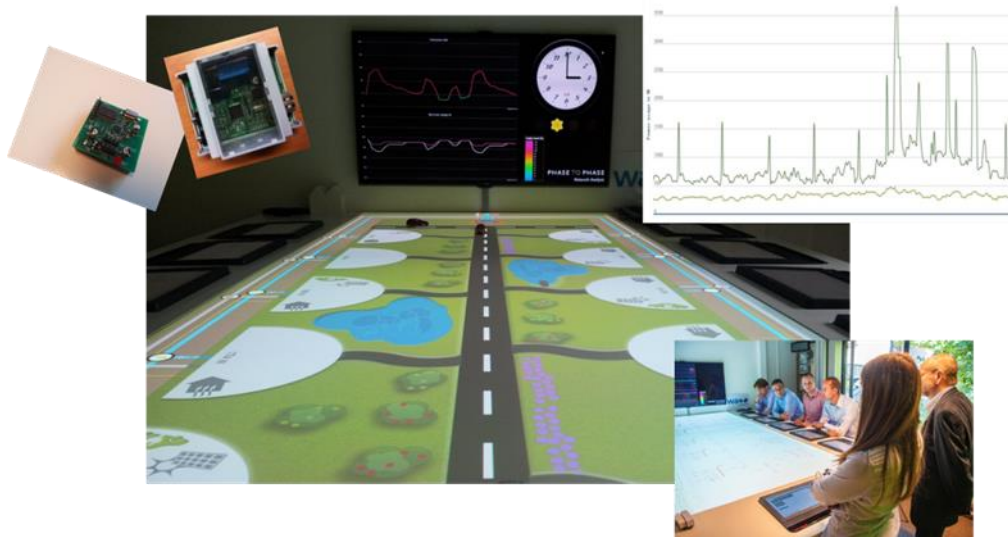


Figure 1.7: Watt connects interactive table

So far, simulations of power flows on the demonstration table for LV distribution networks, which incorporate DG, have shown that, under specific conditions, severe over or under-voltages can occur in the grid. One of the objectives of DNV GL, is to develop control algorithms that can minimize problematic changes to voltage levels. Therefore, the objective of this research is well suited in the Watt connects project and the validation of its results constitutes one of the company's future goals.

## 1.8 Thesis outline

Chapter 1 starts with a brief introduction on the transition electric power system is facing due to the increasing penetration of DG. After a presentation of PV systems and the evolution of their grid integration, the research problem is stated and the objective of the project as well as the research questions and approach are defined.

Chapter 2 presents the requirements, set by the new regulations, regarding the connection of distributed generators, such as PV systems, in the LV network.

Chapter 3 analyses the voltage rise problem and investigates the main voltage support strategies which appear in literature as well as in new DG connection standards. Then, it categorises the strategies based on their communication infrastructure requirements.

---

Chapter 4 presents the details used for the design of the LV network, load and PV-Battery system models. It finishes with a list of the assumptions been made.

Chapter 5 starts with an investigation whether the voltage rise problem is the limiting factor for further PV integration in the LV network model. After an estimation of the PV-integration limits without voltage support, it implements the selected voltage support strategies and tests their attributes as the PV-integration level increases. Then, a comparison of the tested strategies follows.

Chapter 6 ends the thesis report with the conclusions drawn from this research project and outlines the recommendations for possible future work





## Chapter 2

# Regulations

### 2.1 General

Distribution grids must be managed to maintain the voltage level within specified limits and deliver a high quality of power. Consumer electrical appliances are able to work only within certain margins for voltage and frequency. To avoid their degradation, system operators have to ensure that every consumer has access to secure and quality electricity [11].

In the past, system operators did not consider PV to be relevant for the electricity system. As a result, they required every installation to switch off automatically and instantly as soon as a grid problem (e.g. a voltage or frequency deviation) occurred. As distributed generation increased, grid operators realised that new grid codes were urgently needed. The grid codes in some countries have changed dramatically and now require that PV installations not only stay connected during grid disturbances, but also that they be able to actively support system operation. This step was being regarded more and more as absolutely necessary to guarantee reliability and quality of electricity supply [11, 17].

New requirements were introduced progressively, first for installations connected to the HV level, then to the MV level and finally to the LV grid. As an example, Figure 2.1 illustrates the evolution of requirements for PV in Germany as PV deployment was increasing.

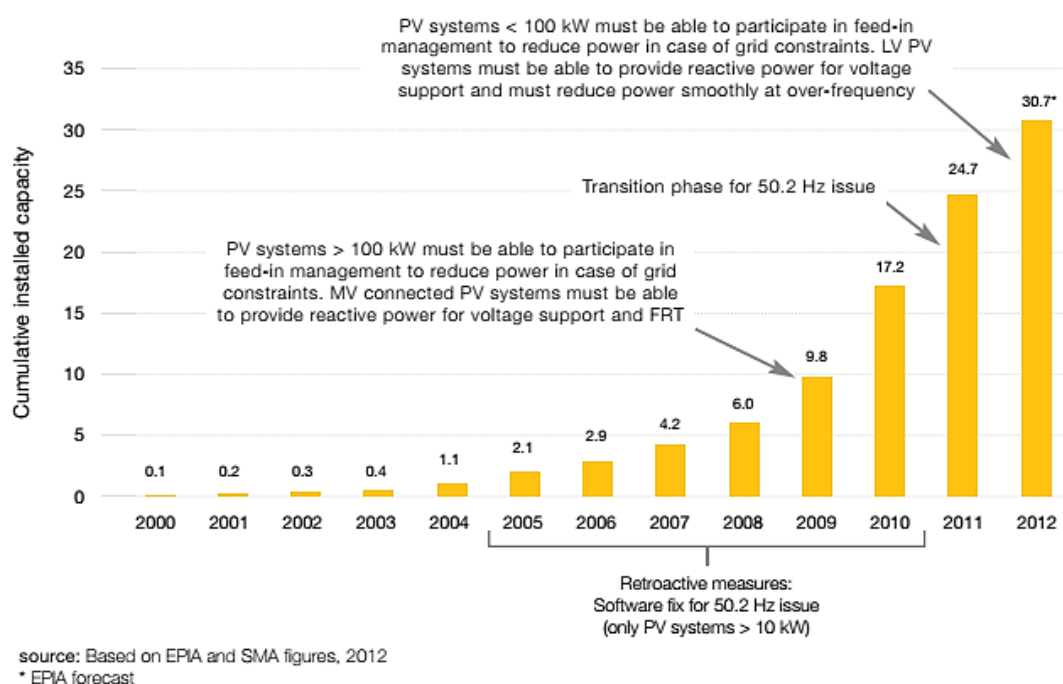


Figure 2.1: Evolution of the German grid codes and regulations compared with PV deployment (GW) [11]

Germany was one of the first European countries which adopted this new approach. Consequently, the change has also been recognised by other countries as being trend-setting for the new role that PV and distributed generation in general got to play [11, 17].

In the rest of this chapter focus is given on the German directive VDE-AR-N 4105 which PV systems connected in the LV network have to follow from 1-1-2012. In addition, references will be made to the European standards EN 50160 (Voltage characteristics of electricity supplied by public electricity networks) and EN 50438 (Requirements for micro-generating plants to be connected in parallel with public low-voltage distribution networks).

## 2.2 Voltage requirements

### 2.2.1 Supply voltage variations

According to the German directive, under normal operating conditions, the magnitude of the voltage change at every PCC of the LV network, caused by all power generating stations connected to this LV network, must not exceed the value of 3 % compared to the voltage when these generating stations were not connected.

$$\Delta V \leq 3\% \quad (2.1)$$

The European standard EN 50160 is also into force and requires the supply voltage variations not to exceed  $\pm 10\%$  of the nominal voltage  $V_n$  (for four-wire three phase systems  $V_n = 230\text{ V}$  between phase and neutral). Specifically, during each period of one week 95 % of the 10 min mean RMS values of the supply voltage shall be within the range of  $V_n \pm 10\%$  and all 10 min mean RMS values shall be within the range of  $V_n + 10\% / - 15\%$  [18].

### 2.2.2 Flicker

Voltage fluctuation causes changes of the luminance of lamps which can create the visual phenomenon called flicker. Flicker is the impression of unsteadiness of visual sensation induced by a light stimulus whose luminance or spectral distribution fluctuates with time. Above a certain threshold flicker becomes annoying. The annoyance grows very rapidly with the amplitude of the fluctuation. At certain repetition rates even very small amplitudes can be annoying [18].

The intensity of flicker annoyance, flicker severity, is evaluated by the following quantities:

- short term severity ( $P_{st}$ ) measured over a period of ten minutes with a flickermeter, a specially designed instrument to measure any quantity representative of flicker [19]
- long term severity ( $P_{lt}$ ) calculated from a sequence of twelve  $P_{st}$ -values over a two hour interval, according to the following expression:

$$P_{lt} = \sqrt[3]{\sum_{i=1}^{12} \frac{P_{st,i}^3}{12}} \quad (2.2)$$

The European standard EN 50438 as well as the German directive VDE-AR-N 4105 state that flicker created by power generating stations with rated currents lower than or equal to 16 A and

higher than 16 A but lower than or equal to 75 A per phase connected to the LV network should comply with the relevant standards EN-IEC 61000-3-3 and EN-IEC 61000-3-11 respectively [20].

Furthermore, EN 50160 requires that under normal operating conditions, during each period of one week the long term flicker severity  $P_{It}$ , caused by voltage fluctuation, should be less than or equal to 1 for 95 % of the time [18].

### 2.2.3 Voltage dips/swells

Voltage dip is defined as the temporary reduction of the RMS voltage at a point in the electrical supply system below a specified start threshold. Typically, a dip is associated with the occurrence and termination of a short circuit or other extreme current increase on the system or installations connected to it. For the purpose of EN 50160 the dip start threshold is equal to 90 % of the reference voltage and the voltage dip duration is from half cycle (10 ms) up to and including 1 min [18]. The interface protection settings required by EN 50438 and VDE-AR-N 4105 are presented in Table 2.1 [20, 21].

Table 2.1: Interface protection settings in case of under-voltage

Standard	Maximum disconnection time	Minimum operate time	Trip value
EN 50438	1.5 s	1.2 s	230 V - 15 %
VDE-AR-N 4105	0.2 s	0.1 s	230 V - 20 %

Voltage swell is defined as the temporary increase of the RMS voltage at a point in the electrical supply system above a specified start threshold. Voltage swells may appear between live conductors or between live conductors and earth. Depending on the neutral arrangement, faults to ground may also give rise to over-voltages between healthy phases and neutral. For the purpose of EN 50160 the swell start threshold is equal to 110 % of the reference voltage and the voltage swell duration is from 10 ms up to and including 1 min [18]. The interface protection settings required by EN 50438 and VDE-AR-N 4105 are presented in Table 2.2 [20, 21].

Table 2.2: Interface protection settings in case of over-voltage

Standard	Maximum disconnection time	Minimum operate time	Trip value
EN 50438	<i>stage 1</i>	3 s	-
	<i>stage 2</i>	0.2 s	0.1 s
VDE-AR-N 4105	0.2 s	0.1 s	230 V + 10 %

### 2.2.4 Voltage unbalance

Voltage unbalance is the condition in a polyphase system in which the RMS values of the line-to-line voltages (fundamental component), or the phase angles between consecutive line voltages, are not all equal. The degree of the inequality is usually expressed as the ratios of the negative and zero sequence components to the positive sequence component [18].

According to EN 50160, under normal operating conditions, during each period of one week, 95 % of the 10 min mean RMS values of the negative phase sequence component (fundamental) of the supply voltage shall be within the range 0 % to 2 % of the positive phase sequence component (fundamental).

VDE-AR-N 4115 puts a limit of 4.6 kVA to the allowed unbalance of power injection of the generating stations connected to the LV network. Hence, a maximum plant power of 13.8 kVA results when using single-phase, uncoupled inverters ( $3 \times 4.6$  kVA) only [21, 22].

### 2.3 Power factor - Reactive power capability

The requirement of the European standard EN 50438 is that the inverter based micro-generators connected to the LV network should operate, under normal steady-state operating conditions, across the statutory tolerance band of nominal voltage, between power factors of 0.9 leading and 0.9 lagging, provided the output active power of the micro-generator is above 20 % of its nominal value. When the active power output is less than 20 % of its nominal value the micro-generator should not exchange more reactive power than 10 % of its nominal active power (Figure 2.2) [20].

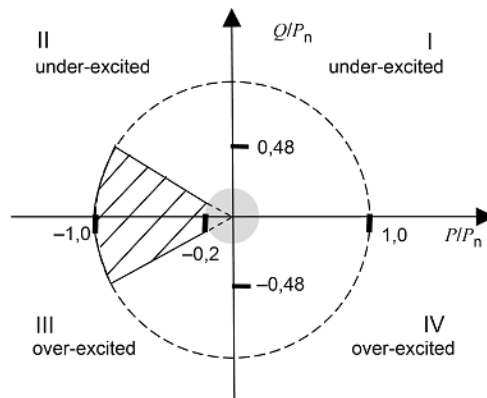


Figure 2.2: Reactive power capability in load reference frame [20]

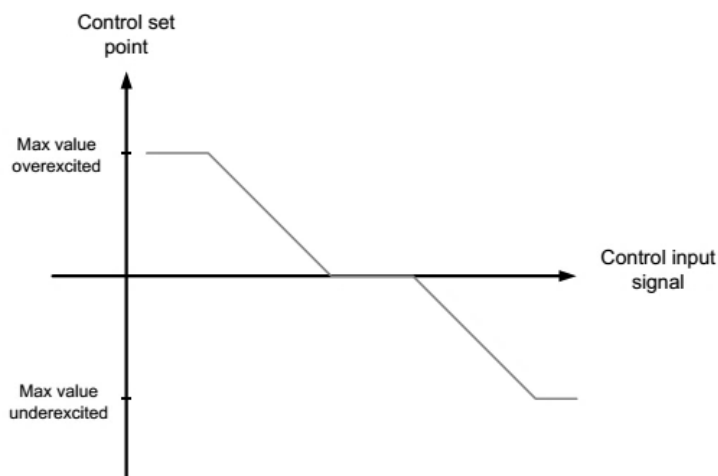


Figure 2.3: Reactive power control characteristic [20]

According to EN 50438 the reactive power control mode should be based on a configurable characteristic curve defined by the DSO (Figure 2.3). The micro-generator shall be capable of operating in the following control modes:

- Q(V), voltage dependent reactive power control
- fixed power factor (fixed PF)
- PF(P), active power dependent power factor

Additional to the characteristic, the dynamic response of the control should be configurable. The dynamics of the control should correspond with a first order filter having a time constant that is configurable in the range of 3 s to 60 s. The time to reach 95 % of a new set point due to a change in voltage will be 3 times the time constant [20].

The German directive VDE-AR-N 4105 requires from the inverters to feed in with power factors up to  $0.95_{\text{lagging/leading}}$  from an apparent plant power of 3.68 kVA whereas, if the plant power exceeds 13.8 kVA, even power factors up to 0.9 must be supported. It suggests that the fixed PF method be used in case of generators with constant active power generation, like CHPs. When it comes to generators with fluctuating generation, it recommends the use of droop-based strategies such as PF(P) and Q(V). It is also more specific in the requirements of the PF(P) characteristic (Figure 2.4).

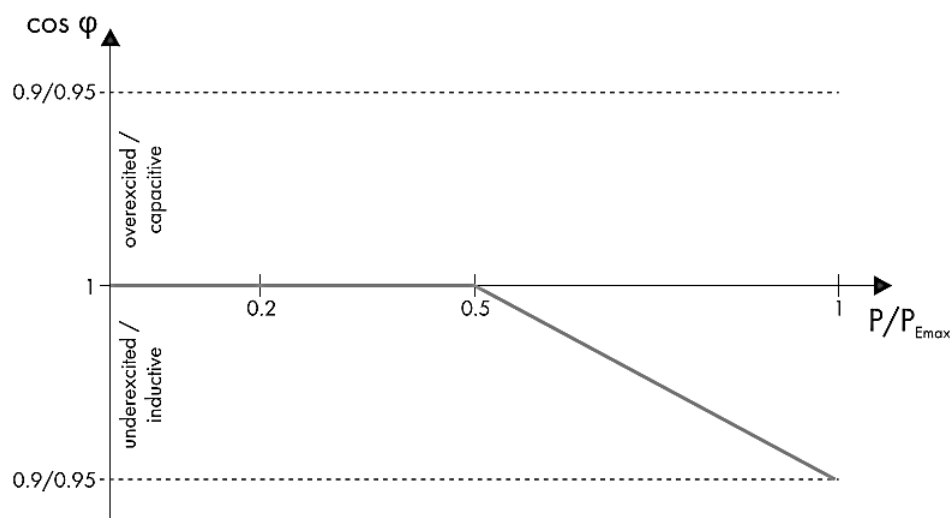


Figure 2.4: PF(P) characteristic according to VDE-AR-N 4105 [22]

The respective inverter must feed in without phase shift up to half of its nominal active power. Thereafter, it is to be steadily increased until it operates at full nominal power with the maximum power factor (underexcited) valid for the respective plant [22].

## 2.4 Active power curtailment

The distribution grid operator should also be able to remotely limit the power of PV plants in increments of no more than 10 % of the nominal power of the plant in the LV grid (in that context, proven increments are 60, 30, or 0 % of the nominal power). Among others, conceivable reasons for a power limitation include the operation of emergency generating units, a short term

overload of the superordinate medium-voltage or transmission grid or a system-endangering frequency increase. This requirement of the German directive applies to all plants with more than 100 kW of power and is otherwise comparable to that in the medium voltage directive [22].

In contrast, the Renewable Energy Sources Act (EEG), valid from the beginning of 2012, applies the remote power limitation capability also to power plants with a nominal power of less than 100 kW<sub>p</sub>. However, operators of PV plants with less than 30 kW<sub>p</sub> are given the choice to skip installing the device for remote power limitation if they accept in return a general limitation of feed-in power to 70 % of the installed generator power [22].

## Voltage rise and mitigation solutions

One of the main impacts of the high number of PV systems and other distributed generators along LV networks is voltage rise. This chapter gives a brief introduction on how PV power feed-in can influence the voltage and presents some of the solutions available to overcome the problem.

### 3.1 Voltage rise in a LV feeder

Without PV generators installed, voltage along distribution feeders would typically drop from the substation to the remote end due to line impedances and loads. With integration of PV generation, voltage profile improves as voltage drop across feeder segments reduces due to reduced power flow through the feeder. However, if PV generation is greater than the local demand at the connection point (CP) of the PV inverter, the surplus power flows back to the grid. The excess power from PV systems may produce reverse power flow in the feeder (Figure 3.1) which would create voltage rise (Figure 3.2). Typical peak time of PV generation is noon, when solar irradiance level is higher. Household demand, on the other hand, is typically lower at this time of the day. LV distribution feeder may therefore experience voltage rise resulting from low load demand and high PV generation [23].

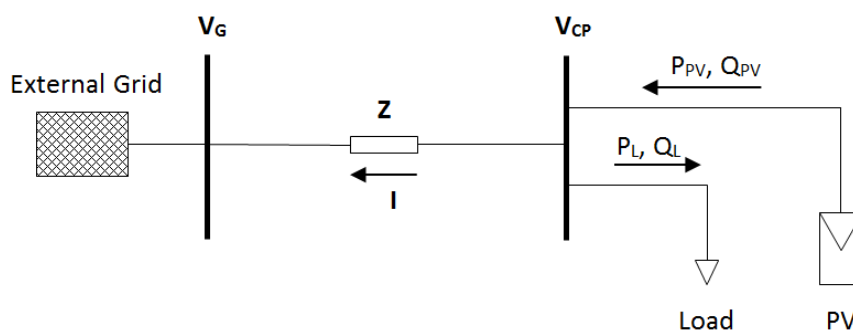


Figure 3.1: Simplified schematic of a PV generator and a load connected to a LV feeder

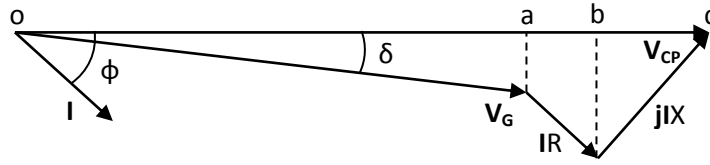


Figure 3.2: Phasor diagram of voltage rise calculation

According to Figure 3.2 and the fact that the voltage angle between  $V_G$  and  $V_{CP}$  is normally very small [24], the voltage rise along the feeder can be approximated as follows:

$$\Delta V = V_{CP} - V_G \approx oc - oa = ac = ab + bc \Rightarrow$$

$$\Delta V \approx IR \cos \varphi + IX \sin \varphi = \frac{V_{CP}IR \cos \varphi + V_{CP}IX \sin \varphi}{V_{CP}} \Rightarrow$$

$$\Delta V \approx \frac{P_{CP}R + Q_{CP}X}{V_{CP}} \approx \frac{P_{CP}R + Q_{CP}X}{V_G} \quad (3.1)$$

Where:

$$P_{CP} = (P_{PV} - P_L) = V_{CP}I \cos \varphi \quad (3.2)$$

$$Q_{CP} = (Q_{PV} - Q_L) = V_{CP}I \sin \varphi \quad (3.3)$$

$$\mathbf{Z} = R + jX \quad (3.4)$$

## 3.2 Solutions to voltage rise problem

Several solutions have been suggested until now in order to cope with the voltage rise phenomenon at high PV penetration levels in LV networks:

- grid reinforcement
- use of MV/LV transformers with on-load tap changers (OLTC)
- reactive power consumption by PV inverters
- active power curtailment
- storage

### 3.2.1 Grid reinforcement

According to equation (3.1), a decrease of the conductor impedance would result in lower voltage rise. In order to achieve that decrease, conductors with larger cross section should be used. That is actually the typical approach applied so far, prior to other solutions contributing to the voltage control, which involved increasing the grid capacity by upgrading the distribution



transformers to a larger power rating or by reinforcing the LV feeders by addition of parallel conductors or replacement of old conductors with higher ampacity ones. However, this is a rather costly procedure, especially when underground cables are used, and as a result DSOs try to avoid or postpone these costs, since network elements such as cables and transformers are by far not used up to their full capacity yet [25].

In Germany, for example, if a PV system cannot be interconnected due to technical reasons, the distribution system operator is obliged, according to German law, to conduct necessary grid reinforcement measures immediately. This is done by either replacing transformers in the grid or reinforcing certain conductors. By law, the costs for these reinforcement measures must be borne by the DSO [15].

### 3.2.2 MV/LV transformers with OLTC

According to EN 50160 the permissible voltage range for customers connected to low voltage distribution grids is  $230\text{ V} \pm 10\%$  (voltage between line and neutral). Currently, voltage regulation within the electricity grid is mainly limited to the OLTC of the HV/MV transformer. Thereby, the voltage at the MV terminals of the transformer can be adapted to current network conditions in order to keep the voltage within the permissible limits. The voltage level at the HV/MV substation is usually set up to 104 % for the high load case. So far the tap changing of a MV/LV transformer is mainly performed off-load and the voltage level may be as high as 106 % [26]. With this setting aiming to cover a high load scenario, a voltage rise of only 4 % of the nominal voltage is allowed until the upper voltage limit is reached under low load conditions and high PV generation.

An effective way of controlling the voltage can be provided by a substation which features an MV/LV transformer with OLTC. The voltage level at the LV bus of the transformer is no longer dependent on the fluctuating voltage level at the MV side, but it may be controlled, for instance, by means of a constant target value and a control range using the variable transformation ratio. A tap change is required when the control range is exceeded. In this way, the allowable voltage rise due to the feed-in of distributed generators would increase from currently 3 % up to 10 % (upper limit set by EN 50160). The usage of this wider voltage band could allow such a high increase of distributed generators that a restriction of new installation may no longer be caused by voltage band limitations but by the exceeding of the ratings of existing network elements [25].

Several OLTC control strategies exist. The more conventional ones use fixed voltage set points at the transformers LV terminal, line-droop compensation or local power flow measurements, while the more high-end ones utilize remote voltage measurement values from smart meters of connected customers. The former could save the investment and operational costs for the additional information and communication technology but may have other technical drawbacks like unintended tap settings, due to a misinterpretation of locally measured values. The latter, on the other hand, may require adaptations in the location of the measurement units when possible changes within the LV network take place [27].

Pilot projects are already under development in order to assess the efficacy of the MV/LV transformers with OLTC. In south-west Germany, for instance, a DSO has equipped one of its

rural MV/LV substations with a regulated 400 kVA transformer prototype in order to test its benefits [28]. The general results were encouraging. However, analysing the data gathered during the first weeks of operation showed that flicker problems can occur when the control algorithm makes the tap-changer switch back and forth in short succession. Still, the solution is not mature enough to be accepted as being feasible [29].

### 3.2.3 Reactive power control strategies

Going back to Figure 3.1 and equation (3.1), assuming that the maximum allowed voltage limit at the connection point has been reached, if one wishes to further increase the amount of injected active power without further increasing the voltage, the solution could be the use of a certain amount of reactive power. Assuming that grid voltage remains unchanged:

$$\frac{P_{CP}'R + Q_{CP}'X}{V_G} = \frac{P_{CP}R + Q_{CP}X}{V_G} \quad (3.5)$$

Thus, one can calculate the change of reactive power required at the connection point, to keep its voltage constant at the maximum voltage allowed, for a certain increase in the injected active power. From the equation above:

$$(P_{CP}' - P_{CP})R + (Q_{CP}' - Q_{CP})X = 0 \Rightarrow \Delta P \cdot R + \Delta Q \cdot X = 0 \Rightarrow$$

$$\Delta Q = -\frac{R}{X}\Delta P \quad (3.6)$$

From equation (3.6), one sees that as the factor  $R/X$  increases, more reactive power injection from the external grid will be required to prevent over-voltage. Thus, the effectiveness of a voltage control through reactive power management depends on the network characteristics. The more inductive the network impedance, the easier the voltage can be controlled via reactive power management [30].

A highly effective way to contribute to grid voltage support is to utilize the ability of modern PV inverters to provide or absorb reactive power while feeding active power into the network. With a reactive power consumption while active power is fed in, the voltage rise can be limited. Modern PV inverters are usually able to operate between 0.9 lagging and leading power factors. When their capacity is increased by around 11 % of their rated active power, the additional capacity can be used for absorbing reactive power from the grid in order to decrease voltage [31, 32].

Various reactive power control methods, without requiring communication infrastructure, have been proposed so far for the grid over-voltage limitation. These strategies can be mainly grouped as:

- fixed power factor (fixed PF)
- PF in terms of injected active power, PF(P)
- voltage-dependent reactive power, Q(V)

Each of these methods is defined by using either a constant value and/or first order piecewise equations that can be easily implemented in the inverter controllers and be modified even remotely [33].

### 3.2.3.1 Fixed PF

According to the German directive VDE-AR-N 4105 the fixed PF method is more suitable for generators with constant active power production, like CHPs. In case of generators with fluctuating generation, it recommends the use of droop-based strategies such as PF(P) and Q(V).

Using the fixed PF method, the absorbed reactive power is proportional to the active power. Thus, in case of PV systems, during low irradiance, the absorbed reactive power will also be as low as the active power generation, by keeping the proportionality equal (Figure 3.3). At 100 % power generation, the generator injects the maximum reactive power possible ( $Q_{lim}$ ), inductive or capacitive.

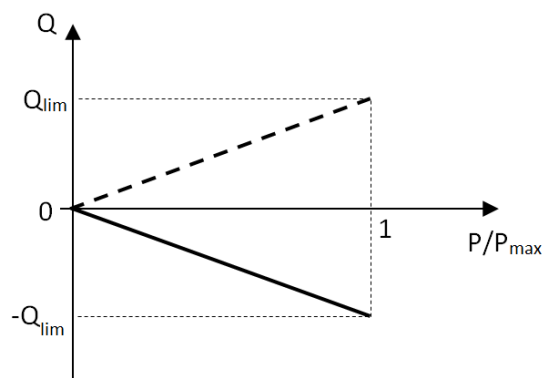


Figure 3.3: Fixed PF characteristic

### 3.2.3.2 PF in terms of injected active power PF(P)

When the power production is low, the potential risk of the grid over-voltage becomes smaller as well, since all produced real power may be consumed locally, without sending excessive power to the MV network. In this case, the reactive power injection will be unnecessary as it apparently creates additional network losses. The PF(P) method can improve this drawback using a characteristic curve such as the one presented in Figure 3.4. A power factor versus active power dependency is defined using a piecewise linear curve. The capacitive part of the curve can be considered optional when only voltage rise is the problem of interest. By adjusting the parameters of this curve the PF(P) control can be modified as required by the DSO.

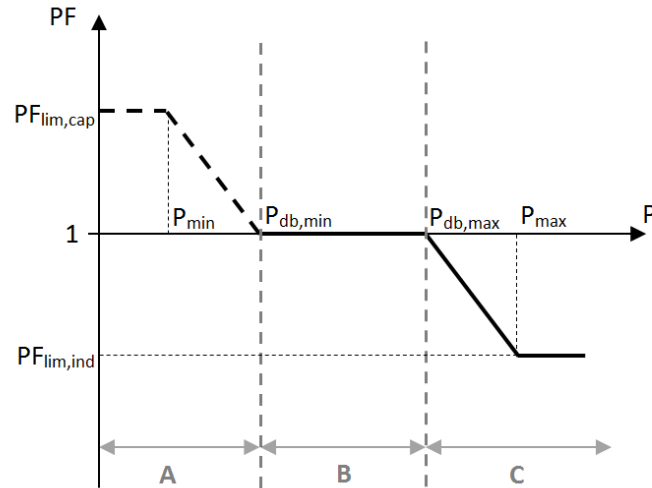


Figure 3.4: PF(P) characteristic

The operational intervals which are presented in Figure 3.4 are explained in Table 3.1.

Table 3.1: Operational intervals of PF(P) characteristic

Interval	Description
A	Capacitive operation of the PV inverter; the main objective is to increase the mains voltage.
B	Dead-band in which the controller is not injecting reactive power for a predefined power range.
C	Inductive operation of the PV inverter; the objective is to decrease the mains voltage.

The relevant parameters which define the PF(P) curve are explained in Table 3.2:

Table 3.2: Parameters of PF(P) characteristic

Parameter	Description
$P_{min}$	Active power threshold below which the PV inverter should operate with the minimum capacitive power factor.
$P_{db,min}$	Minimum active power of dead-band interval. For lower active power values overexcited (capacitive) inverter operation is chosen while for higher values the PV inverter does not inject any reactive power.
$P_{db,max}$	Maximum active power of dead-band interval. For lower values the PV inverter does not inject reactive power while for higher values the underexcited (inductive) inverter operation mode is chosen.
$P_{max}$	Active power threshold above which the PV inverter should operate with the minimum inductive power factor.
$PF_{lim,cap}$	Minimum (capacitive) power factor value that the PV inverter operates.
$PF_{lim,ind}$	Minimum (inductive) power factor value that the PV inverter operates.

One property of this type of control is that inverters will inject reactive power regardless of the location in the feeder. Since all inverters in the network are taking part, an overall better control of the voltage is assumed. However, it may still be the case that the inverters might inject reactive power to the network even though it may not be required (no significant voltage drop or voltage rise situation).

### 3.2.3.3 Voltage-dependent reactive power Q(V)

The methods given so far support the grid voltage indirectly by using only local active power measurement as input. In all these methods, it is assumed that the grid voltage level increases with the produced active power from PV inverters, regardless of load variation. Nevertheless, when the high irradiance level coincides with a significant power demand, then simply the voltage rise may not reach to the critical value. The Q(V) method directly uses local voltage information that is a consequence of the power production and consumption in the neighbourhood [33]. This control needs to take also into account the standard tap changer position of the MV/LV transformer.

The Q(V) control is normally implemented as in Figure 3.5. A reactive power versus voltage dependency is defined using a piecewise linear curve. The optionally dead band, commonly used in medium voltage applications, allows for a delay of reactive power injection in favour of active power yield but can also be omitted [34]. The voltage at the inverter bus terminals is used as an input value to the controller. This voltage may be computed as the averaged RMS value of the three phases and expressed in per unit system. A low pass filter is added to the controller in order to increase stability by making the controller slower (e.g. the inverter will not interact with faster automatic voltage regulators) [29].

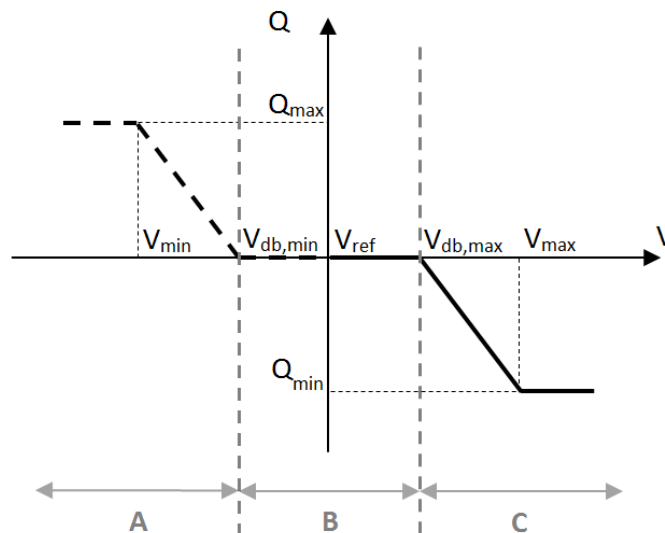


Figure 3.5: Q(V) characteristic

Analysing the Q(V) curve there are several defining parameters and intervals as shown in Figure 3.5. The operational intervals defined are explained in Table 3.3.

Table 3.3: Operational intervals of Q(V) characteristic

Interval	Description
A	Capacitive operation of the PV inverter; the main objective is to increase the mains voltage.
B	Dead-band in which the controller is not injecting reactive power for a predefined voltage range.
C	Inductive operation of the PV inverter; the objective is to decrease the mains voltage.

The relevant parameters shown in the figure above are explained in Table 3.4:

Table 3.4: Parameters of Q(V) characteristic

Parameter	Description
$V_{\min}$	Voltage threshold below which the controller should apply maximum capacitive reactive power at the inverter's terminals.
$V_{\text{db},\min}$	Minimum voltage of dead-band interval. For lower voltages overexcited (capacitive) inverter operation is chosen while for higher values the PV inverter does not inject any reactive power.
$V_{\text{db},\max}$	Maximum voltage of dead-band interval. For lower values the PV inverter does not inject reactive power while for higher values the underexcited (inductive) inverter operation mode is chosen.
$V_{\text{ref}}$	Reference voltage for dead-band selection. This parameter is chosen according to the selected output voltage of the MV/LV transformer at the secondary side (LV side) and in accordance with the voltage tap-setting. This parameter has no other purpose but to correctly determine suitable values for $V_{\text{db},\min}$ and $V_{\text{db},\max}$ .
$V_{\max}$	Voltage threshold above which the controller should apply minimum (inductive) reactive power at the inverter's output terminals.
$Q_{\min}$	Minimum reactive power generated by inverter. This parameter refers to the underexcited reactive power operation of the inverter. The value can reach up to the maximum underexcited reactive power capability of the inverter.
$Q_{\max}$	Maximum reactive power generated by inverter. This parameter refers to the overexcited reactive power operation of the inverter. The value can reach up to the maximum overexcited reactive power capability of the inverter.

Parameter  $V_{\text{ref}}$  may be chosen based on the rated PCC voltage and the position of the tap changer on the MV/LV transformer.

The parameters  $V_{\min}$  and  $V_{\max}$  are usually chosen depending on the applicable lower and higher voltage limits of the inverters. According to EN 50160 the 10 min mean RMS values of the supply voltage should not to exceed  $\pm 10\%$  of the nominal voltage  $V_n$ . When PV inverters are needed to comply also with the German directive VDE-AR-N 4105, an additional limitation must be taken

into account. The value of  $V_{\max}$  should be selected in such a way that the voltage change at the PCC must not exceed 3 % compared to the voltage when distributed generating stations were not connected.

Parameters  $V_{\text{db,min}}$  and  $V_{\text{db,max}}$  are defining the width of the voltage dead-band in which the Q(V) control should not generate any reactive power. This region should restrict the inverters injecting unnecessary reactive power when small variations, around the nominal prescribed value, are present at the LV side of the distribution transformer. A too broad dead-band could also have negative effects, since inverters closer to transformer station might not participate at all in regulating the voltage, while inverters at the remote ends would provide maximum reactive power.

### 3.2.4 Active power curtailment (APC)

Reactive power control may result in higher currents and losses and also in lower power factors at the input of the feeders, especially in LV systems where voltages are less sensitive to reactive power due to more resistive feeder characteristics. In addition, the apparent power of PV inverters might have to be increased in order to provide reactive power without losing part of their active power capability when reactive power has to be injected.

At a first glance, the option of active power curtailment could be seen as very attractive from DSOs, as it postpones grid reinforcement and therefore could be considered, in some cases, as a way to increase PV integration. In Germany, as discussed in paragraph 2.4, all PV systems connected from 2012 onwards are required to provide a remote active power reduction capability. In some other countries, such as Canada, reactive power cannot be injected by inverters connected in the LV system, as it is forbidden for small power producers to interfere with voltage control of the feeder using reactive power [35]. Thus, voltage rise mitigation through reactive power absorption cannot be used in these cases.

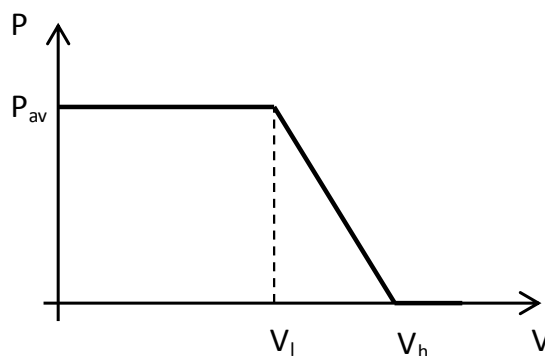


Figure 3.6: P(V) characteristic

As in LV systems the relationship between voltage and active power is stronger than that with reactive power, given the highly resistive line characteristics, droop-based APC methods have been proposed [31, 35]. They are normally implemented as in Figure 3.6.

Up to a lower voltage threshold ( $V_l$ ) no power curtailment is taking place and all the available active power ( $P_{av}$ ) is injected into the grid. When this threshold is exceeded, active power is

linearly reduced and from the time the voltage at the inverter terminals reaches the higher voltage threshold ( $V_h$ ) the PV system ceases its production [35].

The problem of this droop-based APC is that if the parameters of the P(V) curve are the same for all PV inverters in a LV network, PV owners who live at the end of the LV feeders will be the first to be affected by the curtailment while those closer to the MV/LV transformer may even not be affected at all. The specific parameterization of the curve in order to equally share the curtailed total power among all the PV owners makes this method not so easily exploitable.

To avoid unfair treatment and discrimination among PV producers a maximum guaranteed active power injection could be offered to every household connected in the LV network. This limitation could be determined for each LV network as the maximum amount of net generation per household before technical problems, such as voltage rise, start to appear. Then the PV power injection could be higher than the agreed limit by the amount of load consumption at the PCC. This dynamic active power curtailment (DAPC) strategy is presented in Figure 3.7.

Analysis conducted in France showed that for MV rural feeders a 45 % PV capacity increase could be achieved, if the loading level of the feeders were taken into account, for only 5 % loss of the maximum possible PV energy generation throughout a year. Furthermore, for the same capacity increase, this dynamic active power curtailment strategy led to one third of yearly energy losses compared to the basic limitation [36].

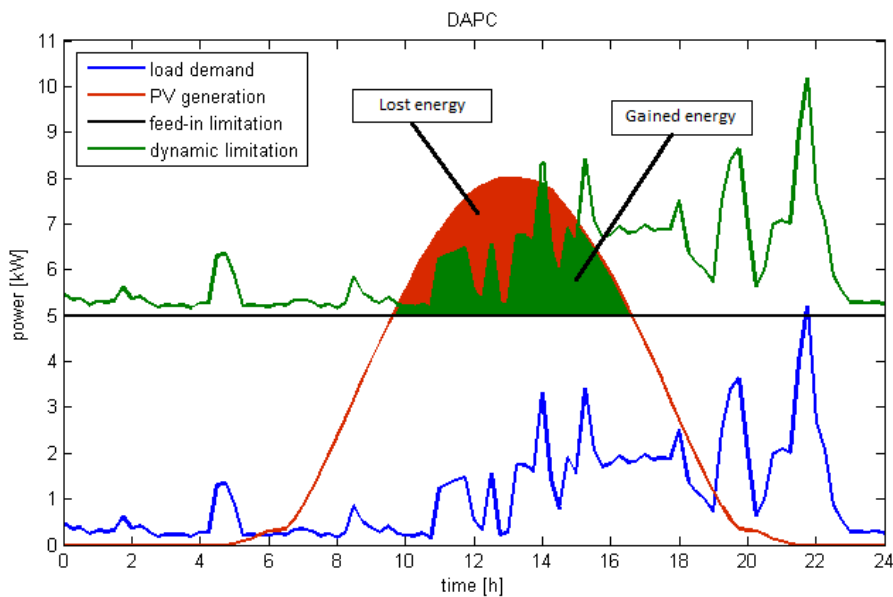


Figure 3.7: Dynamic active power curtailment strategy for a feeder with 5 kW/household maximum net generation

However, implementing such a strategy instead of reinforcing the network or allowing reactive power injection would result to the customer's decision whether to install a PV system of higher capacity or not. In order to motivate the PV system owner to install a larger PV system and produce more power than the value agreed with the DSO, self-consumption incentives could be offered. Self-consumption mechanisms have recently been promoted in several European countries. In some cases, pure net-metering schemes have been developed (such as in Belgium,



Denmark and the Netherlands), while other countries (such as Germany) have favoured mechanisms promoting an instantaneous consumption of the electricity produced [37, 38]. Either demand side management (DSM) techniques or storage solutions could lead the way to an increase in self-consumption [11, 37, 39].

### 3.2.5 Storage

For mitigating voltage rise in a LV distribution feeder with PV, energy storage options have also been proposed. The energy storage system can be a battery (bidirectional power flow) or a controllable AC load (unidirectional power flow, e.g. heat pumps) [29]. When it comes to the battery systems, two concepts in general stimulate the interest. The first concept relies on a battery system which can provide voltage support for the whole feeder from a strategically defined location while the second one is based on a number of distributed battery systems to achieve the same target, for example, one battery system on every location with PV [40].

The centralised storage concept could face the voltage rise problem directly, as charge and discharge control of the battery system could be based on voltage measurements on the most critical nodes of the LV network, where the highest voltage rise is observed. The selection of the position of this central battery system is also of major importance.

On the other hand, the distributed storage option could affect voltage rise only indirectly, as charge and discharge control would be based on the instantly available photovoltaic generation and load demand on the PCC [40]. The surplus of available PV generation can be stored in batteries, which the PV owner will have in his property, in order to use it later in the day when there would be no PV generation. In this way storage could act as the major facilitator for the development of efficient self-consumption as it would increase the local consumption of PV energy at the PCC without constraining the user in his consumption habits [41].

The difference of the concepts, regarding the direct and indirect treatment of voltage rise, lies on their incentives. The DSO would install the battery system, at a strategically defined location, so as to prevent voltage rise situations above the limit as well as to flatten the residual load curve by significantly reducing the peak demand in the evening and avoiding excess reverse power flow in the midday. In contrast, the incentive of a PV system owner to invest in the installation of batteries in his property would be the potential profit from self-consumption.

In order for the concept of distributed storage to directly tackle the voltage rise problem it should be combined either with reactive power absorption of PV inverters [40] or active power curtailment [11]. This combination could positively affect both of the aforementioned strategies.

In the first case (reactive power absorption of PV inverters), it would result in less reactive power demand by the LV network, which otherwise would rise up as the PV penetration increases. Already, utilities in the south-western United States have started to encounter power factor violations of the operating rules, laid down by the regional transmission organizations (RTO) and independent system operators (ISO) who have oversight over their systems, and may incur fines for operating their systems outside of the prescribed conditions [42].

In the second case (active power curtailment), storage would result in less PV generation being curtailed, thus higher revenue for the PV system owner and larger interest from non-owners to

install their own PV systems. This would lead to both higher PV penetration and larger rates of self-consumption in the LV networks.

The main disadvantage of the storage solution is the high cost of batteries. However, a second trend in our society is a fast increasing market share of electric and hybrid cars. This has several advantages: a massive increase in batteries will take place in the future resulting in lower prices and an additional market for used batteries will appear. Batteries of electric and hybrid cars with reduced capacity could still be usable for domestic applications [43].

### 3.3 Categorisation of strategies based on their communication requirements

Based on their communication requirements, three types of voltage support strategies can be distinguished: local, decentralized and central (Figure 3.8) [15].

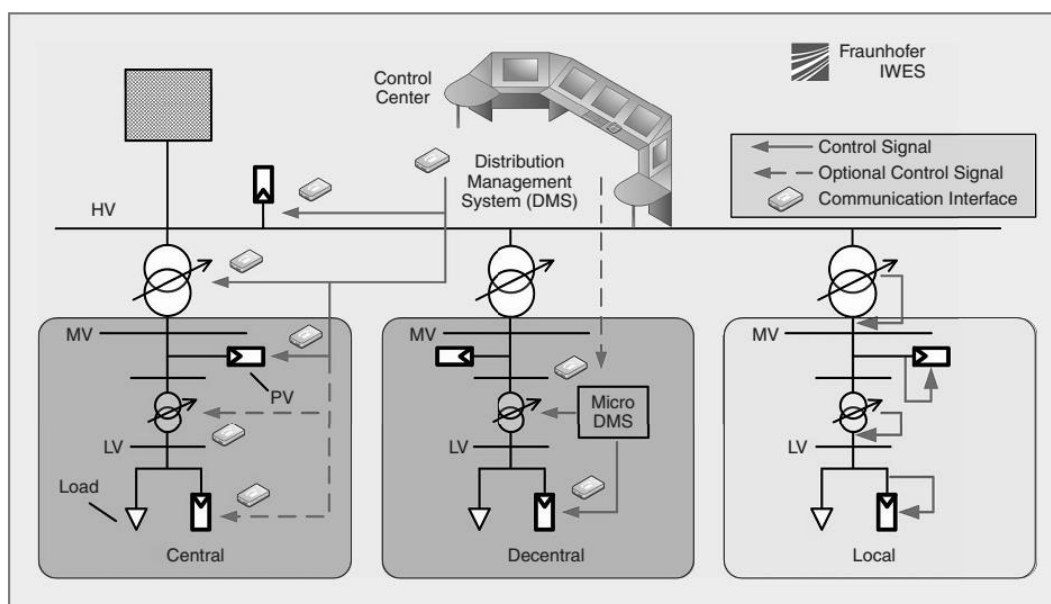


Figure 3.8: Categorisation of voltage support strategies based on their communication requirements [15]

#### 3.3.1 Local strategies

Local control strategies do not require communication devices. The distributed generator reacts to specific grid situations according to predefined parameters and droop functions, as well as measurements (e.g. voltage or frequency) at its PCC.

PV inverters connected to distribution grids, using their active and reactive power control capabilities, can contribute to lowering their impact (in terms of voltage rise) on the grid in times of high solar irradiance. They reduce the need for additional grid reinforcement measures and do not require any additional information and communication infrastructure. Therefore, local voltage control strategies can be easily integrated into the overall grid operation [15].

#### 3.3.2 Decentralised strategies

Decentralized strategies can be achieved via the coordination of several active system components, automated and without regulation by the grid control centre of the system

operator. However, not only local measurements but also an information exchange is required among single controllable entities, such as distribution substations and PV inverters, to increase overall system performance.

### **3.3.3 Central strategies**

In contrast to decentralized voltage support strategies, where subsets of the distribution system are controlled independently, central control aims for coordinated control of the complete system from the distribution system control centre. It thus requires a set of information, with which to establish the current system status, as well as knowledge of the boundaries in which the system needs to operate.

Decentralised and central approaches require significant investment in sensors, communication equipment and control systems, which makes their application to massive DG conditions difficult to implement [44]. As priority seems to be given to local voltage support strategies, in this thesis only this kind of strategies, based on measurements on the PCC of each PV-battery system, are going to be implemented and tested.



---

## Simulation setup

The voltage rise problem in a low voltage network caused by the high penetration of PV systems and the suggested local voltage support strategies, presented in chapter 3, are analysed by a series of RMS simulations as well as load flow calculations. The overall simulation model consists of three main components, which are presented in detail in the following paragraphs:

- the rural test network model
- the load models
- the PV-Battery system models

### 4.1 Rural test network model

In order to test the performance of the studied voltage support strategies in a LV distribution network, a suitable and realistic test network model has to be implemented. The focus of this thesis is on rural distribution networks because, on the one hand, the grid structures there are generally rather weak (low level of interconnection, long distances, low load density, low short circuit power) and, on the other hand, they are confronted with vast available spaces for distributed generation [45]. Moreover, rural areas often have a high percentage of farms which offer even more generous roof space for large PV arrays making the chance of violating voltage limitations even higher [46].

Based on statistical investigations of LV distribution networks in Southern Germany [47], a rural test network model is derived by appropriately selecting its characteristic parameters. Important parameters describing the electrical characteristics of LV distribution networks are [34]:

- the distance between neighbouring house connections
- the typical number of households and feeders as well as the number of households per feeder
- the transformer power per household
- the conductor type (cable, overhead line)

The test network model is implemented in DlgSILENT PowerFactory software. It consists of the external grid, a MV/LV transformer, two feeders, house and farm loads, PV generators and batteries. Figure 4.1 shows the single-phase diagram for the rural network structure.

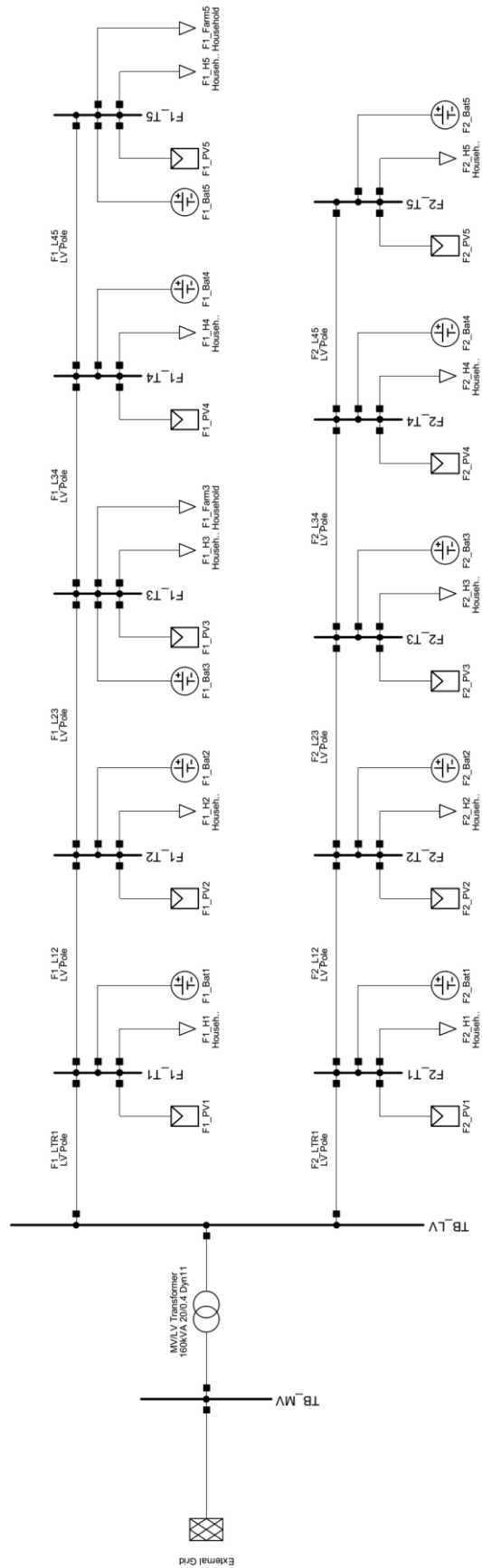


Figure 4.1: Single-phase diagram of the test rural network structure

### 4.1.1 External grid

The LV network is connected to the MV network via the transformer. The parameters of the MV equivalent network of a typical European LV network, based on the Cigre LV benchmark [48], are presented in Table 4.1.

Table 4.1: MV equivalent network parameters

<b>Nominal system voltage (line to line)</b>	20 kV
<b>Short circuit power</b>	100 MVA
<b>R/X ratio</b>	1

The same values are used for the “External Grid” element of the model (Figure 4.2).

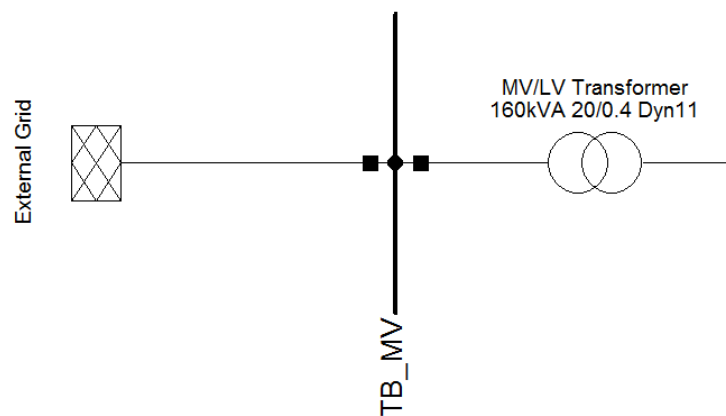


Figure 4.2: External Grid element connected to the MV busbar of the transformer

### 4.1.2 MV/LV transformer

According to a statistical analysis of the LV distribution networks in southern Germany [32, 47], the average transformer power is around 12 kVA per household. Moreover, the most common rated powers of the transformers used are 100 and 160 kVA. Based on the number of households (10) and farms (2) connected to the test network model, the selected rated power for the transformer used in the model is 160 kVA. All the characteristics of the transformer element are presented in Table 4.2 [49].

Table 4.2: Transformer characteristics

<b>Rated power</b>	160 kVA
<b>Rated voltage (primary/secondary)</b>	20/0.4 kV
<b>Short circuit voltage</b>	4 %
<b>Copper losses</b>	2000 W
<b>Iron losses</b>	200 W
<b>Connection</b>	Dyn11

### 4.1.3 Feeders and conductor types

Two feeders are connected to the LV busbar of the MV/LV distribution transformer of the rural test network model. The conductor types, which are used in Europe, can be either cables or overhead lines (OHL). More specifically, in southern Germany both types have the same share in rural LV networks [47]. Thus, either OHLs or cables can be selected in the test network model created. The characteristics of the available conductors are presented in Table 4.3. More details on OHL modelling in PowerFactory software can be found in Appendix A - OHL modelling.

Table 4.3: Characteristics of the conductors available in the model

Type	Material	Size [mm <sup>2</sup> ]	Rated current [A]	Impedance [Ω/km]	R/X impedance ratio
OHL	Aluminium	70	270	0.492 + j0.285	1.7
Cable	Aluminium	120	265	0.254 + j0.069	3.7

According to the same statistical analysis, the distance between neighbouring house connections in the case of rural LV networks in southern Germany varies between around 25 and 150 m (Figure 4.3) [47].

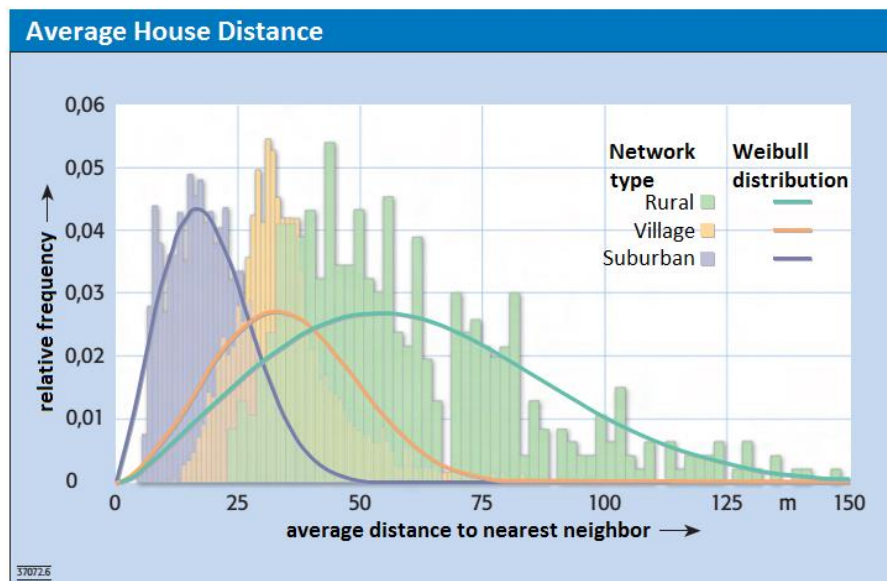


Figure 4.3: Histograms and associated Weibull distribution of the average house distance for rural, village and suburban networks [47]

The lengths of the line segments which are chosen for the test network model are presented in Table 4.4.



Table 4.4: Line segments of the feeders and their corresponding lengths

Line segment	Length [m]
F1_LTR1	20
F1_L12	60
F1_L23	80
F1_L34	80
F1_L45	80
F2_LTR1	50
F2_L12	60
F2_L23	60
F2_L34	60
F2_L45	60

#### 4.1.4 Loads, PV generators and batteries

Five households are connected to each feeder. Additionally, two farms are connected to the first feeder (upper one - Figure 4.1) on terminals 3 and 5, as shown, in more detail, in Figure 4.4. All these households and farms constitute the loads of the test network model. The load models used are further explained in paragraph 4.2.

Ten PV-Battery systems, each one connected to one of the ten PCCs available, constitute the distributed PV generation and storage of the test network model. The components, characteristics and control modes of the PV-Battery system model are further described in paragraph 4.3.

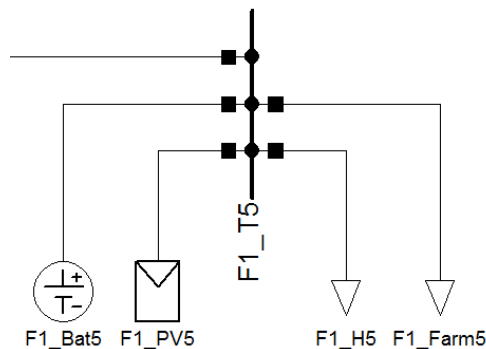


Figure 4.4: Household load, farm load, PV generator and battery system connected to the last terminal of the first feeder

## 4.2 Load model

The frame of the load model is shown in Figure 4.5. Each of its blocks is explained in the following sections.

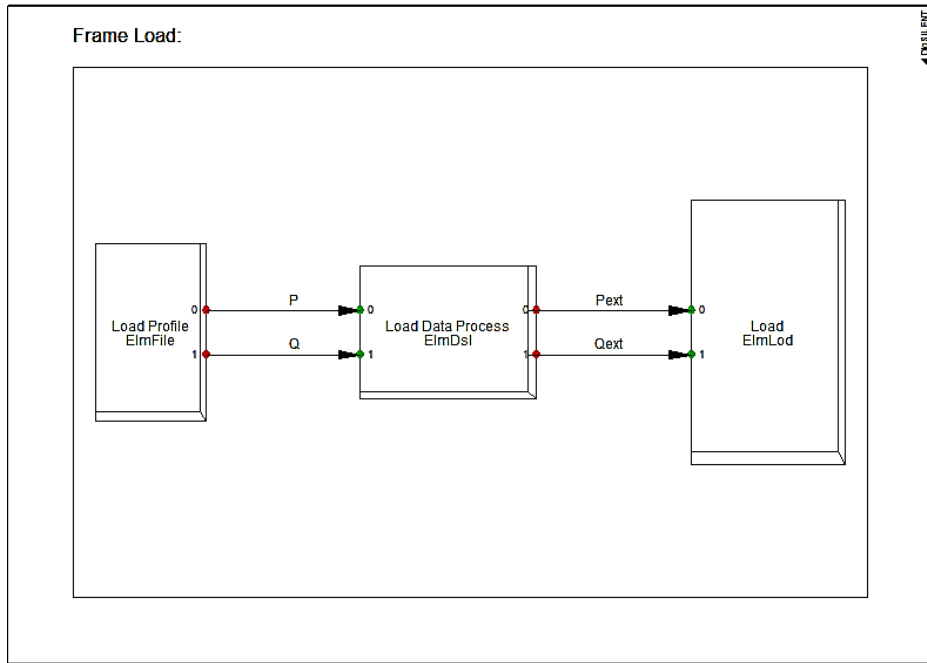


Figure 4.5: Load frame

#### 4.2.1 “Load profile” block

Measurements of electric power consumption in a household, gathered by Électricité de France (EDF) between December 2006 and November 2010, constitute the source of the load profiles used in the case of households [50]. Ten different weekly load profiles, with 15 min average values, corresponding to the summer season, were assigned randomly to the simulated household loads. Figure 4.6 presents an example of a daily load profile used.

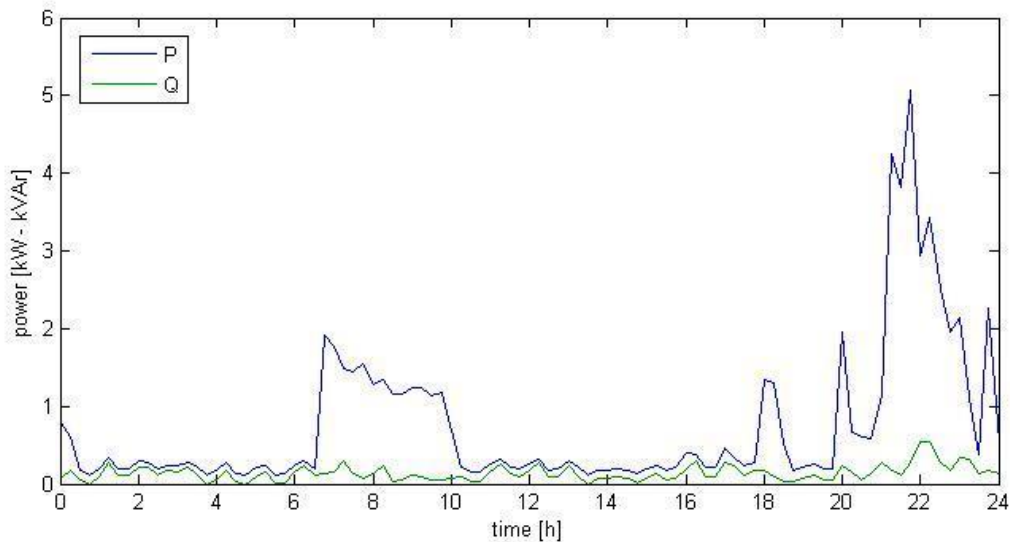


Figure 4.6: Example of daily household load profile

In the majority of the load profiles under consideration there was more intensive electricity consumption in the evening than during the day. This behaviour corresponds to families with employed adults and children going to school. These types of families constitute a high

percentage of the inhabitants in rural single family houses [51]. Thus, the load profiles used can be assumed as a good calculation basis for an important group of users of PV and PV-Battery systems in the simulation scenarios considered.

In the case of farms, daily load profiles were derived from the VDEW standard load profile for German farms, with 15 min average values [52]. Two variations were created, which slightly differ in time and peak power values, and each one was assigned to one farm load. Both farm loads were assumed inductive with a constant power factor of 0.95.

Focusing on the region of southern Germany and more specifically in Bavaria, the average herd size of Bavarian dairy farms is 30.9 cows [53]. Farms in this region have been mostly traditional family farms. Based on this traditional operation the annual energy consumption was considered high and a value of around 1,000 kWh/cow was assumed [54]. Thus the original VDEW load profile was suitably time shifted and scaled for peak load demands of 7 kW (Figure 4.7) and 8 kW, creating two different farm load profiles which correspond to an annual energy consumption of around 28,000 kWh and 32,000 kWh respectively.

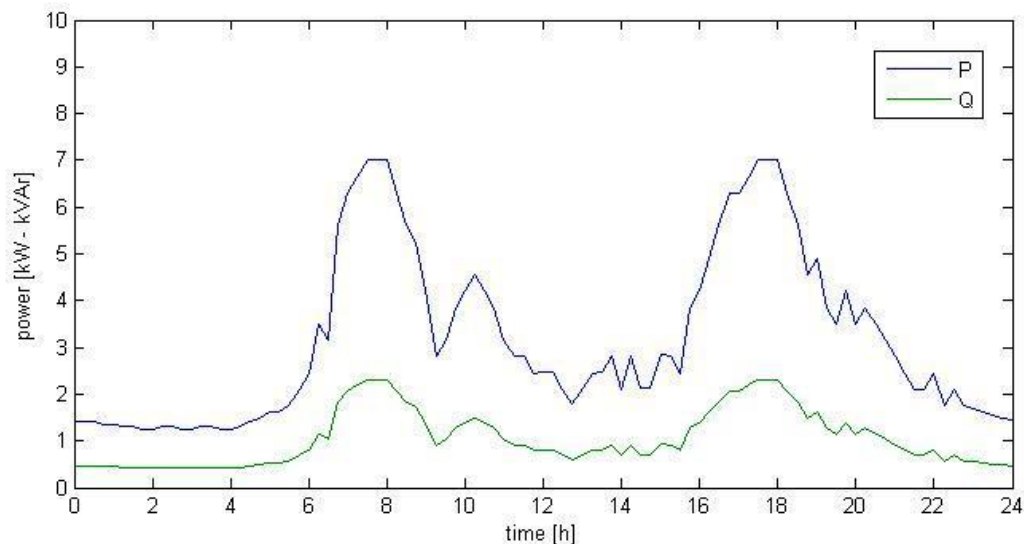


Figure 4.7: Example of farm load profile

#### 4.2.2 “Load data process” block

The role of the “Load data process” block is to allow the user suitably edit the power consumption of the load by scaling the values defined by the load profiles and even set or change the power factor of the load. The inputs and parameters required are presented in Table 4.5 and Table 4.6.

Table 4.5: Inputs of “Load data process” block

Name	Unit	Description
P	MW	Active power consumption as defined by the load profile
Q	MVAr	Reactive power consumption as it may be defined by the load profile

Table 4.6: Parameters of "Load data process" block

Name	Unit	Description
scale	-	Scale factor
ExtCtrl	-	Activation/deactivation of externally controlled (by load profile) reactive power consumption
PF	-	Power factor value in the case of internally defined reactive power consumption

The active and reactive power outputs of the block ( $P_{ext}$ ,  $Q_{ext}$ ) are defined as follows:

$$P_{ext} = scale \cdot P \quad (4.1)$$

$$Q_{ext} = \begin{cases} scale \cdot Q, & ExtCtrl = 1 \\ scale \cdot P \cdot \tan(\cos^{-1} PF), & ExtCtrl = 0 \end{cases} \quad (4.2)$$

The exact DSL model block definition can be found in Appendix B - DSL models' code.

### 4.2.3 "Load" block

The "Load" block definition has as inputs the externally defined active ( $P_{ext}$ ) and reactive ( $Q_{ext}$ ) power consumption of the load as calculated by equations (4.1) and (4.2). The built-in load model in PowerFactory, whose equivalent circuit is presented in Figure 4.8, is associated with the "Load" block definition.

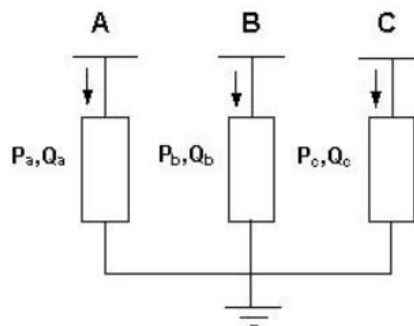


Figure 4.8: 3-phase load model in PowerFactory

## 4.3 PV-Battery system model

The frame of the PV-Battery system model is shown in Figure 4.9. The sections that follow explain one by one the blocks which constitute the overall model.

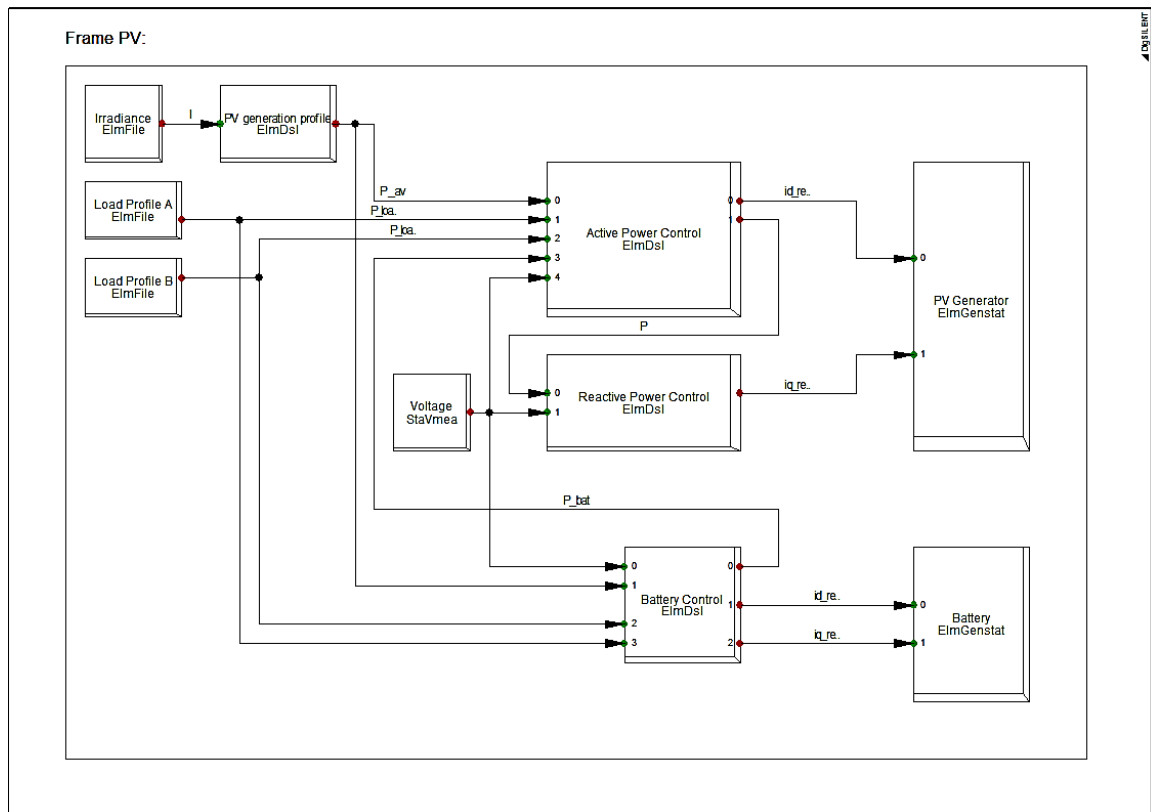


Figure 4.9: PV-Battery system frame

### 4.3.1 “Irradiance” block

Global solar irradiance data on an inclined surface are used as an input to the PV-Battery system model. The corresponding city of the data is Munich. PV panels are assumed to face directly into South with a  $30^\circ$  vertical inclination. More details are presented in Table 4.7.

Table 4.7: Solar irradiance data parameters [55]

<b>Provider</b>	MINES ParisTech - Armines
<b>Site latitude</b>	$48.15^\circ$
<b>Site longitude</b>	$11.58^\circ$
<b>Elevation</b>	519 m
<b>Tilt angle</b>	$30^\circ$
<b>Azimuth angle</b>	$180^\circ$
<b>Albedo of the ground</b>	0.2
<b>Year</b>	2005
<b>Time resolution</b>	15 min

As solar irradiance shows higher values during summer, the PV generation is also higher and voltage rise problem more intense. Hence, a week of June is selected as the study period of the simulation. Thus, irradiance data from 13/06/2005 to 19/06/2005 in  $\text{W/m}^2$  define the output of the irradiance block during the executed simulation (Figure 4.10).

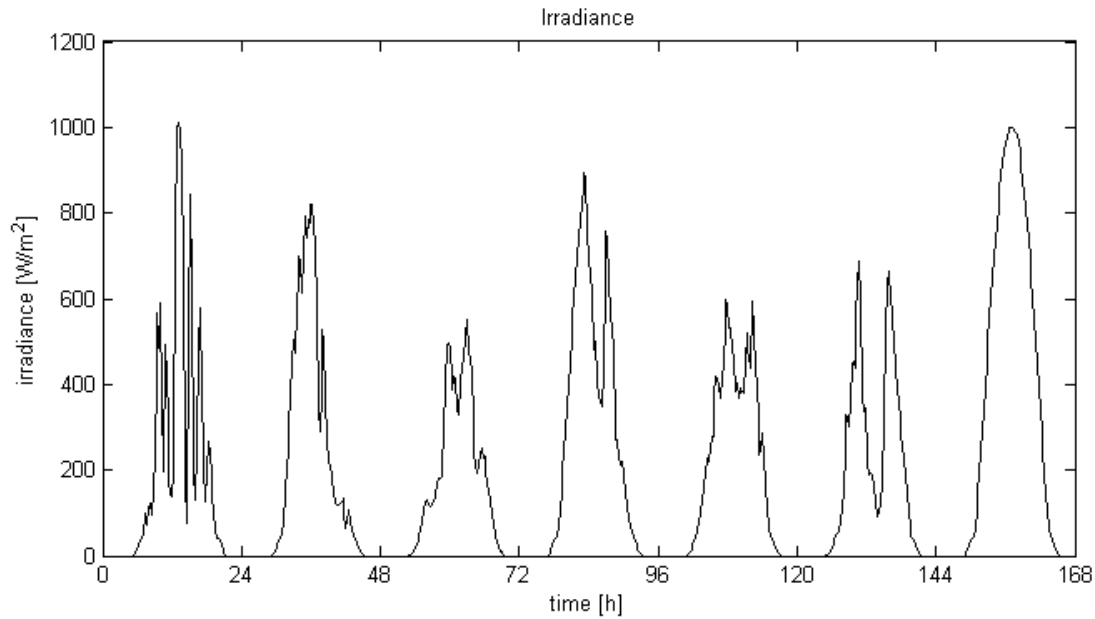


Figure 4.10: Weekly irradiance profile used in the simulations

### 4.3.2 “PV generation profile” block

In order to create a PV generation profile (see also Appendix B - DSL models' code) for each PV system connected to the network, the irradiance profile as well as a selected maximum output power for each PV generator is required. “PV generation profile” block definition has as input the irradiance ( $I$ ) from the “Irradiance” block and as output the available active power ( $P_{av}$ ) in per unit. The per unit power base ( $S_b$ ) of its PV system is defined as the nominal apparent power ( $S_{PV,nom}$ ) of the static generator (see paragraph 4.3.8) associated with the specific PV-Battery system model.

$$S_b = S_{PV,nom} \quad (4.3)$$

Assuming maximum active power generation under  $1000 \text{ W/m}^2$  irradiance conditions, the available active power in p.u. is calculated as follows:

$$P_{av} = \frac{I}{1000} \cdot \frac{P_{max}}{S_b} = \frac{I}{1000} \cdot \frac{P_{max}}{S_{PV,nom}} \quad (4.4)$$

For every PV static generator element the nominal apparent power ( $S_{PV,nom}$ ) in kVA has been selected such that:

$$S_{PV,nom} = \frac{P_{max}}{PF_{lim}} \quad (4.5)$$

Where:

$PF_{lim}$  is the power factor operating limit of the PV generator

$P_{max}$  is the maximum active power capability of the PV generator in kW

### 4.3.3 “Load Profile” blocks

Each of the PV-Battery systems is associated with either a household only or a household and a farm load. Hence, the corresponding load profiles serve as input to the active power controller and battery controller. More information on these load profiles are given in paragraph 4.2.1.

### 4.3.4 “Voltage” block

The Voltage block is associated with the voltage measurement device which is used to measure the AC voltage at each terminal. The measured positive sequence voltage ( $v$ ) in p.u. is then fed as a signal into the active and reactive power controllers as well as to the battery controller.

### 4.3.5 “Active Power Control” block

The role of the “Active Power Control” block is to define the output active power injection of the PV generator, based on the available PV power ( $P_{av}$ ) as well as the possible limitations, control modes and parameters specified by the user. The inputs and parameters required are presented in Table 4.8 and Table 4.9. The exact DSL model can be found in Appendix B - DSL models’ code.

Table 4.8: Inputs of "Active Power Control" block

Name	Unit	Description
$P_{av}$	p.u.	Available PV power as calculated by the “PV generation profile” block
$P_{load,A}$	MW	Household load demand (active power)
$P_{load,B}$	MW	Farm load demand (active power)
$P_{bat}$	MW	Battery power (positive when charging)
$v$	p.u.	Voltage at PV generator’s terminals

Table 4.9: Parameters of "Active Power Control" block

Name	Unit	Description
$S_{PV,nom}$	MVA	Nominal apparent power of the PV static generator
<b>DAPC</b>	-	Activation/deactivation of dynamic active power curtailment mode
$P_{curt,set}$	MW	Active power limitation set by the DSO in case of DAPC
<b>T</b>	s	Time constant of the first-order lag filter (PT1)

Parameter DAPC enables the dynamic active power curtailment mode (see paragraph 3.2.4) when it is set to 1 and disables it when it is set to 0. If DAPC mode is enabled, then an upper limit in the active power injection is set, defined by the following equation:

$$P_{lim} = P_{curt,set} + P_{load,A} + P_{load,B} + P_{bat,charge} \quad (4.6)$$

Where:

$$P_{bat,charge} = \begin{cases} 0, & P_{bat} < 0 \\ P_{bat}, & P_{bat} \geq 0 \end{cases} \quad (4.7)$$

If DAPC is disabled, then all the available active power ( $P_{av}$ ) is injected into the grid.

The time constant (T) required is associated with the first-order lag filter (PT1) which is incorporated in the Active Power Control model (see Appendix B - DSL models' code). Such a filter should be applied after power references in order to make sharp references slow down and avoid output oscillations caused by iterations [31].

The outputs of the block are the active power (P) in p.u. that is going to be injected into the LV network and the direct-axis current ( $i_d$ ) in p.u. which serves as one of the inputs to the PV static generator (see paragraph 4.3.8).

Table 4.10: Outputs of "Active Power Control" block

Name	Unit	Description
P	p.u.	Active power injection into the grid
$i_{d,ref}$	p.u.	Direct-axis current reference for the PV static generator

In order to work in the dq0 rotating frame a Park Transformation would be necessary so as to convert the abc voltage signal. Because of the symmetrical and balanced conditions assumed throughout the simulations and as the dq0 rotating frame is synchronised with the grid voltage (no rotating mechanical parts in a PV inverter), if at  $t=0$  the alignment of the frame is selected properly, so that the d-axis coincides with phase A, then all the q and 0 components are zero and the d component has the magnitude of the positive sequence voltage. Thus:

$$\begin{aligned} v_d &= v \\ v_q &= 0 \\ v_0 &= 0 \end{aligned} \quad (4.8)$$

In general, the active power (P) is related to the d and q-axis voltage and current components through the following equation:

$$P = v_d i_d + v_q i_q \quad (4.9)$$

Thus, as a result of equation (4.8) and (4.9):

$$i_d = \frac{P}{v} \quad (4.10)$$

#### 4.3.6 "Reactive Power Control" block

The role of the "Reactive Power Control" block is to define the reactive power injection of the PV generator based on the control mode, parameters and possible limitations specified by the user. The inputs required are presented in Table 4.11.

Table 4.11: Inputs of "Reactive Power Control" block

Name	Unit	Description
P	p.u.	Active power injection into the grid
v	p.u.	Voltage at PV generator's terminals



The three reactive power based voltage support strategies, presented in chapter 3, are implemented and the user is able to select the one preferred by changing the appropriate parameter (mode) as shown in Table 4.12.

Table 4.12: Reactive power based control strategy selection

mode	Control strategy
0	fixed PF
1	PF(P)
2	Q(V)

The rest of the parameters that need to be defined in the Reactive Power Control model are shown in Table 4.13.

Table 4.13: Parameters of "Reactive Power Control" block

Name	Unit	Description
$PF_{fixed}$	-	Fixed power factor value of the fixed PF mode
$PF_{lim}$	-	Power factor operating limit of the PV generator
$P_{sp}$	-	Ratio of the maximum active power of the PV generator over which the PV system starts absorbing reactive power when the PF(P) mode is selected
$V_{sp}$	p.u.	Voltage set-point over which the PV system starts absorbing reactive power when the Q(V) mode is selected
$V_{max}$	p.u.	Voltage threshold above which the PV system should absorb the maximum possible reactive power when the Q(V) mode is selected
$T$	s	Time constant of the first-order lag filter (PT1)

Figure 4.11 presents the implemented characteristic of the fixed PF strategy. Only the inductive part of that of Figure 3.3 is considered as only voltage rise is the problem of interest in this thesis.

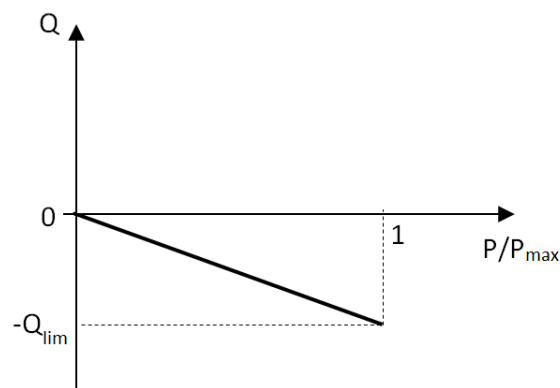


Figure 4.11: Fixed PF characteristic

The equations related to the characteristic of Figure 4.11 are:

$$Q = -P \cdot \tan(\cos^{-1} PF_{fixed}) \quad (4.11)$$

$$Q_{lim} = P_{max} \cdot \tan(\cos^{-1} PF_{fixed}) \quad (4.12)$$

The selected power factor ( $PF_{fixed}$ ) should be within the operational limits of the PV generator. Thus, for the needs of this study:

$$PF_{lim} \leq PF_{fixed} \leq 1 \quad (4.13)$$

In case the controller is set to the PF(P) control mode then the characteristic presented in Figure 4.12 is enabled. This strategy has been extensively described in paragraph 3.2.3.2. However, as shown in Figure 4.12, only the inductive part is considered for the needs of this thesis. Equation (4.14) describes the PF(P) characteristic used:

$$PF = \begin{cases} 1, & \frac{P}{P_{max}} < P_{sp} \\ \frac{1 - PF_{lim}}{P_{sp} - 1} \left( \frac{P}{P_{max}} - P_{sp} \right) + 1, & P_{sp} \leq \frac{P}{P_{max}} \leq 1 \end{cases} \quad (4.14)$$

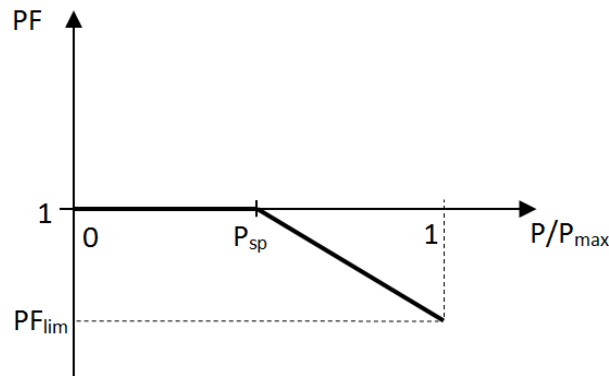


Figure 4.12: PF(P) characteristic

The last control mode is associated with the Q(V) strategy and it is implemented as shown in Figure 4.13.

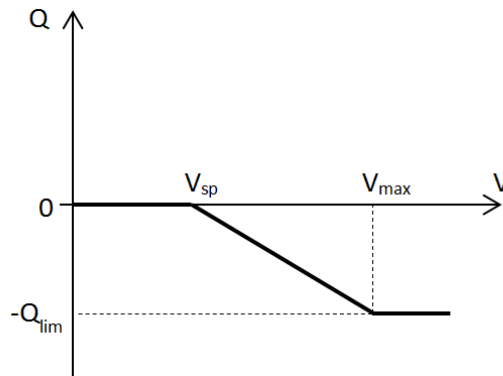


Figure 4.13: Q(V) characteristic

It is based on the following equation:

$$Q = \begin{cases} 0, & V < V_{sp} \\ -\frac{Q_{lim}}{V_{max} - V_{sp}}(V - V_{sp}), & V_{sp} \leq V \leq V_{max} \\ -Q_{lim}, & V > V_{max} \end{cases} \quad (4.15)$$

Where,  $Q_{lim}$  is a function of instantaneous active power injection ( $P$ ) and power factor limit ( $PF_{lim}$ ) of the PV static generator:

$$Q_{lim} = P \cdot \tan(\cos^{-1} PF_{lim}) \quad (4.16)$$

The output of the block is the quadrature-axis current ( $i_q$ ) in p.u. which is connected to the corresponding input ( $i_{q,ref}$ ) of the PV static generator (see paragraph 4.3.8). Regardless of which control mode is used, the reactive power injection of the PV generator is related to the d and q-axis voltage and current components through the following equation:

$$Q = v_q i_d - v_d i_q \quad (4.17)$$

And as a result of equation (4.8) and (4.17):

$$i_q = \frac{Q}{v} \quad (4.18)$$

The exact DSL model can be found in Appendix B - DSL models' code.

### 4.3.7 "Battery Control" block

The role of the "Battery Control" block is to manage the charging and discharging procedure of the battery associated with it. The inputs and parameters required are presented in Table 4.14 and Table 4.15.

Table 4.14: Inputs of "Battery Control" block

Name	Unit	Description
$P_{av}$	p.u.	Available PV power as calculated by the "PV generation profile" block
$P_{load,A}$	MW	Household load demand
$P_{load,B}$	MW	Farm load demand
$v$	p.u.	Voltage at battery's terminals

Table 4.15: Parameters of "Battery Control" block

Name	Unit	Description
<b>EnableStorage</b>	-	Activation/deactivation of the battery
<b>C</b>	MWh	Energy capacity of the battery
$S_{bat,nom}$	MW	Nominal apparent power of the Battery static generator
$S_{PV,nom}$	MW	Nominal apparent power of the PV static generator
<b>T</b>	s	Time constant of the first-order lag filter (PT1)

Battery capacity ( $C$ ), for each household and farm, is selected in such a way that part of PV power generated is stored for later consumption within the day. Unlike autonomous dwellings, for grid-connected ones, a battery system should not necessarily cope with a long period of low PV generation because the grid is available as a back-up. Therefore, the target is on a battery system which makes daily shifts of energy exchange. As no design rules for this purpose are available in the literature [43], battery capacity for each household and farm in the model is selected in such a way that it covers the average electricity demand of the time period between 19:30 and 07:00, which is a period of low or no irradiance.

The objective of the energy management of the battery system is to store the additional PV energy (charge) when PV generation exceeds load demand and to provide energy (discharge) when load demand exceeds PV generation. This functionality is limited by the capacity of the battery system and the maximum charge/discharge rate (equation (4.19)). When the battery is fully charged, the PV energy has to be injected directly into the grid. This energy is not used for local consumption. When the battery is fully discharged the required electricity is provided by the public grid.

As lithium-ion technology is assumed for the batteries, to prevent the effects of battery ageing the active state of charge (SOC) range is limited to 60 % of the initial battery capacity (SOC range: 20 – 80 %). According to the modelling assumptions a constant efficiency ( $n_{bat}$ ) of 95 % is considered for both charging and discharging states [41, 43]. Furthermore, the maximum rate of charge/discharge is limited to 1 C [56]. Hence, the battery power ( $P_{bat}$ ) in p.u. is:

$$P_{bat} = \begin{cases} \frac{P_{PV} - P_{load}}{S_{bat,nom}}, & P_{PV} > P_{load} \cap SOC < 80 \% \\ \frac{P_{load} - P_{PV}}{S_{bat,nom}}, & P_{PV} \leq P_{load} \cap SOC > 20 \% \\ 0, & \text{all other conditions} \end{cases} \quad (4.19)$$

$$-\frac{C}{1h} \cdot \frac{1}{S_{bat,nom}} \leq P_{bat} \leq \frac{C}{1h} \cdot \frac{1}{S_{bat,nom}}$$

Where:

$$P_{PV} = P_{av} \cdot S_{PV,nom} \quad (4.20)$$

$$SOC = a \cdot \frac{S_{bat,nom} \cdot \int P_{bat} dt}{3600 \frac{s}{h} \cdot C} \cdot 100 \% \quad (4.21)$$

$$20 \% \leq SOC \leq 80 \%$$

The coefficient  $a$  used in equation (4.21) is defined as follows:

$$a = \begin{cases} n_{bat}, & P_{PV} > P_{load} \\ \frac{1}{n_{bat}}, & P_{PV} \leq P_{load} \end{cases} \quad (4.22)$$

The other outputs of the block, the direct-axis current ( $i_d$ ) and the quadrature-axis current ( $i_q$ ) in p.u. serve as input to the Battery static generator (see paragraph 4.3.8) and are calculated, using equations (4.19), (4.8), (4.9) and (4.17) as follows:

$$i_d = -\frac{P_{bat}}{v} \quad (4.23)$$

$$i_q = 0$$

The exact DSL model can be found in Appendix B - DSL models' code

### 4.3.8 "PV Generator" and "Battery" blocks

In PowerFactory a static generator can serve as a model of any kind of static (no rotating) generator, such as:

- photovoltaic generators
- fuel cells
- storage devices
- HVDC terminals
- reactive power compensators
- wind generators

In the case of the PV-Battery system model, the two static generators used serve as the interface of the PV and battery system, respectively, to the LV network. Their inputs are the direct and quadrature axis reference currents which are associated with the active and reactive power injected into the grid, as defined by their corresponding controllers.

## 4.4 General simulation assumptions

The following general simulation assumptions apply:

- Household and farm loads are assumed to be balanced and 3-phase connected. No voltage dependency is taken into account for loads as well.
- No daily variation was assumed for farm load profiles.
- Every PV generator and battery system is considered to be 3-phase connected.
- Irradiance is considered the same for all household and farm PV systems.
- The maximum active power generation for all the household PV systems is the same. The same applies to farm PV systems although at different level than that of households.
- No inverter and cable losses are taken into account for the PV-Battery systems.
- The efficiency of the PV panels is regarded constant and based on STC conditions.
- Voltage at the MV side of the transformer is assumed constant thus no voltage variation in the MV grid is taken into account



---

## Implementation and test results

In this chapter the LV network model is firstly tested under high PV integration to verify that the voltage rise problem indeed appears. Then the local voltage support strategies, presented in chapter 3, are activated and tested one by one, as well as their combination with battery storage, in order to check their effectiveness and behaviour for different PV-integration levels.

### 5.1 High PV integration without voltage support

Referring to a study performed by a German DSO, the average installed power for PV systems on residential rooftops is  $10 \text{ kW}_p$ , whereas on farm buildings it is  $27 \text{ kW}_p$  [34]. Assuming that every household and farm PV system of the test network model can produce power up to  $10 \text{ kW}$  and  $27 \text{ kW}$  respectively, it should be checked whether the voltage at the network's terminals violates or not the limit set by the German directive VDE-AR-N 4105.

Since off-load tap of LV distribution transformer is usually adjusted by estimating voltage drop with maximum nominal load, only low load condition should be considered to investigate voltage rise [57]. As the MV level is not part of the simulation's interest, the voltage on the MV side of the transformer is set fixed to 1 p.u.. It is also assumed that the maximum voltage at each LV terminal must not exceed 1.03 p.u. in order to fulfil the requirements.

Thus, in order to cover the worst case scenario in terms of voltage rise, maximum PV generation and low load conditions (base load of load profiles) are assumed, as a minimum load would always be present in the system. Figure 5.1 and Figure 5.2 present the voltage profile along each feeder of the LV network for both conductor types and for this worst case load flow calculation.

It is observed that voltage rise, for both feeders, is more intense when OHLs are used. Feeder 1 exhibits higher voltage rise than feeder 2 because of the higher total PV generation, due to the farm PV systems that are connected into it. Its last three terminals clearly exceed the 3 % limit in the case of OHL, while only the last two terminals exceed the limit in the case of cables. Although none of the terminals of feeder 2 exhibits voltage higher than 1.03 p.u. when cables are used, in the case of OHLs its last two terminals experience voltage rise slightly above the limit.

The transformer and conductor loading for this worst case scenario are presented in Table 5.1. As it is observed they do not constitute limiting factors for this operating condition of the network under study.

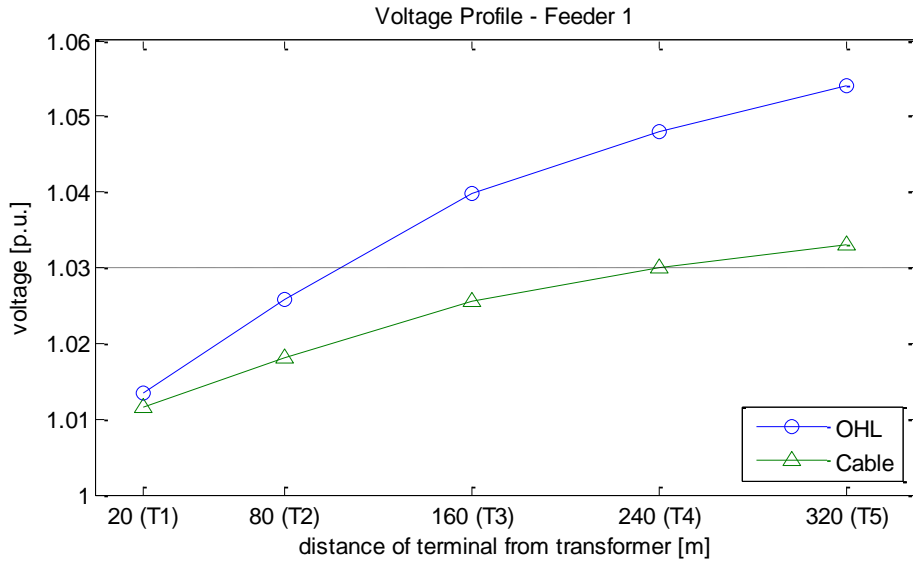


Figure 5.1: Voltage profile of feeder 1 under low load and high PV generation conditions (10 kW/household and 27 kW/farm) for both conductor types

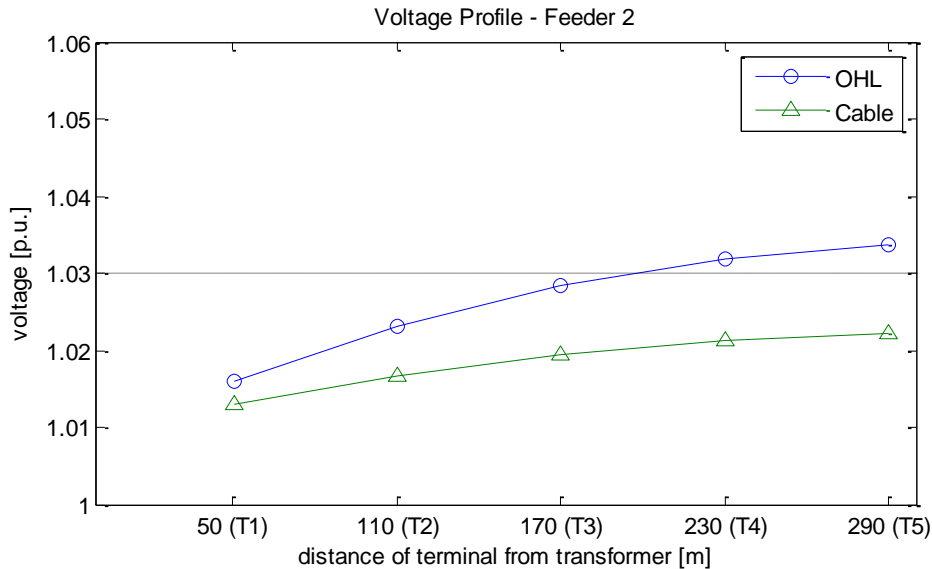


Figure 5.2: Voltage profile of feeder 2 under low load and high PV generation conditions (10 kW/household and 27 kW/farm) for both conductor types

Table 5.1: Transformer and conductor loading for the worst case conditions (low load – high PV generation)

Conductor	Transformer loading	Maximum conductor loading
OHL	78.5 %	41.5 %
cable	79.5 %	42.8 %

It is also a matter of interest whether the voltage limit is violated not only under low load conditions but also under normal load conditions. For this purpose, weekly simulations are executed, for both conductor types, using the load profiles presented in paragraph 4.2.1 and the irradiance data presented in paragraph 4.3.1. As observed in Figure 5.1, the weakest point of the



test network is the fifth terminal of the first feeder. Thus, voltage measurements for this terminal are shown in Figure 5.3.

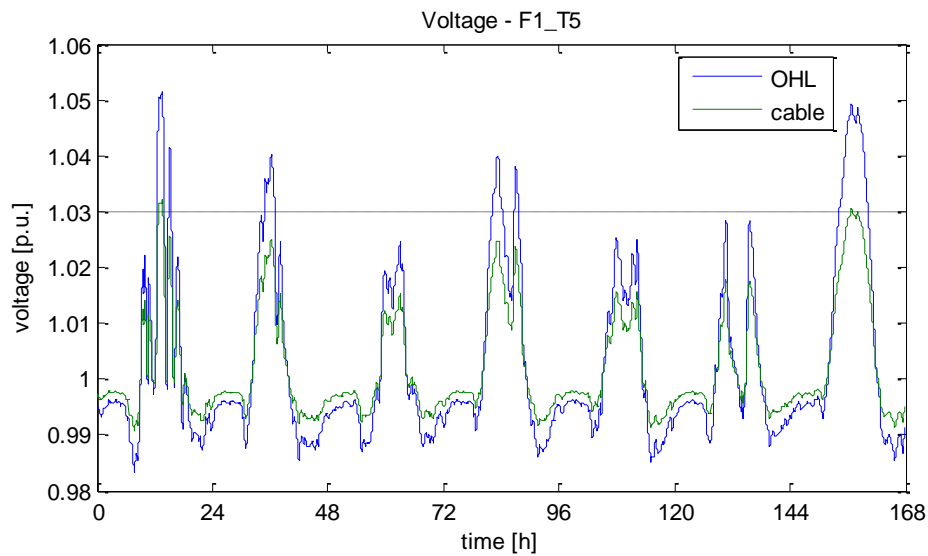


Figure 5.3: Voltage measurements for the weakest point of the network under normal load conditions and high PV integration (10 kW/household and 27 kW/farm) throughout the weekly simulation

The results show that the 3 % limit set by the German directive is clearly exceeded during the simulations, when the irradiance observed is high (see Figure 4.10). It is also clear that the problem is more intense when overhead lines are used. Therefore, voltage support strategies are required to keep voltage under the limit when PV integration in the test LV network is high. The level of PV integration over which voltage rise problem appears is studied in paragraph 5.3.

## 5.2 Voltage sensitivity analysis of test network

Before implementing the studied voltage support strategies suggested, which are based on active and reactive power control, it would be useful to check the voltage sensitivity of the test network to active and reactive power variations. Both cases of overhead lines and cables are tested.

In general, voltage sensitivity analysis can be used for estimating the voltage variation due to a small change in active or reactive power injection at a certain location. Voltage sensitivity matrices for a network can be derived for both active and reactive power by solving non-linear load flow equations using the Newton–Raphson algorithm, which provides a linear model around the given operating point. The same matrices can be used to identify critical locations in relation to load/generation conditions. Elements of resultant sensitivity matrices give the most effective places to support voltage by regulating Q and P at related nodes. Moreover P-V and Q-V sensitivity matrices can be compared to each other for a specific network to determine which system parameter input (P or Q) has dominant impact on grid voltage. The most remote node in the feeder, presents the highest sensitivity value, thus it is the most critical location for active power injection in relation to voltage variation [31, 40].

One can therefore calculate the expected small changes in angle ( $\theta$ ) and amplitude (V) of the voltage for a given small change in the active and reactive power values:

$$\begin{bmatrix} \Delta P \\ \Delta Q \end{bmatrix} = \begin{bmatrix} \frac{\partial P}{\partial \theta} & \frac{\partial P}{\partial V} \\ \frac{\partial Q}{\partial \theta} & \frac{\partial Q}{\partial V} \end{bmatrix} \cdot \begin{bmatrix} \Delta \theta \\ \Delta V \end{bmatrix} = \mathbf{J} \cdot \begin{bmatrix} \Delta \theta \\ \Delta V \end{bmatrix} \quad (5.1)$$

Where:

$\mathbf{J}$  is the system Jacobian matrix which is updated at each load flow iteration, until convergence tolerance is satisfied. Solving equation (5.1) for  $\Delta \theta$  and  $\Delta V$  the sensitivity matrix  $\mathbf{S}$  arises:

$$\begin{bmatrix} \Delta \theta \\ \Delta V \end{bmatrix} = \mathbf{S} \cdot \begin{bmatrix} \Delta P \\ \Delta Q \end{bmatrix} = \begin{bmatrix} S_{\theta_P} & S_{\theta_Q} \\ S_{V_P} & S_{V_Q} \end{bmatrix} \cdot \begin{bmatrix} \Delta P \\ \Delta Q \end{bmatrix} \quad (5.2)$$

The voltage sensitivity matrix is composed of four sub-matrices with partial derivatives that portray the variation in the voltage magnitude and angle of the buses due to variations in active and reactive power at each bus. The diagonal elements of  $S_{V_P}$  and  $S_{V_Q}$  represent the voltage variation at a bus due to a variation of active and reactive power respectively at the same point. The non-diagonal elements describe the voltage variation at a bus due to the variation in active and reactive power at a different point on the network.

Applying this technique on the test network model, voltage sensitivities are calculated. Regarding the worst case condition of voltage rise problem, the operating point is selected the same as that of the previous paragraph (low load demand – 10 kW/household and 27 kW/farm PV generation).

Figure 5.4 and Figure 5.5 plot the voltage sensitivity magnitudes of the diagonal elements of  $S_{V_P}$  and  $S_{V_Q}$  for the two types of conductors (OHL and cable) that have different R/X impedance ratios (Table 4.3). We should recall from equation (3.6) that, as the R/X ratio increases, higher values of reactive power injection from the external grid will be required to prevent overvoltage. Thus, the effectiveness of a voltage support strategy through reactive power management in the test network is higher in case overhead lines are used as conductors.

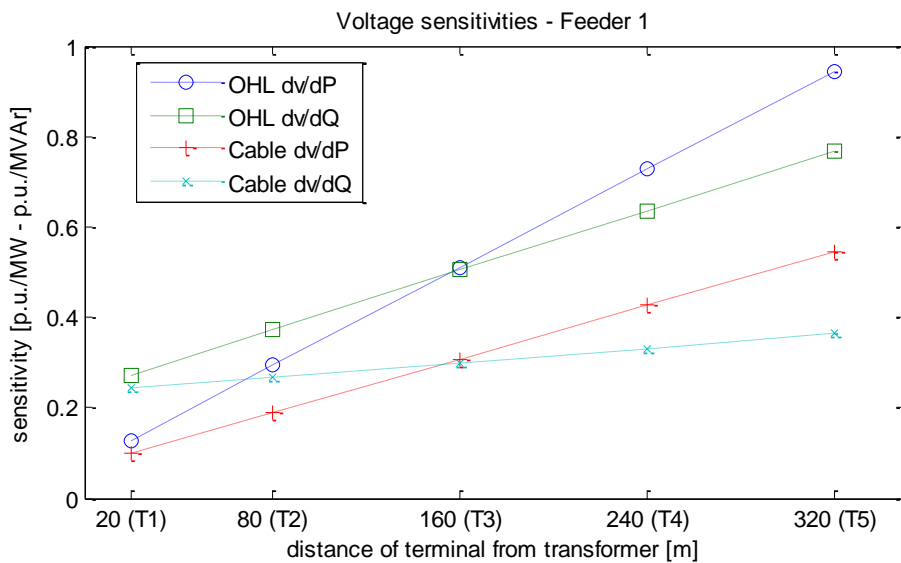


Figure 5.4: Voltage sensitivities to P and Q variation for the terminals of feeder 1

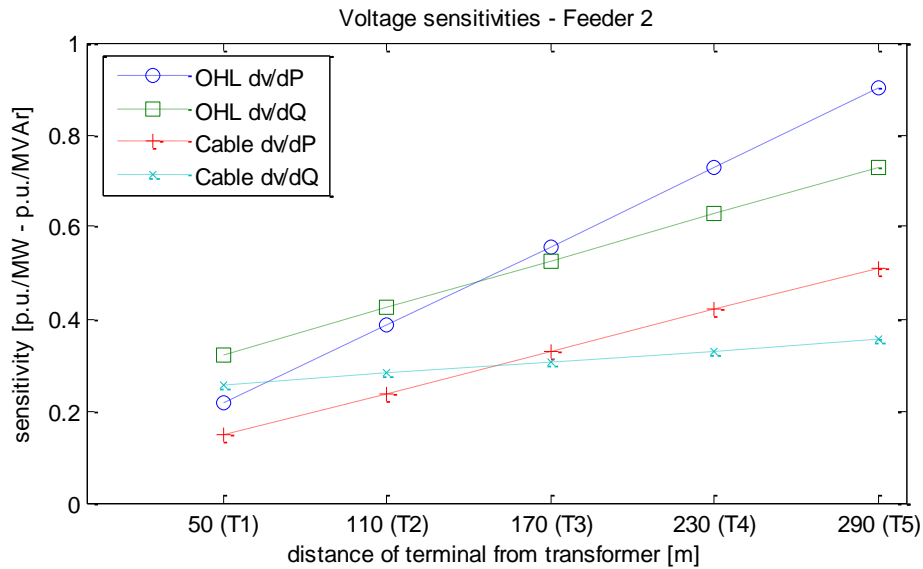


Figure 5.5: Voltage sensitivities to P and Q variation for the terminals of feeder 2

With bigger impedance (OHL case, see Table 4.3), there is always higher voltage impact by both active and reactive power variations. It is also observed from Figure 5.4 and Figure 5.5 that  $S_{V_Q}$  is higher than  $S_{V_P}$  at the terminals which are closer to the transformer. This happens because of their shorter distance to the transformer. Therefore, short-circuit reactance of the transformer becomes dominant over the short-circuit resistance at these locations. As the distance to the transformer increases along the feeder, line resistance contributes more on the impedance so that the active power control becomes more effective on the voltage support than the reactive power control.

### 5.3 Reactive power control strategies

Recalling the German directive, PV inverters should be capable to feed in with power factors up to 0.95 from an apparent PV system power of 3.68 kVA, while if PV system power exceeds 13.8 kVA, even power factors up to 0.9 must be supported. Thus during the simulation all the household PV systems can be controlled to absorb reactive power with a power factor up to 0.95 whereas the two farm PV systems can be controlled up to 0.9.

It should be mentioned here that, because of the statistics presented in paragraph 5.1, a ratio 2.7:1 is considered for the assigned maximum active power injections of farm and household PV systems throughout all the simulations and load flow calculations of this thesis. Selecting, for example, a maximum PV power of 6 kW for a household PV system means that a farm PV system has a capability of generating up to 16.2 kW ( $2.7 \cdot 6$  kW). Therefore, from this point forward, when a value is mentioned for the maximum active power feed-in of a household PV system, it would mean that a farm PV system injects 2.7 times this value.

One question that arises is:

*“What is the PV hosting capacity of this test LV network depending on the power factor under which the maximum active power of each PV generator is fed into it?”*

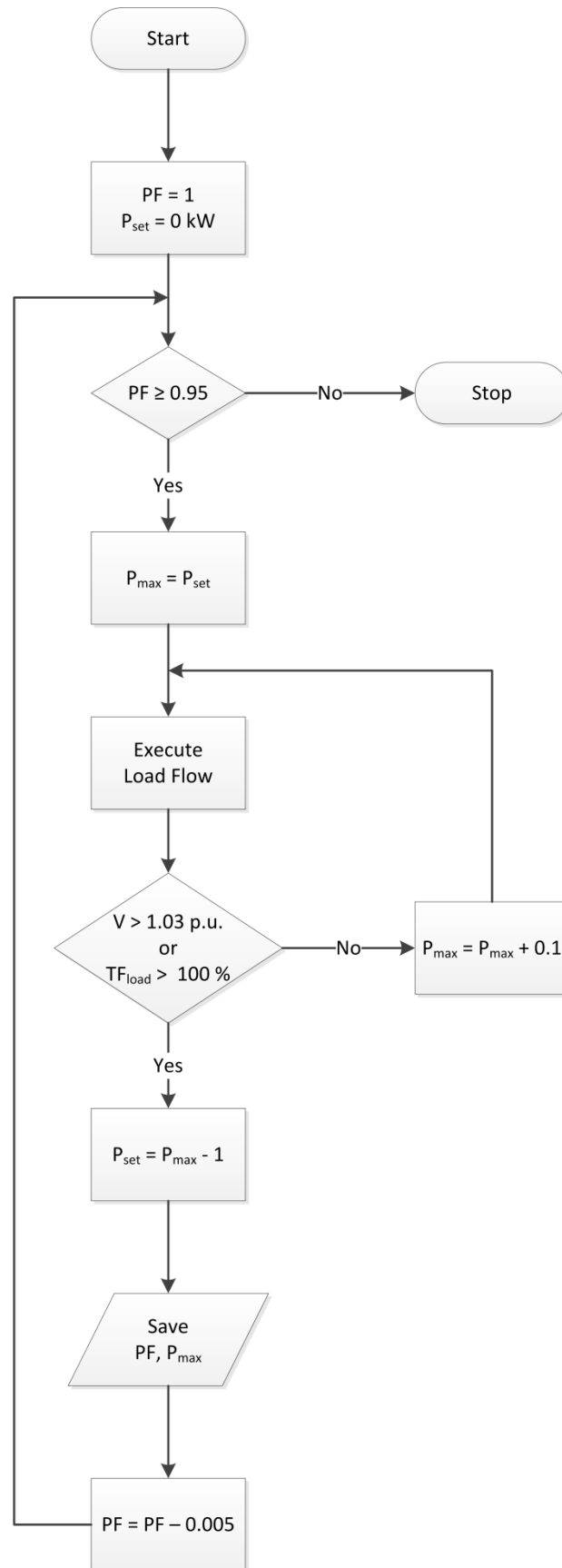


Figure 5.6: Flowchart of the script executed to calculate the PV hosting capacity of the network for different power factors of the PV generators

In order to answer this question, a script is written in DPL (see Appendix C - DPL commands) and its flowchart is presented in Figure 5.6. The script takes into account the worst case scenario, thus low load conditions are assumed.

PV hosting capacity is defined as the maximum PV integration for which the network still operates satisfactorily [30]. It is determined in such a way that PV power production per household and farm is increased until a limiting factor reaches its corresponding limit levels [33]. Regarding the worst-case condition in the sense of voltage rise, low load conditions are assumed. The PF is decreased from 1 to 0.95 for households with a 0.005 step and from 1 to 0.9 for farms with a 0.1 step. Thus eleven measurements in total are taken. For each PF set the active power injection of each household PV system is increased with a 0.1 kW step (0.27 kW for farm PV systems) and PV hosting capacity of the LV network is determined as soon as either:

- the voltage at a terminal exceeds 1.03 p.u., or
- the loading of the transformer or a line section exceeds 100 % of its rated power

This method to estimate the maximum PV integration in the network has the advantage of creating a uniform distribution of PV power across the entire LV network. Practical cases may differ from this situation though. The script was executed for both OHL and cables usage. The results are presented in Table 5.2 and plotted in Figure 5.7.

Table 5.2: PV hosting capacity of the network for the range of permitted power factors of the PV generators

Power Factor		PV hosting capacity [kW] (OHL)				PV hosting capacity [kW] (Cable)			
Household	Farm	Household	Farm	Total	Gain	Household	Farm	Total	Gain
<b>1</b>	<b>1</b>	5.6	15.1	75.0	0%	9.0	24.3	120.6	0%
<b>0.995</b>	<b>0.99</b>	6.4	17.3	85.8	14%	10.4	28.1	139.4	16%
<b>0.990</b>	<b>0.98</b>	6.9	18.6	92.5	23%	11.2	30.2	150.1	24%
<b>0.985</b>	<b>0.97</b>	7.3	19.7	97.8	30%	11.9	32.1	159.5	32%
<b>0.980</b>	<b>0.96</b>	7.7	20.8	103.2	38%	12.0	32.4	160.8	33%
<b>0.975</b>	<b>0.95</b>	8.1	21.9	108.5	45%	11.9	32.1	159.5	32%
<b>0.970</b>	<b>0.94</b>	8.5	23.0	113.9	52%	11.8	31.9	158.1	31%
<b>0.965</b>	<b>0.93</b>	8.9	24.0	119.3	59%	11.7	31.6	156.8	30%
<b>0.960</b>	<b>0.92</b>	9.4	25.4	126.0	68%	11.6	31.3	155.4	29%
<b>0.955</b>	<b>0.91</b>	9.9	26.7	132.7	77%	11.5	31.1	154.1	28%
<b>0.950</b>	<b>0.9</b>	10.4	28.1	139.4	86%	11.4	30.8	152.8	27%

The results show that in case of overhead lines the test LV network can host up to 86 % more PV capacity with reactive power based voltage support strategies than without support. Voltage rise is the limiting criterion for all the hosting capacity levels. When cables are used as conductors, reactive power injection relocates the limiting criterion of hosting capacity from voltage towards transformer loading from a certain hosting capacity upwards. This shift happens at approximately 12 kW per household PV system which leads to an increase of only 33 % in total PV capacity of the test network compared to the unity power factor case. However, maximum PV hosting capacity in case of cables is around 15 % more than in case of overhead lines.

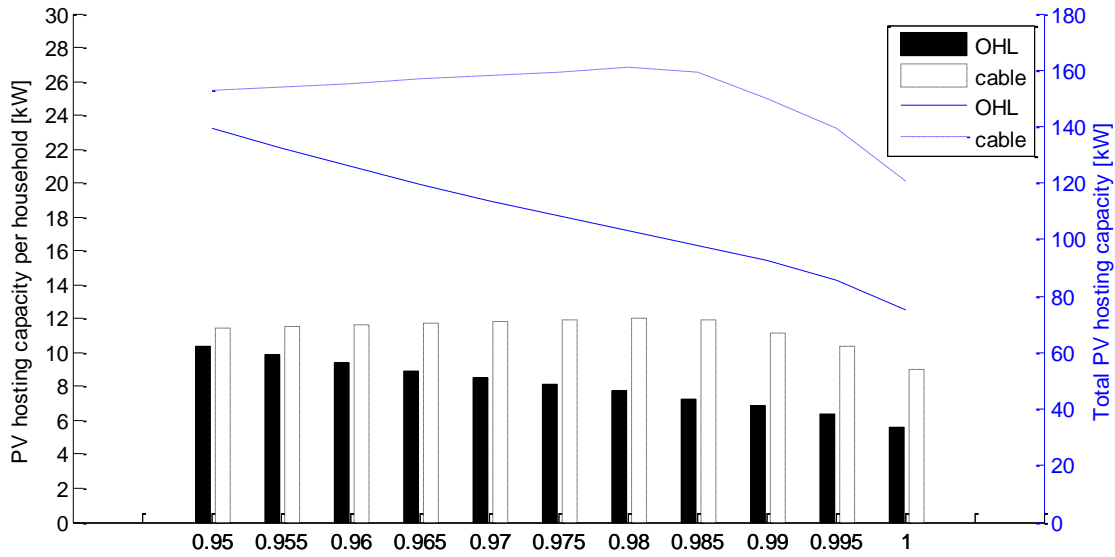


Figure 5.7: Plot of the PV hosting capacity with respect to the power factor of a household PV system

Line loading cannot be a limiting factor in this network, under the simulated operating conditions, as the thermal rating of both conductor types used is higher than that of the transformer, thus in any studied case the transformer would be overloaded first.

From the analysis so far it is becoming clear that voltage rise problems are more intense in case overhead lines are used, comparing conductors of almost equal current rating (Table 4.3). Hence, for the rest of the analysis and simulations executed, implementing the studied voltage support strategies, only the case of overhead lines is considered.

### 5.3.1 PF(P) control mode

In order to check the effectiveness and behaviour of the PF(P) voltage support strategy, the corresponding control mode is activated in the reactive power controllers of the PV-Battery systems. Then a series of simulations, under normal load conditions, are executed for PV integration levels from 6 up to 10 kW/household, with a step of 1 kW/household.

Following the German directive, the  $P_{sp}$  parameter (see Table 4.13) of the PF(P) characteristic, presented in Figure 4.12, is set to 0.5. This means that when the PV power production exceeds half of the PV system's maximum power, the power factor starts linearly decreasing up to the power factor limit (see paragraph 5.3) and reactive power is absorbed.

It should be noticed that the selection of the value for the  $P_{sp}$  parameter can influence the behaviour of the PF(P) strategy. For example, in the case of the test LV network under study, if the active power threshold, over which PV generators start absorbing reactive power, is selected larger than 5.6 kW, then the resulting characteristic could still cause voltage rise problems in case of low irradiance and low load conditions, but it would be efficient for higher values of irradiance. This case is presented in Figure 5.8, for 9 kW/household PV-integration level. The red line represents the problematic characteristic whose threshold is set to 7 kW and the green one the suggested by the German regulation whose threshold is set to 4.5 kW ( $P_{sp} = 0.5$ ). The blue markers indicate the hosting capacity limit as given in Table 5.2.

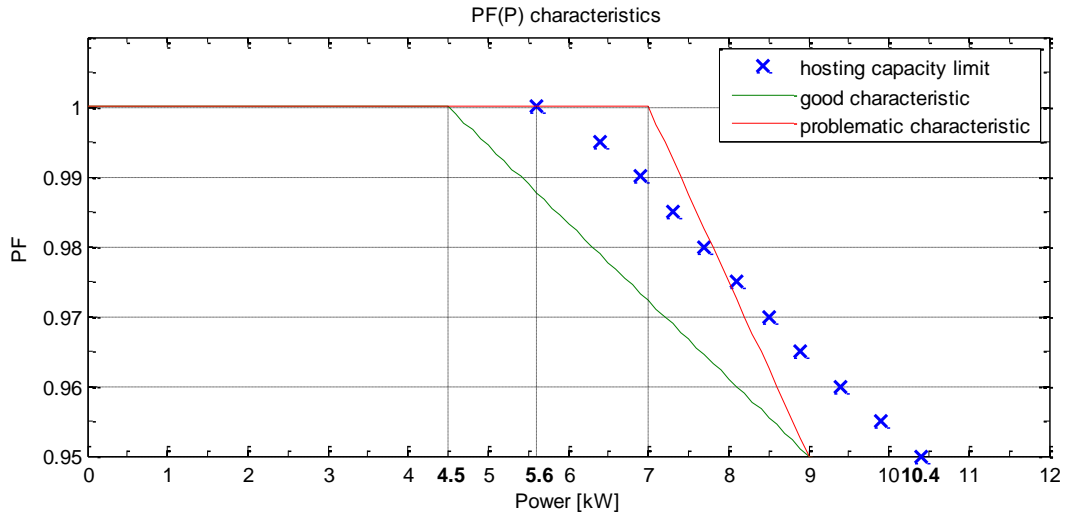


Figure 5.8: Selection of the appropriate PF(P) characteristic

In order to test the validity of the PF(P) voltage support strategy in case of maximum PV hosting capacity (10.4 kW/household), a characteristic with  $P_{sp} = 0.5$  and  $P_{max} = 10.4$  kW is compared with the hosting capacity limits as presented in paragraph 5.3. It is observed that every point of the suggested PF(P) characteristic is below the hosting capacity limits which makes the PF(P) strategy suitable for all the tested PV-integration levels.

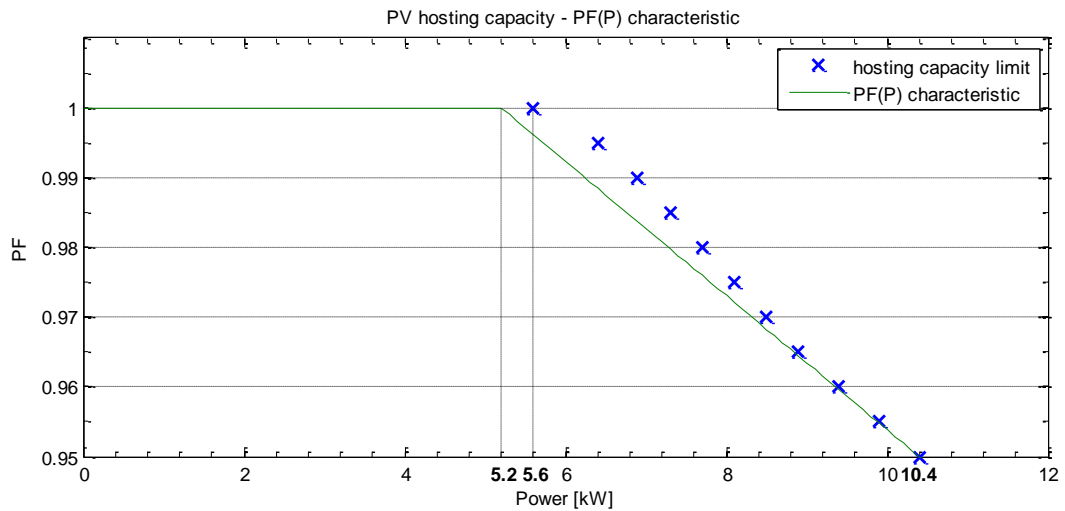


Figure 5.9: Comparison of the selected PF(P) characteristic with the hosting capacity limits in case of maximum PV hosting capacity

**5.3.1.1 PF(P) without storage**

As resulted by the series of simulations, PF(P) strategy manages to keep the voltage below the limit set by the German regulation. Figure 5.10 presents the voltage of the weakest terminal for 6 and 10 kW/household PV-integration levels.

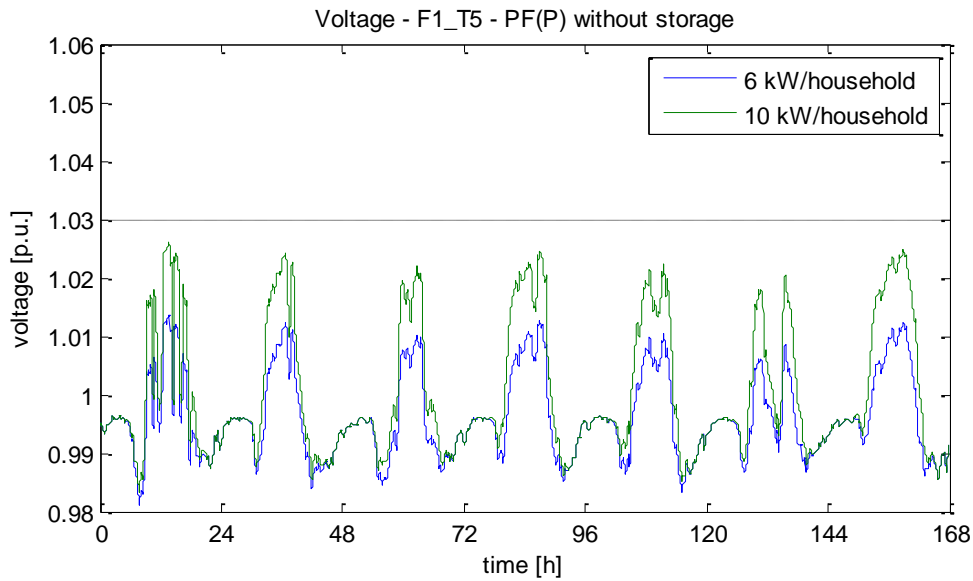


Figure 5.10: Voltage at the weakest terminal in case of PF(P) strategy without storage

The active and reactive power injection by a household PV system, for a maximum active power of 10 kW, is presented in Figure 5.11. It can be noticed that when the active power generated by a PV system is below 5 kW (half of the maximum active power) no reactive power is absorbed.

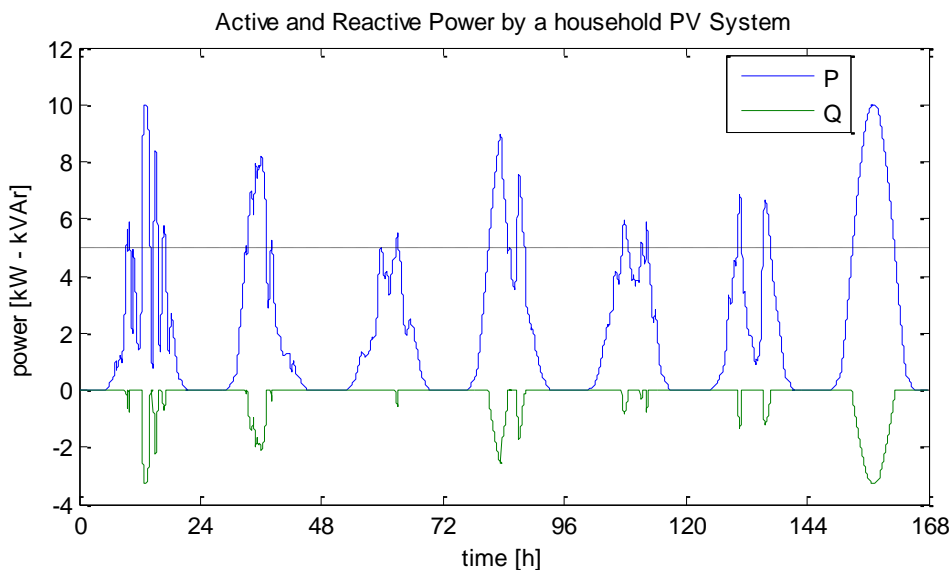


Figure 5.11: Active and reactive power injection of a household PV system for a PV-integration level of 10 kW/household

### 5.3.1.2 PF(P) with battery storage

The same series of simulations are executed again but now the battery storage option is also activated. The results concerning the voltage at the weakest terminal are presented in Figure 5.12, for 6 and 10 kW/household PV integration levels.



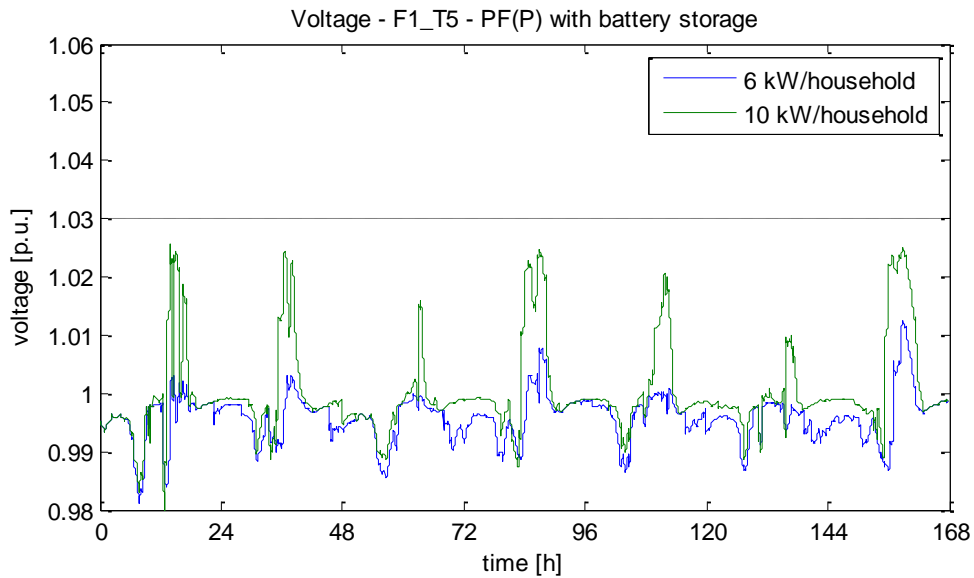


Figure 5.12: Voltage at the weakest terminal in case of PF(P) strategy with battery storage

Long time periods when the voltage is very close to 1 p.u. are observed, which indicate battery charging and discharging states. When batteries are fully charged there is still some voltage rise which is kept below the limit via the reactive power absorption of PV systems. The active and reactive power injection by a household PV system, for a maximum active power of 10 kW, is the same as the one presented in Figure 5.11.

Figure 5.13 presents an example of the state of charge of a battery system during a weekly simulation. It is shown that the target of daily shifts of energy exchange, as discussed in paragraph 4.3.7 is achieved.

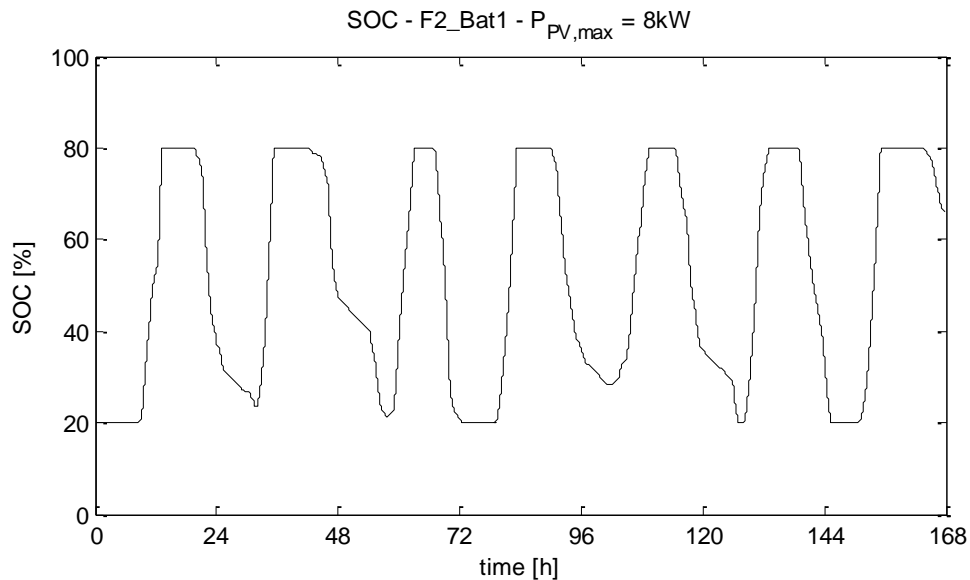


Figure 5.13: State of charge of one of the household battery systems throughout the weekly simulation

### 5.3.2 Q(V) control mode

The next voltage support strategy that is tested is Q(V). The corresponding control mode is activated in the reactive power controllers and a series of simulations, under normal load conditions, are executed for the same PV-integration levels as with the PF(P) strategy (6 – 10 kW/household).

As stated by the German regulation, the droop characteristic of the Q(V) strategy should be provided by the authorised distribution system operator. Therefore, a droop characteristic specific for the LV network under consideration should be specified. First, it should be studied how the selection of the parameters  $V_{sp}$  and  $V_{max}$  can influence the behaviour of the Q(V) strategy.

Given a voltage measurement ( $v$ ), the amount of reactive power that should be absorbed depends of the selection of parameters  $V_{sp}$ ,  $V_{max}$  as explained in Figure 5.14. For the first parameter, a value larger than or equal to the network's nominal voltage can be selected, thus  $V_{sp} \geq 1$  p.u., creating a dead band which delays the reactive power consumption, if it is unnecessary. Increasing  $V_{sp}$  results to lower reactive power absorption ( $|q'| < |q|$ ) as shown in Figure 5.14a. For the second parameter, a value lower than or equal to the limit specified by the German guideline has to be selected, thus  $V_{max} \leq 1.03$  p.u. Figure 5.14b shows that decreasing  $V_{max}$  results to higher reactive power consumption ( $|q'| > |q|$ ).

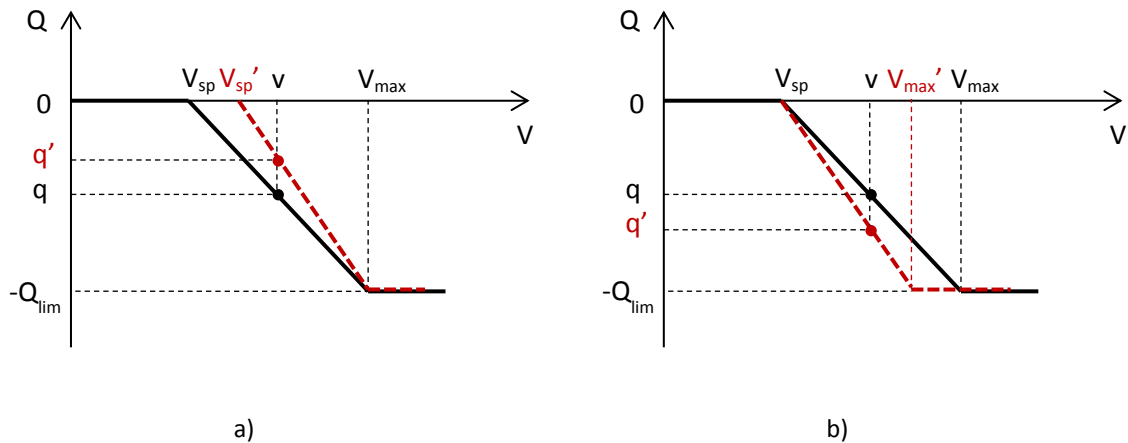


Figure 5.14: Sensitivity of Q(V) characteristic in the selection of its parameters: a) for the  $V_{sp}$  parameter, b) for the  $V_{max}$  parameter

Parameter  $V_{sp}$  is set to one, thus no dead-band is used, so as not to burden the whole reactive power load to the PV systems at the end of the feeders, where voltage would be higher in case of reverse active power flow. When it comes to parameter  $V_{max}$ , the aim is to select the highest value possible so as to avoid a possible excessive demand of reactive power, which leads to losses and is undesirable.

Wanting to specify the highest value of  $V_{max}$  which allows for each PV-integration level the use of the Q(V) strategy, a script is written in DPL (see Appendix C - DPL commands) and its flowchart is presented in Figure 5.15. The script takes into account the worst case scenario, thus low load conditions are assumed. The results are presented in Table 5.3.

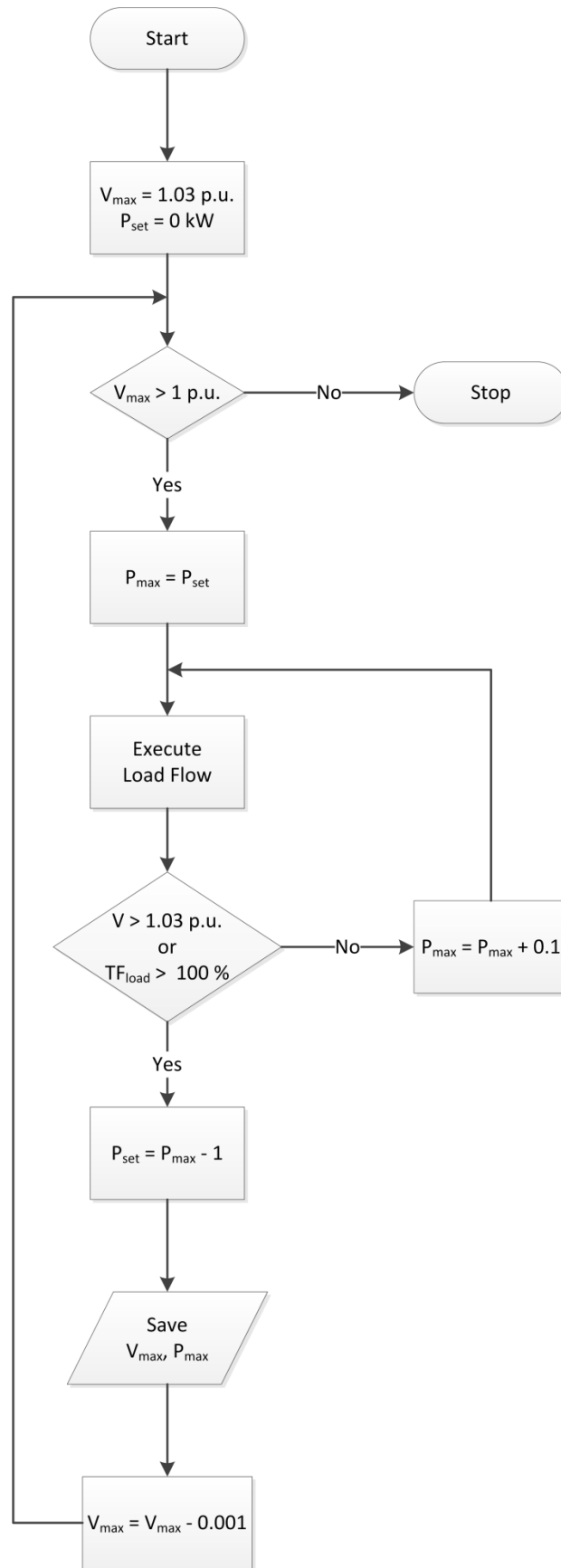


Figure 5.15: Flowchart of the script executed to calculate the highest value of  $V_{\max}$  which allows for each PV-integration level the use of Q(V) strategy

Table 5.3: PV hosting capacity with respect to  $V_{\max}$  parameter

$V_{\max}$ [p.u.]	PV hosting capacity [kW/household]	$V_{\max}$ [p.u.]	PV hosting capacity [kW/household]
<b>1.030</b>	8.6	<b>1.015</b>	9.7
<b>1.029</b>	8.7	<b>1.014</b>	9.7
<b>1.028</b>	8.8	<b>1.013</b>	9.7
<b>1.027</b>	8.8	<b>1.012</b>	9.8
<b>1.026</b>	8.9	<b>1.011</b>	9.8
<b>1.025</b>	9.0	<b>1.010</b>	9.9
<b>1.024</b>	9.1	<b>1.009</b>	9.9
<b>1.023</b>	9.2	<b>1.008</b>	9.9
<b>1.022</b>	9.3	<b>1.007</b>	9.9
<b>1.021</b>	9.4	<b>1.006</b>	10.0
<b>1.020</b>	9.5	<b>1.005</b>	10.0
<b>1.019</b>	9.5	<b>1.004</b>	10.0
<b>1.018</b>	9.6	<b>1.003</b>	10.1
<b>1.017</b>	9.6	<b>1.002</b>	10.1
<b>1.016</b>	9.6	<b>1.001</b>	10.1

The results of Table 5.3 are also verified through simulations with low load conditions and finally the selected values for  $V_{\max}$  for each PV-integration level, are specified (Table 5.4). It can be observed that for a PV-integration level of 10 kW/household, a very steep Q(V) characteristic is required, which is logical as the network reaches close to its maximum possible hosting capacity for the specified power factor limits of PV systems connected to it (see paragraph 5.3).

Table 5.4: Selection of  $V_{\max}$  parameter for different PV-integration levels

PV-integration level [kW/household]	$V_{\max}$ [p.u.]
<b>6</b>	1.030
<b>7</b>	1.030
<b>8</b>	1.030
<b>9</b>	1.023
<b>10</b>	1.003

### 5.3.2.1 Q(V) without storage

The target to maintain the voltage at every terminal below 1.03 p.u., using the Q(V) voltage support strategy, is achieved as it is shown in Figure 5.16, which plots the voltage of the weakest terminal for 6 and 10 kW/household PV-integration levels.

A characteristic of the Q(V) strategy is that not all PV systems contribute the same to the reactive power consumption that is required to keep the voltage under the specified limit. That happens because, in case of reverse power flow, the voltage at connection points closer to the MV/LV transformer is lower than the voltage at the end of the feeder. Thus, PV systems at the end of the feeder may consume the maximum of their reactive power capability while PV systems closer to the transformer may consume a very small amount of reactive power. This fact is presented in Figure 5.17. It is clear that due to lower voltage magnitude at terminal 2 than at

terminal 4 of feeder 1, the reactive power consumption of the PV system of terminal 2 is also lower than that of terminal 4.

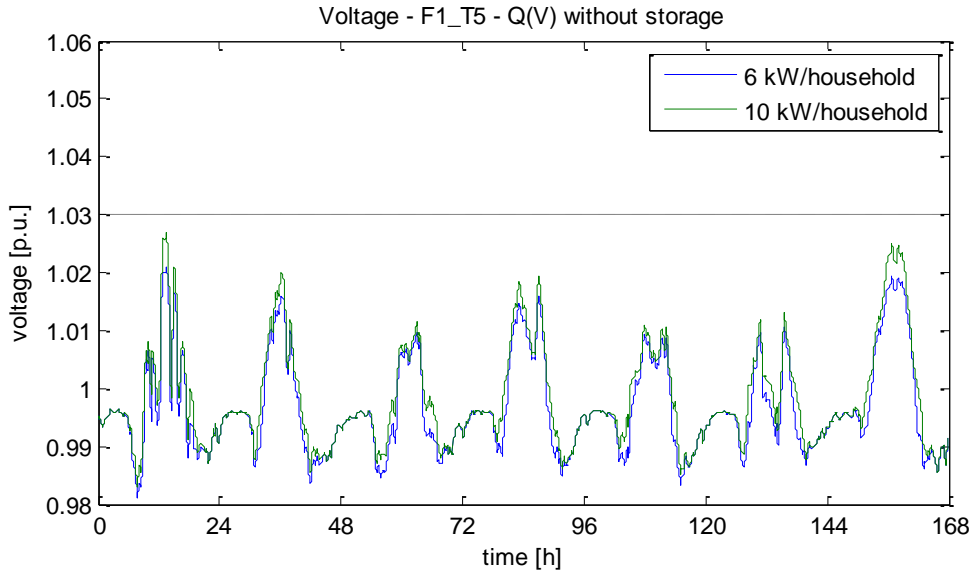


Figure 5.16: Voltage at the weakest terminal in case of Q(V) strategy without storage

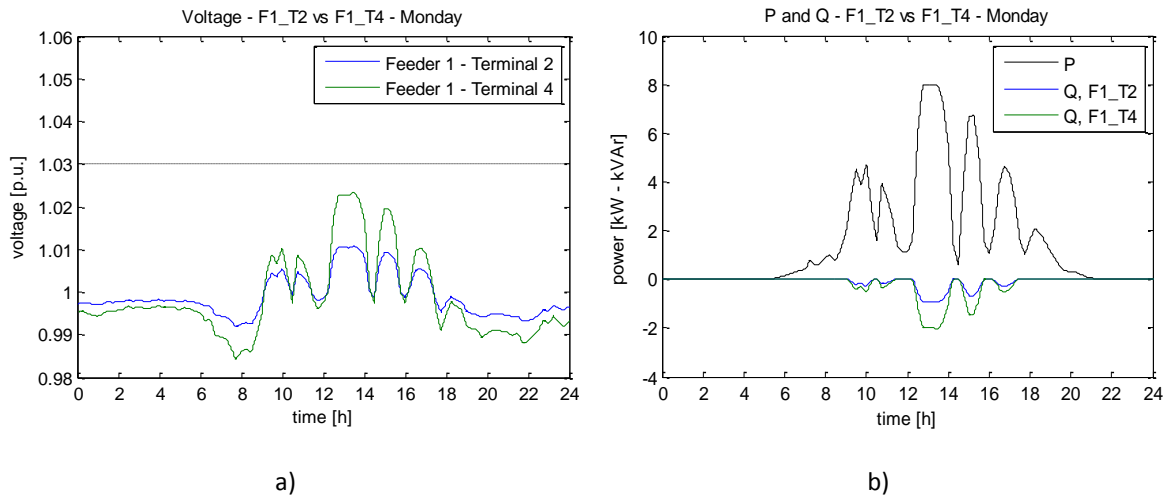


Figure 5.17: Comparison of the behaviour of Q(V) strategy at different terminals: a) daily voltage measurements, b) active and reactive power injection

**5.3.2.2 Q(V) with battery storage**

The same series of simulations are executed activating the battery storage option. The results concerning the voltage at the weakest terminal are presented in Figure 5.18, for 6 and 10 kW/household PV-integration levels.

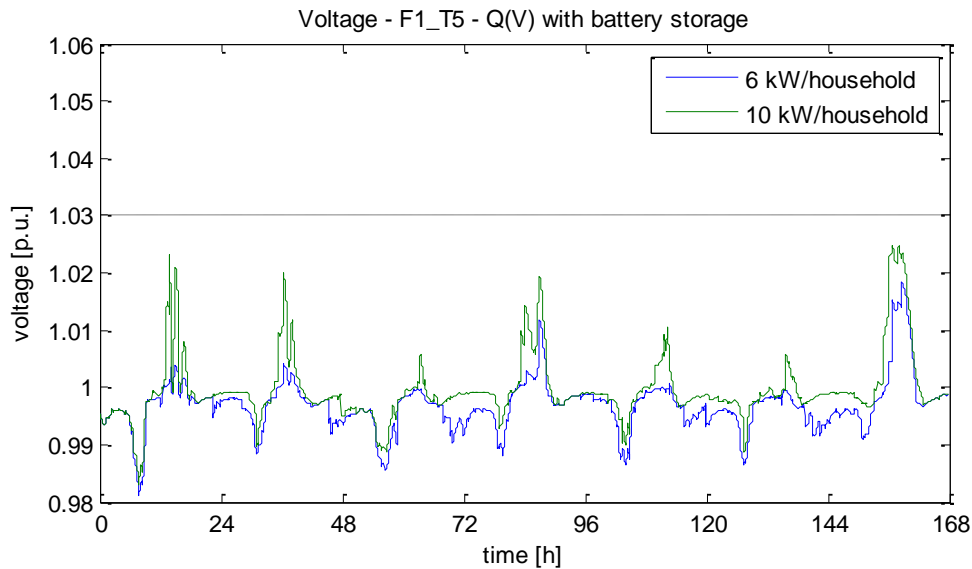


Figure 5.18: Voltage at the weakest terminal in case of Q(V) strategy with battery storage

### 5.3.3 Comparison of reactive power based voltage support strategies

Both reactive power based voltage support strategies, with and without battery storage, succeed in mitigating voltage rise problem up to a PV-integration level of 10 kW/household. However, when increasing the PV integration level of the test LV network, a question regarding grid losses arises:

*“How grid losses are influenced by the increase of PV-integration level?”*

Figure 5.19 presents grid losses during the weekly simulation, which consist of the transformer and line losses, for PV-integration levels from 6 - 10 kW/household, using PF(P) and Q(V) voltage support strategies, with and without battery storage. In the same figure, grid losses are plotted for the case that no voltage support is provided. It is shown in paragraph 5.3 that up to a PV-integration level of 5 kW/household no voltage support is actually required. However, comparing the resulting curves, for PV-integration levels greater than 6 kW/household, differences in grid losses are observed.

PF(P) and Q(V) strategies without storage exhibit greater grid losses than the case no voltage support strategy is activated. This difference is due to the increased reactive power flow in the network caused by the reactive power control of PV systems in order to mitigate voltage rise. It is observed that for a range of 6 – 9 kW/household, Q(V) strategy leads to lower grid losses than PF(P) strategy. This is reversed for the PV-integration level of 10 kW/household, when Q(V) strategy shows higher losses mainly due to its steep characteristic curve that requires high reactive power absorption from all PV systems. Although the same tendency appears between PF(P) and Q(V), when battery storage is also enabled, grid losses are lower than the case no voltage support strategy is activated because of self-consumption that lowers the active power flow in the network.

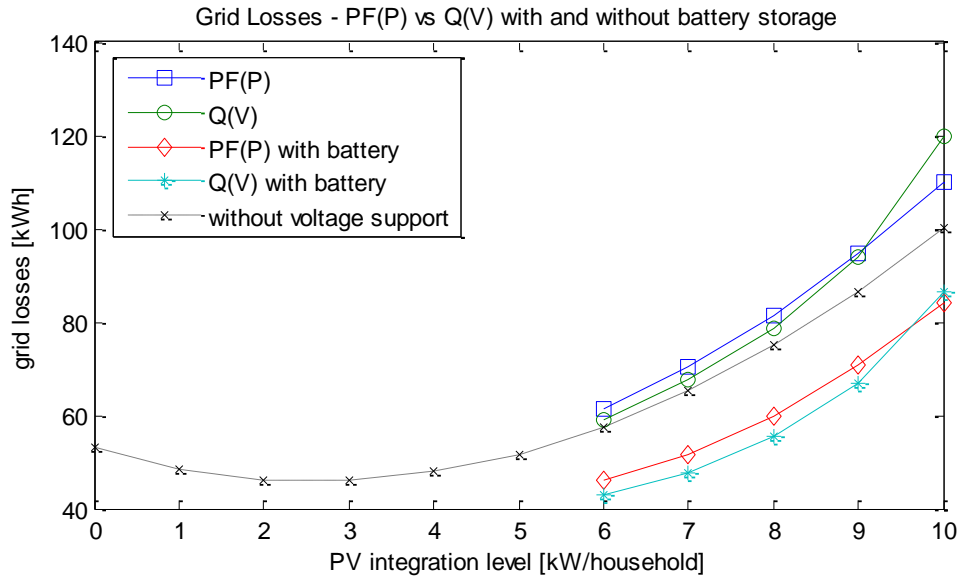


Figure 5.19: Weekly grid losses comparison for the reactive power control strategies

However, apart from grid losses, significant battery losses also appear in case battery storage is used (Figure 5.20). They are independent of the reactive power strategy used as the charging/discharging control algorithm depends only on the local active power generation and consumption (see paragraph 4.3.7). It seems that the reduction of grid losses, in case battery storage is used, is by far less than the increase in battery losses, thus the LV network seems to be less efficient. Nevertheless, more information would be required regarding losses caused by the reactive power flow in other voltage levels of the transmission and distribution system.

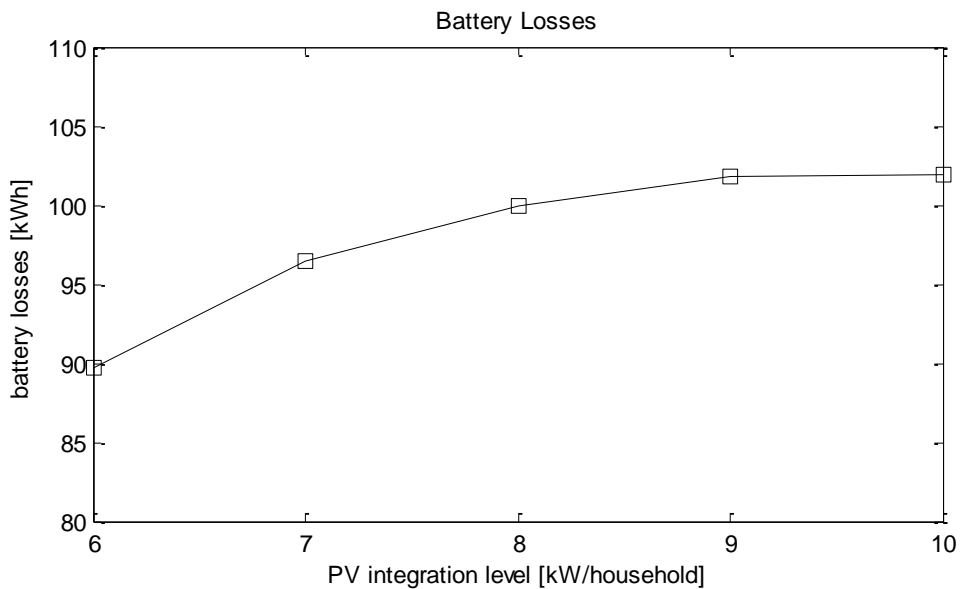


Figure 5.20: Weekly losses of all the battery systems

The reactive power consumed additionally enlarges the loading of the grid equipment and demands measures for compensation. The more reactive power is consumed by distributed generators, such as PV systems, the higher the need from transmission system operators (TSO) to provide the lack of reactive power in their grids. Therefore, an effective concept of reactive

power consumption is needed in order to increase the hosting capacity of distribution networks without causing additional measures in other places or network levels.

Figure 5.21 shows the trend of the maximum reactive power demand from the external grid, using PF(P) and Q(V) strategies, with and without storage, as the PV-integration level increases. Q(V) strategies exhibits better results than PF(P) ones especially in the range of 6 – 9 kW/household. It should be noted that the increase in maximum reactive power demand from the external grid throughout the simulations reached up to around 700 % comparing with the case that no voltage support is considered. This fact may lead to the requirement of supplemental reactive power compensation systems, which means additional investments from the power system operators.

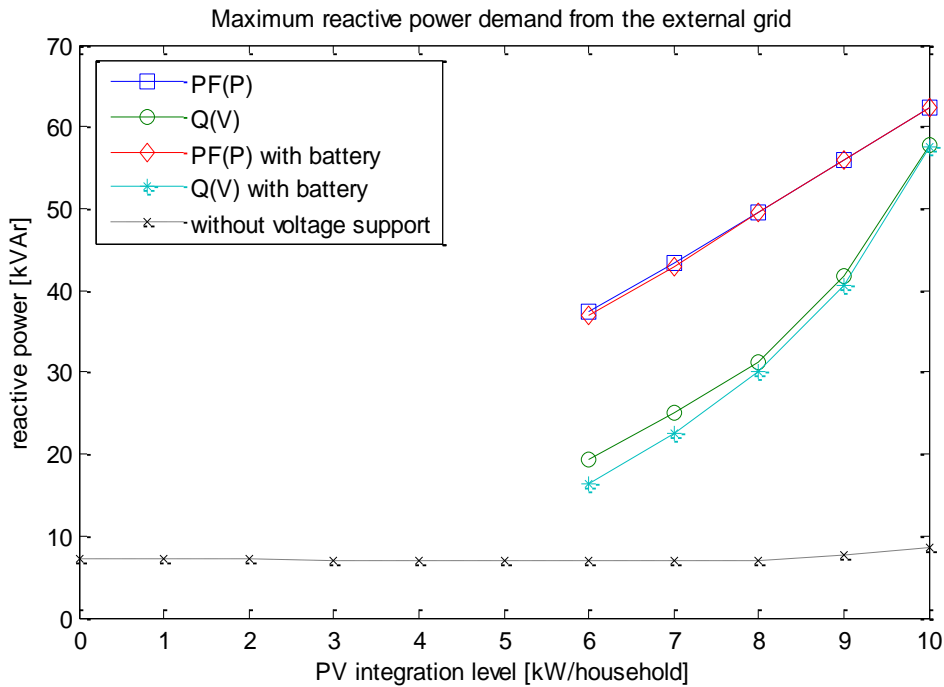


Figure 5.21: Maximum reactive power demand from the external grid

Besides the increase in hosting capacity, and eventually in PV energy yield, through the use of these reactive power based voltage support strategies, it is also important how much reactive power in time has to be provided to reach a certain PV-integration level. A way to evaluate this criterion can be through a quality index defined as follows [34]:

$$quality\ index = \frac{\int P_{PV,tot} dt}{\int S_{PV,tot} dt} \quad (5.3)$$

The numerator is the total PV energy yield of all PV systems of the network throughout the simulation and the denominator is the corresponding apparent “energy”:

$$P_{PV,tot} = \sum_{i=1}^{10} P_{PV,i} \quad (5.4)$$



$$S_{PV,tot} = \sum_{i=1}^{10} \sqrt{P_{PV,i}^2 + Q_{PV,i}^2} \quad (5.5)$$

An example of the difference in reactive power consumption by a PV system connected in the network, between the PF(P) and Q(V) strategies is shown in Figure 5.22. The apparent power, whose integral is used in the denominator of the quality index, is also plotted in the same figure. It can be observed that, for this PV-integration level, PF(P) strategy consumes more reactive power than Q(V) one, while both succeed in keeping the voltage below the permitted limit. Apart from the increased losses caused to the grid, costs for the compensation of reactive power may also be relevant, if the DNO has to compensate its reactive power flows. Furthermore, the more reactive power is consumed by a PV inverter the more it is loaded thus its lifetime can be negatively influenced [58].

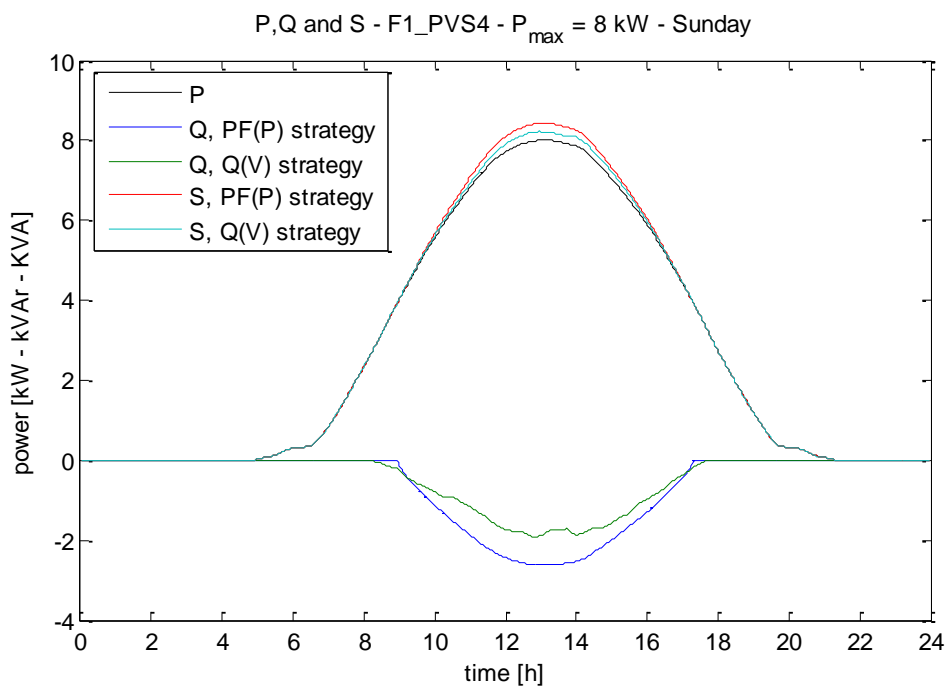


Figure 5.22: Difference in reactive power requirement between PF(P) and Q(V) strategies

Figure 5.23 plots the quality index for the PV-integration range of 6 – 10 kW/household. Because of the dependence of reactive power consumption only on active power production, the quality index is the same and constant in case of PF(P) strategies. In contrast, the reduction of the quality index in case of Q(V) strategies reveals that the ratio of reactive power demand over time per active power generation over time gets higher as PV-integration level and eventually energy yield increases.

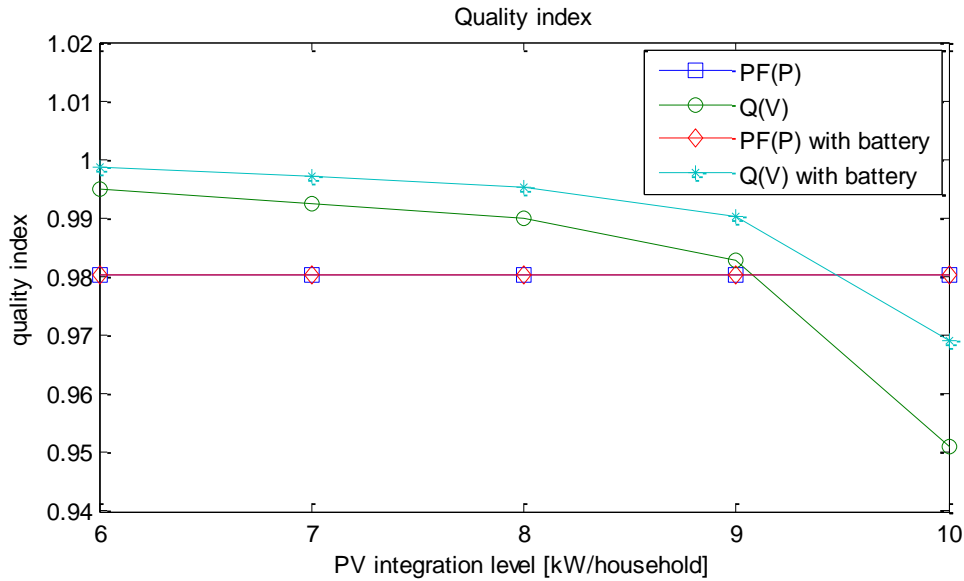


Figure 5.23: Quality index comparison among the reactive power control strategies

Q(V) strategies present higher quality indices than PF(P) ones for a range of 6 – 9 kW/household, although this is reversed for the PV-integration level of 10 kW/household. Moreover, the quality index is higher for the Q(V) strategy with battery storage than for the same strategy without storage as at times battery systems are in charging state, voltage at their terminals is lower and thus also lower reactive power absorption is demanded by the reactive power controllers.

## 5.4 Dynamic active power curtailment strategies

DAPC control mode, as presented in paragraph 4.3.5, is activated in the active power controller of the PV-Battery systems, while the reactive power controller is set to unity fixed power factor (no reactive power is absorbed by PV systems). The effectiveness and behaviour of DAPC voltage support strategy is then tested through, a series of simulations, under normal load conditions, for PV integration levels from 6 - 10 kW/household, with a step of 1 kW/household.

The DPL script, whose flowchart is presented in Figure 5.6, is executed again, but now only under unity power factor and no load conditions, in order to estimate the highest possible value for  $P_{\text{curt,set}}$  parameter, as defined in Table 4.9. This parameter is selected to match the maximum net generation per household over which voltage rises above the limit at the weakest terminal of the network. The estimated value for the maximum net generation of the studied network is 5 kW/household.

### 5.4.1 DAPC without storage

The target to maintain the voltage at every terminal below 1.03 p.u., using the DAPC voltage support strategy, is achieved as it is shown in Figure 5.24, which plots the voltage of the weakest terminal for 6 and 10 kW/household PV integration levels.

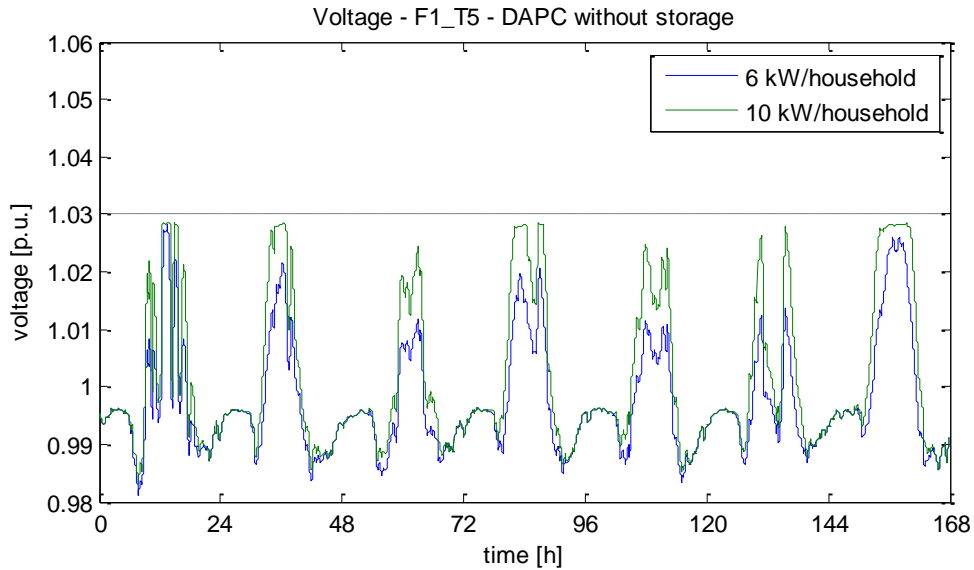


Figure 5.24: Voltage at the weakest terminal in case of DAPC strategy without storage

An example of the operation of the DAPC control mode is presented in Figure 5.25. The dynamic limitation curve is the “load demand” curve offset by the net generation limit. In this way, the area between the “ideal PV generation” and “actual PV generation” curves corresponds to the PV energy loss due to the power curtailment.

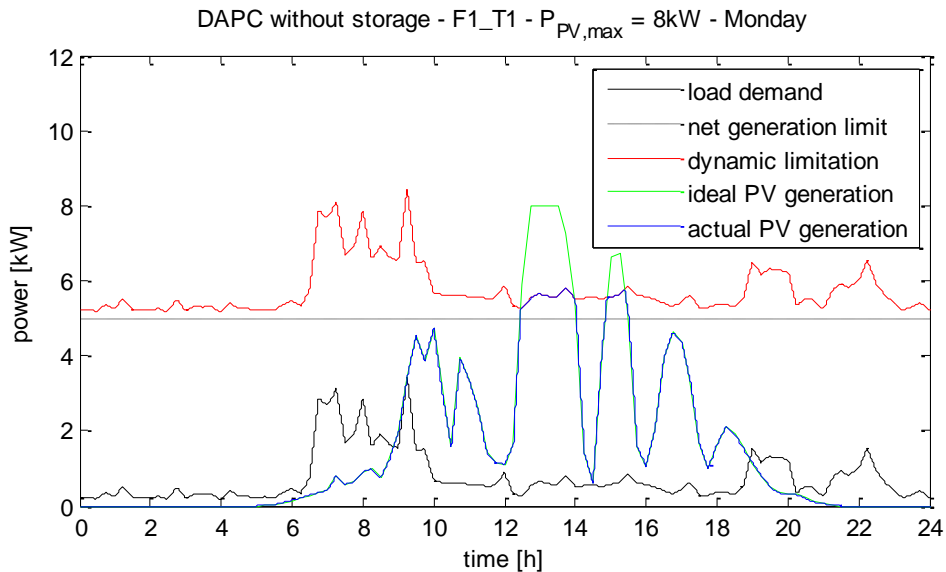


Figure 5.25: Operation of DAPC strategy without storage for one of the PV systems connected in the network

#### 5.4.2 DAPC with battery storage

Activating the battery storage option the same series of simulations are executed again. The results concerning the voltage at the weakest terminal are presented in Figure 5.26, for 6 and 10 kW/household PV integration levels. As it turns out, the target to limit the voltage below 1.03 p.u. is achieved.

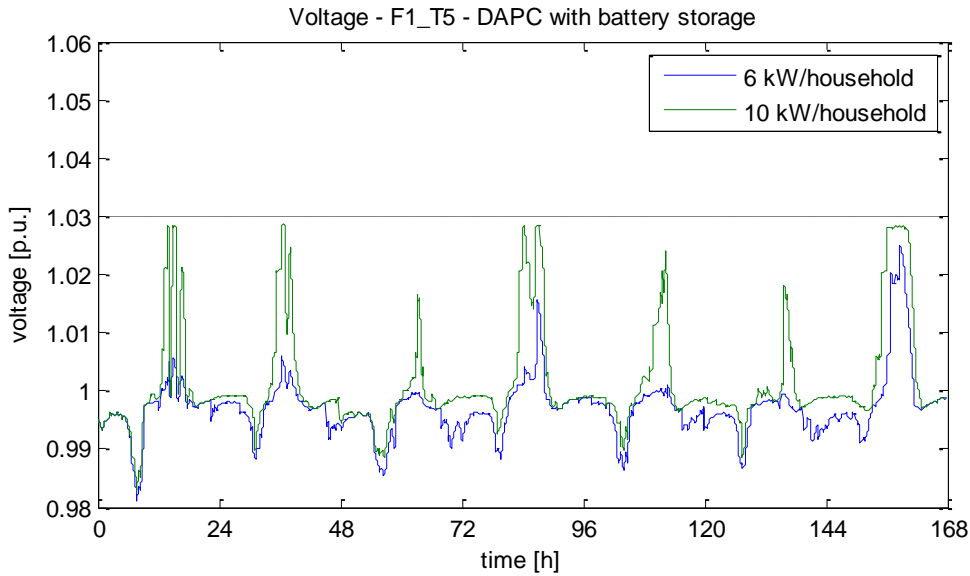


Figure 5.26: Voltage at the weakest terminal in case of DAPC strategy with battery storage

An example of the operation of the DAPC control mode with battery storage is presented in Figure 5.27. In this case, the dynamic limitation curve is the “load demand” curve plus the opposite of the charging part of the “battery power” curve offset by the net generation limit. The area between the “ideal PV generation” and “actual PV generation” curves corresponds to the PV energy loss due to the power curtailment and as it can be observed, it is smaller than that of Figure 5.25.

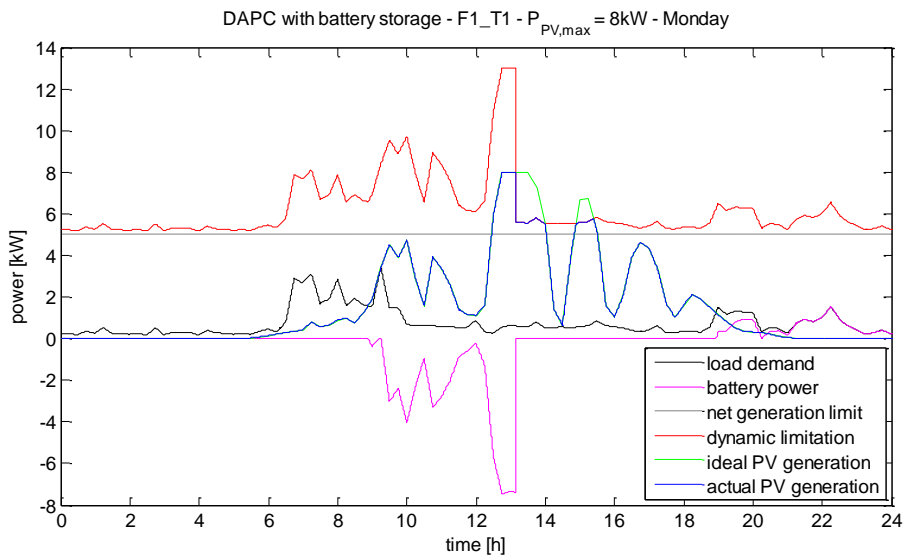


Figure 5.27: Operation of DAPC strategy with battery storage for one of the PV systems connected in the network

### 5.4.3 Comparison of the DAPC voltage support strategies

Both DAPC voltage support strategies, with and without battery storage, succeed in mitigating voltage rise problem. However, as in the case of reactive power based strategies, they are compared to each other based on a set of selected criteria.

The first comparison is related to grid losses and the results are presented in Figure 5.28. Both alternatives exhibit grid losses less than the case without voltage support due to the curtailed active power which would cause losses by flowing in the grid. Because of the self-consumption scheme, when battery storage is activated, grid losses are even lower than the case without storage. On the other hand, battery losses appear as a result of batteries' energy exchange (see Figure 5.20).

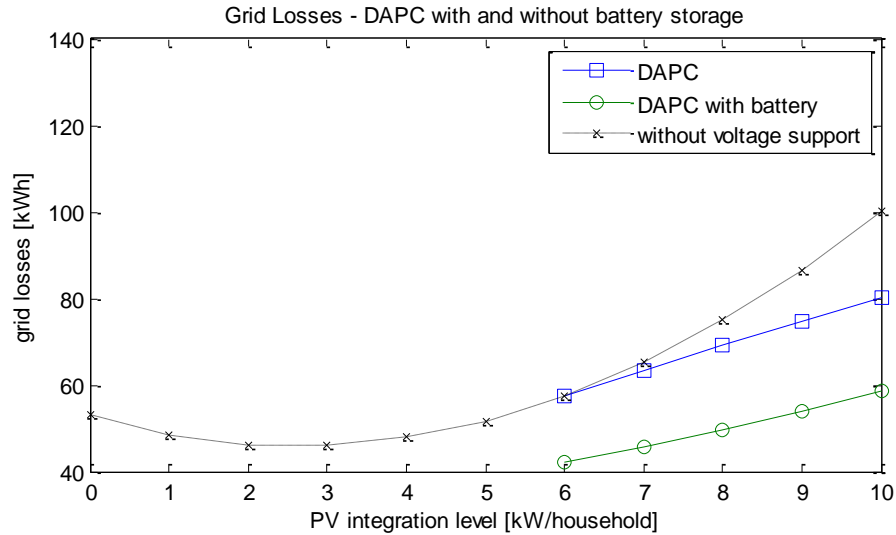


Figure 5.28: Weekly grid losses comparison for the DAPC strategies

As a result of the active power curtailment, a part of the possible PV energy yield, throughout the study period, is consequently curtailed. Yield loss, which is defined in equation (5.6), is plotted for both DAPC alternatives, in Figure 5.29.

$$\text{Yield loss} = \frac{\text{actual yield}}{\text{maximum possible yield}} \cdot 100\% \quad (5.6)$$

It is observed that as PV-integration increases, yield losses become rather significant. The differences between the cases with and without storage lie on the availability of the batteries to store a portion of the energy that otherwise would be curtailed.

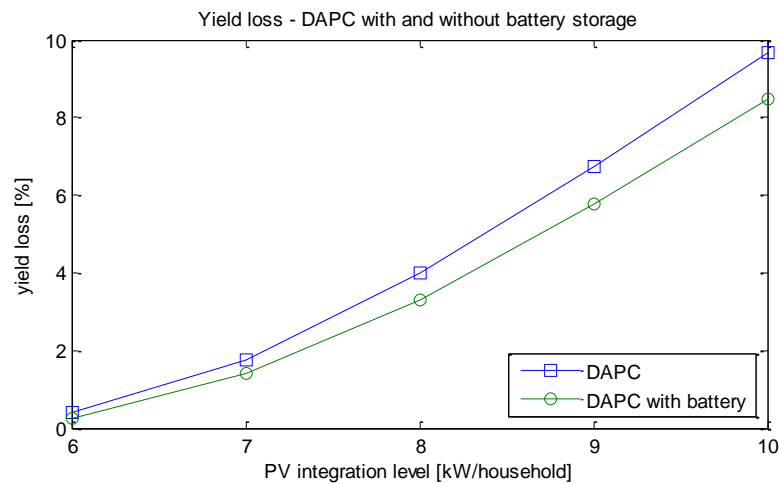


Figure 5.29: Yield losses comparison

## 5.5 Overall comparison

It is clear from the analysis so far that the studied voltage support strategies perform differently in the following evaluation criteria:

- grid losses
- battery losses
- maximum reactive power demand
- reactive power performance (quality index)
- yield loss

An overview of the performance of all the strategies in the criteria above is presented in Figure 5.30. A difficulty arises in the overall comparison among them as there is not a unique one which performs the best in all the criteria.

### 5.5.1 Formulation of an overall evaluation criterion

When there are more than one objective that a solution method is expected to satisfy, then the need for an overall evaluation criterion (OEC) arises [59]. In engineering an overall index is not so common because of the following difficulties:

- Units of measurement – the criteria of evaluations in engineering and science are generally different and the same applies to their units.
- Relative weighting – Not all the criteria of evaluation are of equal importance.
- Sense of the quality characteristic (QC) – The quality characteristic indicates the direction of desirability of the evaluation numbers. Depending on the criteria and how they are measured, QC can be “bigger is better”, “smaller is better”, or “nominal is the best”. Unless the quality characteristics of different criteria are the same, the evaluation numbers cannot be readily combined.

In the case of the criteria set for the evaluation of the studied strategies all the above difficulties are valid. This situation is summarised in Table 5.5.

Table 5.5: Differences of evaluation criteria

Criterion	Symbol	Unit	Relative weighting	Quality characteristic
Grid losses	$L_G$	kWh	$W_{LG}$	<i>smaller is better</i>
Battery losses	$L_B$	kWh	$W_{LB}$	<i>smaller is better</i>
Maximum Q demand	$Q_{max}$	kVAr	$W_{Qmax}$	<i>smaller is better</i>
Q performance	$P_Q$	-	$W_{PQ}$	<i>bigger is better</i>
Yield loss	$L_Y$	%	$W_{LY}$	<i>smaller is better</i>

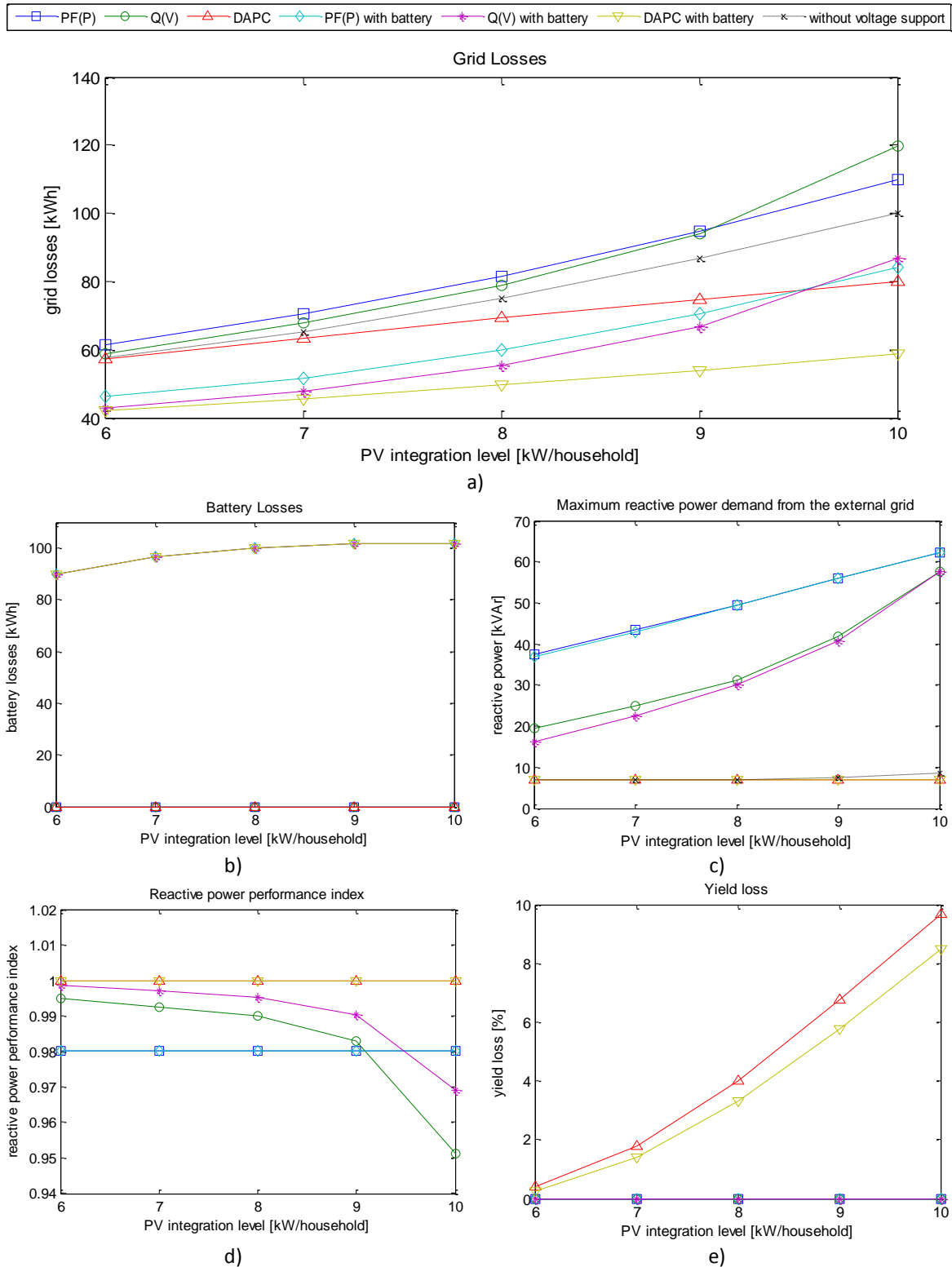


Figure 5.30: Overview of the performance of all strategies in the evaluation criteria: a) grid losses, b) battery losses, c) maximum reactive power demand from the external grid, d) reactive power performance index and e) yield loss

Therefore, what is needed is a properly formulated OEC number representing the overall performance of the tested strategies. In order to combine the different criteria, they must first be normalised and weighted accordingly. Then, for each PV-integration level  $i$  and for each strategy  $j$ , an OEC is formulated as follows:

$$\begin{aligned}
OEC_{i,j} = & \left(1 - \frac{L_{G,i,j} - \min\{L_{G,i}\}}{\max\{L_{G,i}\} - \min\{L_{G,i}\}}\right) \cdot W_{L_G} + \left(1 - \frac{L_{B,i,j} - \min\{L_{B,i}\}}{\max\{L_{B,i}\} - \min\{L_{B,i}\}}\right) \cdot W_{L_B} \\
& + \left(1 - \frac{Q_{max,i,j} - \min\{Q_{max,i}\}}{\max\{Q_{max,i}\} - \min\{Q_{max,i}\}}\right) \cdot W_{Q_{max}} + \frac{P_{Q,i,j} - \min\{P_{Q,i}\}}{\max\{P_{Q,i}\} - \min\{P_{Q,i}\}} \cdot W_{P_Q} \quad (5.7) \\
& + \left(1 - \frac{L_{Y,i,j} - \min\{L_{Y,i}\}}{\max\{L_{Y,i}\} - \min\{L_{Y,i}\}}\right) \cdot W_{L_Y}
\end{aligned}$$

Before all evaluation criteria can be combined, their QCs must all be the same. By choosing an OEC number with a “bigger is better” QC, all the criteria with “smaller is better” QC are properly converted to the desired QC by subtracting the normalising fraction from 1. The numerator in each term is calculated by subtracting the smaller magnitude of all the strategies from the one associated with the specific strategy whose OEC is being calculated. The denominator is the positive difference between the best and the worst magnitude for the criteria.

An average OEC is then calculated for each strategy, taking into account the OEC values of each PV-integration level, as follows:

$$OEC_{av,j} = \frac{1}{5} \cdot \sum_{i=1}^5 OEC_{i,j} \quad (5.8)$$

### 5.5.2 Relative weighting of the evaluation criteria

In order to calculate the relative weights of the evaluation criteria, eight independent experts (DNV GL – Energy consultants, a DNO consultant, a TU Delft professor and a TU Delft PhD candidate) were asked to determine the ranking of the various criteria. This procedure was conducted through the use of a multicriteria-analysis software which combines a pairwise comparison method and a “Fuzzy Logic” algorithm to determine and quantify the comparative importance of the criteria.

The experts were asked to determine the ranking of the criteria twice as there are two main stakeholders involved in the operation of the LV network with connected PV systems, namely the DNO and PV system owners. The relative weights of the evaluation criteria were thus calculated for both the perspectives of a DNO and a PV system owner (Table 5.6).

Table 5.6: Relative weights of the evaluation criteria

Criterion	Relative weights [%]	
	DNO	PV system owner
Grid losses	23.3	12.6
Battery losses	12.6	25.9
Maximum Q demand	24.4	13.8
Q performance	24.2	19.6
Yield loss	15.5	28.2



### 5.5.3 Choosing the best strategy

As it is indicated by the weights obtained, the choice of the best strategy heavily depends on the perspective of the involved stakeholders. Grid losses, for example, are a major issue for a DNO while they are of minor importance for a PV system owner. The reverse is valid for battery losses while the performance of a reactive power based strategy is of common interest.

Figure 5.31 presents the ranking of the strategies based on their average OEC value, as it is calculated from equation (5.8). It is observed that the best voltage support strategy for a DNO is DAPC with battery storage while for a PV system owner this strategy ranks in the second lowest position. Q(V) strategy seems to be superior for an owner of a PV system but it ranks fourth in the DNO's preference. Thus a conflict of interests seems to arise.

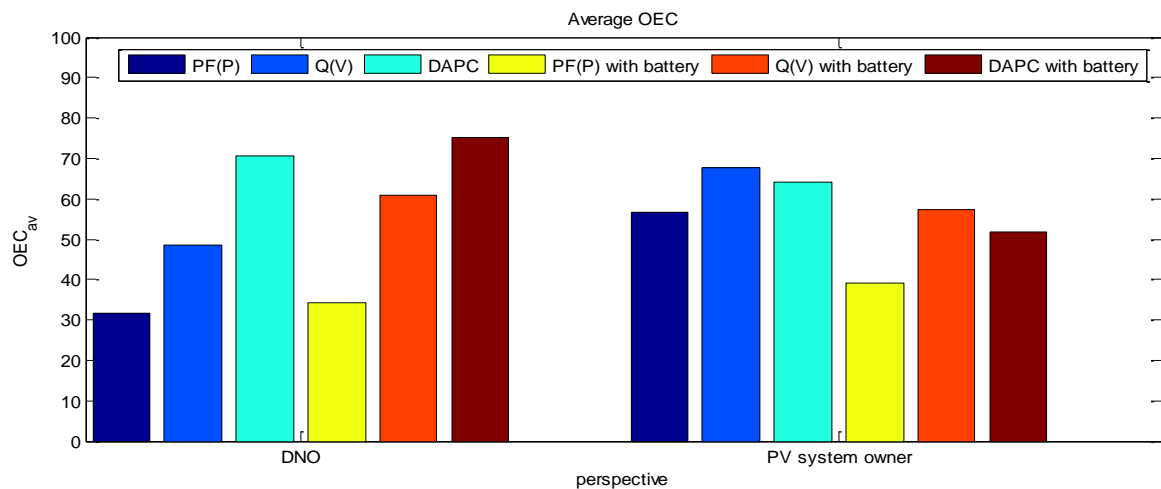


Figure 5.31: Ranking of the studied voltage support strategies

An interesting observation is how the overall performance of each strategy varies according to the PV-integration level. Figure 5.32 and Figure 5.33 present the OEC values of the studied strategies with respect to the PV-integration level for a DNO's perspective and a PV system owner's perspective respectively.

For the former, DAPC strategy, with and without battery storage, gathers a high score considering the whole studied PV-integration range. Q(V) strategies, while comparable with DAPC ones at lower PV-integration levels, they present a declining trend, as the integration increases, and finally gather the lowest scores at 10 kW/household. These are even lower than the ones of PF(P) strategies, which are the most unfavourable of all for the range of 6-9 kW/household. For the same range, the DNO clearly favours the option of battery storage, considering the same type of strategy.

On the other hand, a PV system owner would prefer to avoid the battery storage option, considering the same type of strategy. Q(V) strategies, while generally the most preferable ones, show a downward trend and finally gather the lowest scores at 10 kW/household. On the contrary, PF(P) alternatives, while generally the least favourable, tend to be the predominant choice at 10 kW/household. Finally, when it comes to DAPC strategies, they are in the second place from 6 to 8 kW/household but present rather competitive at 9 and 10 kW/household.

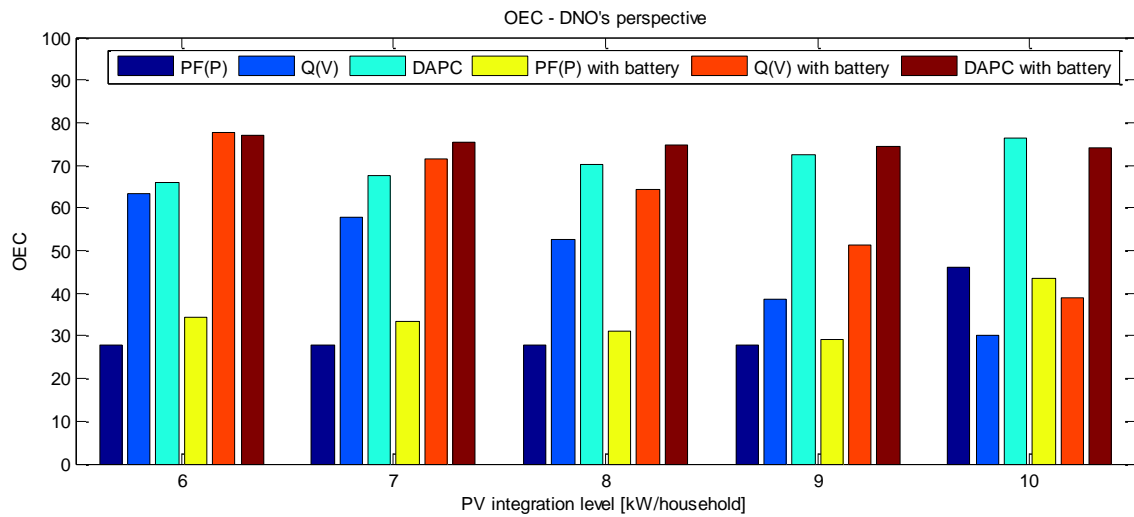


Figure 5.32: OEC comparison with respect to the PV-integration level according to the DNO's perspective

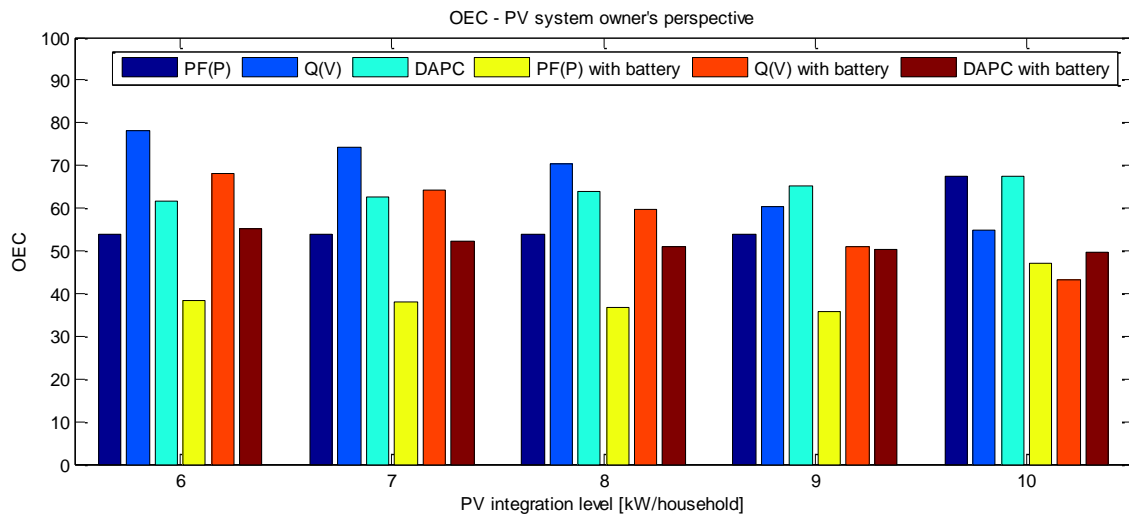


Figure 5.33: OEC comparison with respect to the PV-integration level according to the PV system owner's perspective

---

## Conclusions and future work

In this chapter the conclusions extracted from this study as well as some recommendations for future work are presented.

### 6.1 Conclusions

#### 6.1.1 Main conclusions

The test and comparison of the studied voltage support strategies led to the following main conclusions:

- All studied strategies manage to mitigate the voltage rise problem, in the test network, for the range of 6-10 kW/household PV integration, achieving 86% more PV hosting capacity than the case without voltage support.
- The comparison of all the three type of strategies studied, with and without the storage option, and the selection of the best candidate proves not to be an easy procedure. Each strategy may be more appropriate regarding a specific criterion for a specific PV-integration level but may be disadvantageous considering another criterion and another PV-integration level. The viewpoints of the main stakeholders involved (DNO, PV system owner) are also different regarding the relative importance of each criterion.
- Through the help of energy experts from various professional positions, the overall evaluation criterion, which is introduced in the form of a score number, reveals the overall preference of a DNO for DAPC strategy with battery storage in contrast to the overall preference of a PV system owner for Q(V) strategy without storage.
- The preference of each stakeholder varies with respect to the PV-integration level. Generally, a DNO seems to favour active power curtailment and local battery storage while a PV system owner would prefer a reactive power based strategy without storage.

#### 6.1.2 Specific findings

##### Integration of PV systems in LV networks:

- Power systems face a transition from centralized to distributed generation and specifically renewable generation, such as PV, due to electricity market opening, environmental awareness and increasing electricity demand. Most PV systems are connected to the LV distribution network, especially in rural areas where vast available space is offered on rooftops of houses and farms. However, rural networks are generally rather weak (low level of interconnection, long distances, low load density, low short circuit power) and thus more prone to voltage rise situations when the power consumed is lower than the power produced.

- Grid codes and regulations set the limits to voltage variations in order to secure power quality and define the requirements for the connection of DG in the LV network. The possible violation of the upper voltage limit, in cases of low consumption and high generation, places an obstacle to the integration of more RES in the power systems and consequently hinders the global target to achieve a sustainable future energy supply.
- Load flow calculations, on a suitably designed rural LV network model, show that for conductors (OHL and cables) with the same ampacity the problem is more intense in the case OHLs are used instead of cables. Conductor and transformer loadings do not initially constitute a problem in further PV integration.

#### **Voltage sensitivity of a LV network on active and reactive power:**

- The implementation of local voltage support strategies, based on reactive power absorption by PV inverters and active power curtailment, are suggested by the new connection standards.
- Voltage sensitivity analysis on active and reactive power on the test network's terminals shows that, comparing the two types of conductors, both sensitivities present higher values in the case of OHLs than in the case of cables. Thus both active and reactive power based voltage support strategies are more effective in mitigating the voltage rise problem when OHLs are used.
- For both conductor types voltage sensitivity in active power is lower than the one in reactive power for terminals closer to the transformer as short-circuit reactance becomes dominant over the short-circuit resistance at these locations. As the distance to the transformer increases along the feeder, line resistance contributes more on the impedance and as a result voltage sensitivity in active power is higher than the one in reactive power for the terminals which are deeper in the feeder. Hence, reactive power based voltage support strategies are more effective in case of PV systems connected close to the transformer while for PV systems connected deeper in a LV feeder active power based strategies seem more suitable.

#### **Reactive power based voltage support strategies and battery storage:**

- By allowing PV inverters to absorb reactive power a significant increase in the network's PV hosting capacity can be achieved while keeping the voltage level under the specified upper limit. For the test rural LV network this increase reached up to 86 %. Reactive power absorption can relocate the limiting criterion of hosting capacity from voltage towards transformer or conductor loading limitation from a certain hosting capacity upwards, as it was shown in the case of cable usage on the test network.
- The parameterisation of PF(P) characteristic needs attention as it may lead to violation of upper voltage limit in low irradiance conditions while being effective in higher irradiance, if it is not carefully designed.
- Using PF(P) strategy, inverters will absorb reactive power regardless of their location in the feeder. As a result inverters might absorb reactive power even though it may not be required (no significant voltage rise situation).
- Q(V) characteristic also requires attention in its parameterisation so as not to lead to excessive unnecessary reactive power demand.

- Using Q(V) strategy, not all PV systems contribute the same to the reactive power consumption that is required to keep the voltage under the specified limit. That happens because, in case of reverse power flow, the voltage at connection points closer to the MV/LV transformer is lower than the voltage at the end of the feeder. Thus, PV systems at the end of the feeder may consume the maximum of their reactive power capability while PV systems closer to the transformer may consume a very small amount of reactive power.
- The performance of Q(V) strategy in all criteria (grid losses, maximum reactive power demand from the external grid, quality index) appears better than that of PF(P) one up to a certain PV integration level but gets worst in most criteria as the network reaches close to its maximum possible hosting capacity for the specified power factor limits of PV systems connected to it.
- The presence of battery storage in each PV system connected to the network improves self-consumption and as a result grid losses and reactive power demand decrease. However, battery losses are introduced.

#### **Dynamic active power curtailment strategies and battery storage:**

- DAPC strategy succeeds in mitigating the voltage rise problem at the cost of yield loss which becomes rather significant as the PV-integration level increases. Grid losses appear less than the case without voltage support due to the curtailed active power which would cause losses by flowing in the grid.
- Because of the self-consumption scheme, when battery storage is activated, grid losses are even lower than the case without storage. On the other hand, battery losses appear as a result of batteries' energy exchange.

## **6.2 Recommendations for future work**

Possible tasks suggested for future work can be:

- Validation of the results on Watt connects interactive table in order to incorporate the (unpredictable) customer's behaviour.
- Substitution of the designed LV test network with actual ones and comparison of the results in order to investigate the range of the possible differences.
- Prolongation of the time period of study to a full year to include the seasonal variation of PV generation and its impact on the evaluation criteria.
- Economic evaluation of the studied voltage support strategies, maybe the most crucial deciding factor for the selection of the best candidate strategy.
- Implementation and test of other voltage support solutions like OLTC transformers and storage at the distribution substation level or other strategically defined location.



## Appendix A - OHL modelling

The physical geometry of overhead lines for a typical European LV network is shown in Figure A.1 and the specifications of the model used are given in Table A.1 [48, 60].

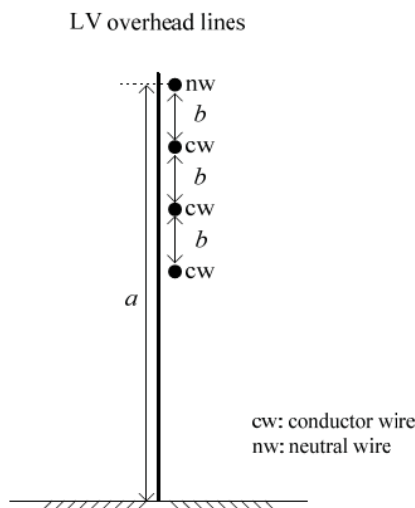


Figure A.1: Geometry of overhead lines for a typical European LV network [48]

Table A.1: Characteristics of the OHLs used in the model [48, 60]

Material	Size [mm <sup>2</sup> ]	Outer diameter [mm]	GMR [mm]	DC-Resistance [Ω/km]	Ampacity [A]	a [m]	b [m]
Al	70	10.5	3.98	0.4367	270	8	0.3

In PowerFactory's environment, in order to model the selected OHLs, the "TypTow" tower geometry type is used and the electrical parameters are provided by the phase impedance matrix. As neutral wires are not included in this type the phase impedance matrix after Kron reduction is used (Table A.2) [48].

Table A.2: Phase impedance matrix after Kron reduction (Ω/km) [48]

Phase	A	B	C
A	0.616 + j0.588	0.131 + j0.306	0.141 + j0.245
B	0.131 + j0.306	0.628 + j0.566	0.147 + j0.276
C	0.141 + j0.245	0.147 + j0.276	0.650 + j0.527

Regarding the option of cable usage, the already available type, in PowerFactory's library, NA2XY 3x120 mm<sup>2</sup>, is chosen in order to match the ampacity of the conductor used as OHL, for loading comparison purposes throughout the simulations.





## Appendix B - DSL models' code

### “Load Data Process” block definition:

```
model Pext,Qext = 'BlkDef Load Data
Process' (P,Q;;scale,PF,ExtCtrl_Q,base_load,P_base,Q_base;)
  Pext=scale*select(base_load, P_base, P)
  Qext=scale*select(base_load, Q_base, select(ExtCtrl_Q, Q,
P*tan(acos(PF))))
```

### “PV generation profile” block definition:

```
model P_av = 'BlkDef PV generation profile' (I;;PF_lim;)
  inc(P_av)=0
  inc(I)=0
  P_av=lim((I/1000)*PF_lim,0,PF_lim) ! available active power in p.u.
```

### “Active Power Control” block definition:

```
model id_ref,P = 'BlkDef Active Power
Control' (P_av,P_load_A,P_load_B,P_bat,u;x;S_nom,DAPC,P_curt_set,T;P_load
,P_curt_lim,P_lim,P_bat_charge)
  inc(P)=0
  inc(x)=0
  P_load=P_load_A+P_load_B
  P_bat_charge=select(P_bat>0,P_bat,0)
  P_curt_lim=(P_curt_set+P_load+P_bat_charge)/S_nom
  P_lim=select(DAPC<0.5,P_av,P_curt_lim)
  P=lim(P_av,0,P_lim)
  limits(T)=(0,)
  x.=(P-x)/T
  id_ref=x/u
```

### “Reactive Power Control” block definition:

```
model iq_ref = 'BlkDef Reactive Power
Control' (u,P;x;mode_Q,PF_fixed,PF_lim,u_max,u_sp,P_sp,T;Q,Q_0,Q_1,Q_2,Q_
lim,PF_P)
  inc(Q)=0
  inc(x)=0
  Q_0=select(P<0.2*PF_lim,0,-P*tan(acos(PF_fixed)))
  PF_P=lim(((PF_lim-1)*(P-P_sp*PF_lim))/(PF_lim*(1-P_sp))+1,PF_lim,1)
  Q_1=-P*tan(acos(PF_P))
  Q_lim=-P*tan(acos(PF_lim))
  Q_2=lim((u-u_sp)/(u_max-u_sp)*Q_lim, Q_lim,0)
  Q=select(mode_Q<0.5,Q_0,select(mode_Q<1.5,Q_1,Q_2))
  limits(T)=(0,)
  x.=(Q-x)/T
  iq_ref=-x/u
```

**"Battery Control" block definition:**

```

model P_bat,id_ref,iq_ref = 'BlkDef Battery
Control'(u,P_av,P_load_A,P_load_B;x1,x2;EnableStorage,S_PV_nom,C,S_bat_n
om,T;P_load,P_bat_av,SOC,eff)
  inc(x1)=20
  inc(x2)=0
  inc(P_bat)=0
  P_load=P_load_A+P_load_B
  P_bat_av=lim(P_av*S_PV_nom-P_load,-C,C)
  eff=select(P_bat_av>0,0.95,1/0.95)
  x1.=eff*P_bat_av/3600/C*100
  SOC=select(EnableStorage<0.5,20,limstate(x1,20,80))
  P_bat=select(EnableStorage<0.5,0,select(SOC>20.and.SOC<80,P_bat_av,0))
  x2.=(P_bat/S_bat_nom-x2)/T
  id_ref=-x2/u
  iq_ref=0

```

## Appendix C - DPL commands

### Hosting capacity depending on the PF settings:

```

double P_set,P_max, v_max, line_maxload, trafo_maxload, a, b, PF_f,PF_h,
       volt_F1, volt_F2, load_F1, load_F2, load_trafo;
int nso, err, j, check_volt_lim, check_load_lim;
set s;
object o;
string str1;

j=MyRes.Clear();
v_max=1.03;           ! voltage limit [p.u.]
line_maxload=100;    ! maximum line loading [%]
trafo_maxload=100;   ! maximum transformer loading [%]
s=PV_Set.All();      ! set of PV static generators
nso=s.Count();

PF_f=1.00;           ! initial PF for farm PV systems
PF_h=1.00;           ! initial PF for household PV systems
P_set=0.005;         ! initial active power production of a household
PV System
while (PF_f>0.89)    ! lower limit of PF for the while loop
{
  P_max=P_set;
  do
  {
    o=s.First();
    for (o=s.First(); o; o=s.Next())
    {
      str1=o:loc_name;
      a=strstr(str1, 'F1_PV3');
      b=strstr(str1, 'F1_PV5');
      if (a+b>=-1)
      {
        o:pgini=2.7*P_max;      ! for a farm PV system active power
production is 2.7 times higher
        o:cosgini=PF_f;
      }
      else
      {
        o:pgini=P_max;
        o:cosgini=PF_h;
      }
      o:pf_recap=1;
      o:iv_mode=0;
    }
    ResetCalculation();
    err=Ldf.Execute();
    if (err)
    {
      output('Load Flow Problem');
      exit();
    }
  }
  else
  {

```

```

volt_F1=F1_Bus:m:u1;
volt_F2=F2_Bus:m:u1;
load_F1=F1_Line:c:loading;
load_F2=F2_Line:c:loading;
load_trafo=Trafo:c:loading;
check_volt_lim=volt_F1>=v_max.or.volt_F2>=v_max;
check_load_lim=load_F1>=100.or.load_F2>=100.or.load_trafo>=100;
if (check_volt_lim.and..not.check_load_lim)
{
    P_set=P_max;
}
else
{
    if (check_load_lim)
    {
        P_set=P_max-0.001000;
    }
    else
    {
        P_max+=0.000100;
    }
}
}
}
while
(volt_F1<v_max.and.volt_F2<v_max.and.load_F1<100.and.load_F2<100.and.loa
d_trafo<100)
    P=P_max*1000-0.1;
    pf=PF_f;
    MyRes.Write();
    PF_f-=0.01;
    PF_h-=0.005;
}
MyRes.Flush();
j=MyRes.Draw();
Export:pResult=MyRes;
Export:iopt_exp=6;
Export:f_name='C:\Thesis\Simulations\PF_Pmax.csv';
Export.Execute();

```

### Calculation of $V_{max}$ for Q(V) strategy:

```

double P_set,P_max, v1, v2, line_maxload, trafo_maxload, a, b,
    volt_F1, volt_F2, load_F1, load_F2, load_trafo,
    S_nom_h, S_nom_f, Q_lim_h, Q_lim_f,q_max_h,q_max_f;
int nso, err, j, check_volt_lim, check_load_lim;
set s;
object o;
string str1;

ResetCalculation();
j=MyRes.Clear();
line_maxload=100;           ! maximum line loading [%]
trafo_maxload=100;        ! maximum transformer loading [%]
s=PV_Set.All();           ! set of PV static generators
nso=s.Count();

q_max_h=PF_lim_h*tan(acos(PF_lim_h));
q_max_f=PF_lim_f*tan(acos(PF_lim_f));

```

```

v1=1.0000;           ! define v_sp (=v1) parameter of Q(V)
characteristic
v2=1.0300;           ! initial v_max (=v2) parameter of Q(V)
characteristic
P_set=0.0050;        ! initial active power production of a
household PV System

while (v2>v1)
{
  P_max=P_set;
  S_nom_h=P_max/PF_lim_h;
  S_nom_f=2.7*P_max/PF_lim_f;
  Q_lim_h=-P_max*tan(acos(PF_lim_h));
  Q_lim_f=-2.7*P_max*tan(acos(PF_lim_f));
  do
  {
    o=s.First();
    for (o=s.First(); o; o=s.Next())
    {
      str1=o.loc_name;
      a=strstr(str1, 'F1_PV3');
      b=strstr(str1, 'F1_PV5');
      if (a+b>=-1)
      {
        o:sgn=S_nom_f;
        o:pgini=2.7*P_max;           ! for a farm PV system active power
production is 2.7 times higher
        o:Pmax_uc=S_nom_f;
        o:P_max=S_nom_f;
        o:cosgini=1;
        o:pf_recap=1;
        o:iv_mode=2;
        o:ddroop=((v1-v2)*S_nom_f*100)/Q_lim_f;
        o:usetp=v1;
        o:q_min=-q_max_f;
        o:q_max=q_max_f;
      }
      else
      {
        o:sgn=S_nom_h;
        o:pgini=P_max;
        o:Pmax_uc=S_nom_h;
        o:P_max=S_nom_h;
        o:cosgini=1;
        o:pf_recap=1;
        o:iv_mode=2;
        o:ddroop=((v1-v2)*S_nom_h*100)/Q_lim_h;
        o:usetp=v1;
        o:q_min=-q_max_h;
        o:q_max=q_max_h;
      }
    }
  }
  ResetCalculation();
  err=Ldf.Execute();
  if (err)
  {
    output('Load Flow Problem');
    exit();
  }
  else
  {

```

```

volt_F1=F1_Bus:m:u1;
volt_F2=F2_Bus:m:u1;
load_F1=F1_Line:c:loading;
load_F2=F2_Line:c:loading;
load_trafo=Trafo:c:loading;
check_volt_lim=volt_F1>=v_max.or.volt_F2>=v_max;
check_load_lim=load_F1>=100.or.load_F2>=100.or.load_trafo>=100;
if (check_volt_lim.or.check_load_lim)
{
    P_set=P_max;
}
else
{
    P_max+=0.0001;
    S_nom_h=P_max/PF_lim_h;
    S_nom_f=2.7*P_max/PF_lim_f;
    Q_lim_h=-P_max*tan(acos(PF_lim_h));
    Q_lim_f=-2.7*P_max*tan(acos(PF_lim_f));
}
}
while
(volt_F1<v_max.and.volt_F2<v_max.and.load_F1<100.and.load_F2<100.and.loa
d_trafo<100)
    Pmax=P_max*1000-0.1;
    v_2=v2;
    MyRes.Write();
    v2-=0.0010;
}
MyRes.Flush();
j=MyRes.Draw();
Export:pResult=MyRes;
Export:iopt_exp=6;
Export:f_name='C:\Thesis\Simulations\Q_V_Hosting_Capacity.csv';
Export.Execute();

```

# Bibliography

- [1] A. von Meier, *Electric power systems: a conceptual introduction*. Hoboken, New Jersey: Wiley, 2006.
- [2] N. Jenkins, G. Strbac, and J. B. Ekanayake, *Distributed generation*. London, United Kingdom: The Institution of Engineering and Technology (IET), 2010.
- [3] A.-M. Borbely and J. F. Kreider, *Distributed generation: the power paradigm for the new millennium*: CRC Press LLC, 2001.
- [4] P. Kundur, *Power system stability and control*: McGraw-Hill, Inc., 1994.
- [5] J. D. Bouford and C. A. Warren, "Many states of distribution," *Power and Energy Magazine, IEEE*, vol. 5, pp. 24-32, 2007.
- [6] M. H. Bollen and F. Hassan, *Integration of distributed generation in the power system*: Wiley-IEEE Press, 2011.
- [7] M. Zeman, "Photovoltaic systems," in *Solar cells*, ed.
- [8] B. M. Wilamowski and J. D. Irwin, *The industrial electronics handbook, Power Electronics and Motor Drives*, 2nd ed.: CRC Press, 2011.
- [9] A. Malla and A. Niraula, "Importance of balance of system in a solar PV application."
- [10] EPIA and Greenpeace, "Solar generation: solar photovoltaic electricity empowering the world," 2011.
- [11] EPIA, "Connecting the Sun," 2012.
- [12] EPIA, "Global market outlook for photovoltaics 2013-2017," 2013.
- [13] EPIA, "Market report 2013," 2013.
- [14] J. Widén, E. Wäckelgård, J. Paatero, and P. Lund, "Impacts of distributed photovoltaics on network voltages: Stochastic simulations of three Swedish low-voltage distribution grids," *Electric Power Systems Research*, vol. 80, pp. 1562-1571, 2010.
- [15] J. von Appen, M. Braun, T. Stetz, K. Diwold, and D. Geibel, "Time in the sun: the challenge of high PV penetration in the German electric grid," *Power and Energy Magazine, IEEE*, vol. 11, pp. 55-64, 2013.
- [16] (30/04/2014). *Watt connects*. Available: <http://www.wattconnects.com/>
- [17] T. Degner, G. Arnold, M. Braun, D. Geibel, W. Heckmann, and R. Brundlinger, "Utility scale PV systems: grid connection requirements, test procedures and European harmonisation," *Photovoltaics International*, 2009.
- [18] "EN 50160 Voltage characteristics of electricity supplied by public electricity networks," ed, 2010.
- [19] "EN-IEC 61000-3-3 Electromagnetic compatibility (EMC) - Part 3-3: Limits - Limitation of voltage changes, voltage fluctuations and flicker in public low-voltage supply systems, for equipment with rated current  $\leq 16$  A per phase and not subject to conditional connection," ed, 2013.
- [20] "EN 50438 Requirements for micro-generating plants to be connected in parallel with public low-voltage distribution networks," ed, 2013.
- [21] B. I. Craciun, T. Kerekes, D. Sera, and R. Teodorescu, "Overview of recent Grid Codes for PV power integration," in *Optimization of Electrical and Electronic Equipment (OPTIM), 2012 13th International Conference on*, 2012, pp. 959-965.
- [22] SMA, "PV Grid Integration," 2012.
- [23] M. J. E. Alam, K. M. Muttaqi, and D. Sutanto, "Distributed energy storage for mitigation of voltage-rise impact caused by rooftop solar PV," in *Power and Energy Society General Meeting, 2012 IEEE*, 2012, pp. 1-8.
- [24] T. A. Short, *Electric Power Distribution Handbook*: CRD Press, 2004.

- [25] D. Geibel, T. Degner, T. Reimann, B. Engel, T. Bulo, J. P. Da Costa, *et al.*, "Active intelligent distribution networks — Coordinated voltage regulation methods for networks with high share of decentralised generation," in *Integration of Renewables into the Distribution Grid, CIREN 2012 Workshop*, 2012, pp. 1-4.
- [26] T. Degner, G. Arnold, T. Reimann, P. Strauß, B. Engel, and M. Breede, "Increasing the photovoltaic-system hosting capacity of low voltage distribution networks," presented at the 21st International Conference and Exhibition on Electricity Distribution (CIREN), Frankfurt, 2011.
- [27] T. Stetz, F. Marten, and M. Braun, "Improved Low Voltage Grid-Integration of Photovoltaic Systems in Germany," *Sustainable Energy, IEEE Transactions on*, vol. 4, pp. 534-542, 2013.
- [28] C. Korner, M. Hennig, K. Handt, and R. Schmid, "Gaining experience with a regulated distribution transformer in a smart grid environment," in *Integration of Renewables into the Distribution Grid, CIREN 2012 Workshop*, 2012, pp. 1-4.
- [29] A. Constantin, R. D. Lazar, and S. B. Kjær, "Voltage control in low voltage networks," Danfoss Solar Inverters A/S2012.
- [30] B. Bletterie, A. Gorsek, B. Uljanic, B. Blazic, A. Woyte, T. Vu Van, *et al.*, "Enhancement of the Network Hosting Capacity – Clearing Space for/with PV," presented at the 25th EU PVSEC, Valencia, Spain, 2010.
- [31] E. Demirok, D. Sera, R. Teodorescu, P. Rodriguez, and U. Borup, "Evaluation of the voltage support strategies for the low voltage grid connected PV generators," in *Energy Conversion Congress and Exposition (ECCE), 2010 IEEE*, 2010, pp. 710-717.
- [32] G. Kerber, R. Witzmann, and H. Sappl, "Voltage limitation by autonomous reactive power control of grid connected photovoltaic inverters," in *Compatibility and Power Electronics, 2009. CPE '09.*, 2009, pp. 129-133.
- [33] E. Demirok, P. Casado Gonzalez, K. H. B. Frederiksen, D. Sera, P. Rodriguez, and R. Teodorescu, "Local Reactive Power Control Methods for Overvoltage Prevention of Distributed Solar Inverters in Low-Voltage Grids," *Photovoltaics, IEEE Journal of*, vol. 1, pp. 174-182, 2011.
- [34] D. Mende, Y. T. Fawzy, D. Premm, and S. Stevens, "Increasing the hosting capacity of distribution networks for distributed generation using reactive power control - Potentials and Limits," presented at the 2nd Solar Integration Workshop, Lisbon, Portugal, 2012.
- [35] R. Tonkoski, L. A. C. Lopes, and T. H. M. El-Fouly, "Coordinated Active Power Curtailment of Grid Connected PV Inverters for Overvoltage Prevention," *Sustainable Energy, IEEE Transactions on*, vol. 2, pp. 139-147, 2011.
- [36] C. Gaudin, A. Ballanti, and E. Lejay, "Evaluation of PV curtailment option to optimize PV integration in distribution network," in *Integration of Renewables into the Distribution Grid, CIREN 2012 Workshop*, 2012, pp. 1-4.
- [37] EPIA, "Self consumption of PV electricity," ed, 2013.
- [38] SMA, "SMA smart home: The system solution for more independence," ed.
- [39] G. G. Pillai, G. A. Putrus, and N. M. Pearsall, "The potential of demand side management to facilitate PV penetration," in *Innovative Smart Grid Technologies - Asia (ISGT Asia), 2013 IEEE*, 2013, pp. 1-5.
- [40] F. Marra, Y. T. Fawzy, T. Bulo, and B. Blazic, "Energy storage options for voltage support in low-voltage grids with high penetration of photovoltaic," in *Innovative Smart Grid Technologies (ISGT Europe), 2012 3rd IEEE PES International Conference and Exhibition on*, 2012, pp. 1-7.
- [41] M. Braun, K. Büdenbender, D. Magnor, and A. Jossen, "Photovoltaic self-consumption in Germany - Using Lithium-Ion storage to increase self-consumed photovoltaic energy," presented at the 24th European Photovoltaic Solar Energy Conference, Hamburg, Germany, 2009.



- [42] C. A. Hill, M. C. Such, C. Dongmei, J. Gonzalez, and W. M. Grady, "Battery Energy Storage for Enabling Integration of Distributed Solar Power Generation," *Smart Grid, IEEE Transactions on*, vol. 3, pp. 850-857, 2012.
- [43] G. Mulder, F. D. Ridder, and D. Six, "Electricity storage for grid-connected household dwellings with PV panels," *Solar Energy*, vol. 84, pp. 1284-1293, 2010.
- [44] P. M. S. Carvalho, P. F. Correia, and L. A. F. Ferreira, "Distributed Reactive Power Generation Control for Voltage Rise Mitigation in Distribution Networks," *Power Systems, IEEE Transactions on*, vol. 23, pp. 766-772, 2008.
- [45] T. Bülo, G. Bettenwort, D. Geibel, T. Degner, A. Seibel, J. P. d. Costa, *et al.*, "Voltage control in active, intelligent distribution networks," presented at the 27th EU PVSEC, 2012.
- [46] G. Arnold, M. Braun, T. Reimann, T. Stetz, and B. Valov, "Optimal reactive power supply in distribution networks - Technological and economic assessment for PV-systems," presented at the 24th EU PVSEC, Hamburg, 2009.
- [47] G. Kerber and R. Witzmann, "Statistical Distribution Grid Analysis and Reference Network Generation," *ew*, vol. 107, pp. 22-26, 2008.
- [48] K. Strunz, "CIGRE-EU-LV-Benchmark," 2013.
- [49] S. Electric, "Use and maintenance of oil-immersed distribution transformers - Elvim range," ed.
- [50] G. Hébrail and A. Bérard, "Individual household electric power consumption Data Set ", É. d. France, Ed., ed: UCI Machine Learning Repository, 2012.
- [51] M. Braun, K. Büdenbender, T. Stetz, and U. Thomas, "Activation of energy management in households," presented at the ETG Congress, Düsseldorf, 2009.
- [52] O. Kalab, "Standardisierte Lastprofile," ed: Wirtschaftskammer Oberösterreich.
- [53] J. Mačuhová and B. Haidn, "Labour input on Bavarian dairy farms with conventional or automatic milking," presented at the International conference of agricultural engineering, Valencia, Spain, 2012.
- [54] K. Bonkoß, J. Neiber, and D. S. Nesor, "Energy savings in dairy farming," ed: Bayerische Landesanstalt für Landwirtschaft, 2012.
- [55] (28/10/2013). *Solar radiation data*. Available: [http://www.soda-is.com/eng/services/services\\_radiation\\_free\\_eng.php](http://www.soda-is.com/eng/services/services_radiation_free_eng.php)
- [56] A. U. Schmiegel, P. Knaup, A. Meissner, C. Jehoulet, H. Schuh, M. Landau, *et al.*, "The Sol-ion system: a stationary PV battery system," presented at the 5th International Renewable Energy Storage Conference (IRES), 2010.
- [57] E. Demirok, D. Sera, R. Teodorescu, P. Rodriguez, and U. Borup, "Clustered PV inverters in LV networks: An overview of impacts and comparison of voltage control strategies," in *Electrical Power & Energy Conference (EPEC), 2009 IEEE, 2009*, pp. 1-6.
- [58] T. Stetz, M. Kraiczy, M. Braun, and S. Schmidt, "Technical and economical assessment of voltage control strategies in distribution grids," *Progress in Photovoltaics: Research and Applications*, vol. 21, pp. 1292-1307, 2013.
- [59] R. K. Roy. (04/04/2014). *Overall Evaluation Criteria (OEC)*. Available: <http://nutek-us.com/wp-oec.html>
- [60] Suedkabel, "Overhead Line Conductors," ed.

